https://doi.org/10.5194/egusphere-2023-2091
Preprint. Discussion started: 29 January 2024


# Climate Affects Global Basin-Related Metallogeny

Chuang Zhang [a]*

[a] Beijing Research Institute of Uranium Geology, China National Nuclear Corporation, Beijing 100029, China

* Corresponding author: zhangc198506@126.com

## Abstract

The basin-related hydrothermal mineral deposits are the products of metal deposition in a relatively small area from metal-rich saline brines that source from basins. Recent studies have confirmed that the metal-rich ore-forming fluids were formed in semi-arid to arid environments, and are the products of a complex system involving precipitation, weathering, groundwater, precipitation-dissolution reactions, and evaporation. The evaporation is the main reason for the buildup of metals in saline brines. The formation of metal-rich saline brines is commonly accompanied by the formation of evaporites.

The statistical results of basin-related mineral deposits worldwide show that there are two metallogenic periods after the great oxidation event: 2.1-1.4Ga (Period I) and 0.8Ga to present (Period II), with few scattered between these two periods (metallogenic quiescence period). In addition, Metallogenic Period II has five metallogenic peaks: ~380-340Ma (II-1), ~300-240Ma (II-2), ~160-100Ma (II-3), 60-40Ma (II-4), and one specific stratiform Cu metallogenic concentration period of ~580-500Ma (II-5). These two metallogenic periods and five peaks are coupled with the widespread development of saline deposits in time. The basin-related ore deposits are mainly symmetrically occurring in 10°-60° in paleo-latitudes, which is consistent with the occurring latitudes of evaporites.

The metallogenic quiescence period corresponded to the scarcity of saline deposits and was probably caused by the combination of a lack of hydrological closed basins and arid to semi-arid environments during 1.4-0.8 Ga. This quiescence period was coupled with the booming of

https://doi.org/10.5194/egusphere-2023-2091
Preprint. Discussion started: 29 January 2024


stromatolites and the extremely thin continents, both of which suggest an Earth with flat continents that were covered by a hot and wet climate, and the widely developed shallow marine environments of the major continents at middle and low altitudes during 1.4-0.8 Ga.

**Keywords:**

Climate, Basin-related mineral deposits, Mesoproterozoic, Saline giants, Stromatolite

## 1. Introduction

For more than thirty years, geologists have strived to unlock the secrets of secular distribution of many types of ore deposits in Earth's history (e.g., Meyer, 1981, 1988; Sawkins, 1984; Groves et al., 2005a, b; Holland, 2005; Leach et al., 2010; Cuney, 2010), such as sediment-hosted Pb-Zn deposits (e.g., Sangster, 1990; Goodfellow and Lydon, 2007), and sediment-hosted stratiform Cu deposits (e.g., Kirkham, 1989; Kirkham et al., 1994; Hitzman et al., 2010). There are three principal factors that have influenced the global pattern of metallogenesis: long-term global tectonic trends (e.g., Barley and Groves, 1992; Goldfarb et al., 2010), the evolution of the hydrosphere-atmosphere, which is inextricably related to the tectonic recycling (e.g., Slack and Cannon, 2009; Bekker et al., 2010), and the secular decrease in global heat production (e.g., Holland, 1984; Sawkins, 1990; Barley and Groves, 1992; Farquhar et al., 2014). The plate tectonic evolution has been increasingly emphasized as a factor that led to the formation of many famous mineral provinces (e.g., Rona, 1980; Mitchell and Garson, 1981; Sawkins, 1984; Groves et al., 2005a; Robb, 2005, 2020). Nevertheless, due to the lack of a reasonable understanding of the formation processes of ore-forming fluids for basin-related ore deposits, there are ambiguities in the correlation between global metallogeny and the complex Earth history of supercontinent assembly and breakup during the Phanerozoic (e.g., Leach et al., 2005, 2010; Hitzman et al., 2010).

The availability of information on important mineral deposits worldwide is steadily increasing, significant advances have been achieved in understanding long-term secular changes in the Earth

https://doi.org/10.5194/egusphere-2023-2091
Preprint. Discussion started: 29 January 2024


System, and data gaps for defining broad temporal distributions of ore types are becoming smaller. However, there continues to be one significant gap in our understanding of the secular distribution of many types of ore deposits in time and space (e.g., Robb, 2005; Goldfarb et al., 2010). If we shift our perspective from ore-deposit centric to one centered on ore-forming fluids (e.g., Richard et al., 2013, 2014; Zhang et al., 2022, 2023a, 2023b), the global distribution pattern of basin-related mineral deposits (e.g., SEDEX and MVT Pb-Zn deposits, sediment-hosted stratiform Cu deposits, Unconformity related U deposits) in time and space would be understood more easily. Recently, some researchers have begun to study the metal-rich fluids in developing basins, so as to reveal the formation processes of paleo-ore-forming fluids for the basin-related ore deposits (e.g., Li and Barnes, 2019; Zhang et al., 2022, 2023a, b). The goal of this paper is to provide a new perspective into the climate controls on the formation of metal-rich fluids, and therefore controls the formation of basin-related ore deposits.

The present is the key to the past. Metalliferous saline brines in basins are the ore-forming fluids for basin-related ore deposits, such as unconformity-related U deposits, MVT Pb-Zn deposits, and redbed Cu deposits (e.g., Leach et al., 1997, 2005; Zhang et al., 2022). This paper covers six main subjects: (1) the description of major types of basin-related ore deposits, in particular SEDEX and MVT Pb-Zn deposits, sediment-hosted stratiform Cu deposits, and basin-related hydrothermal type U deposits; (2) the formation processes of metal-rich saline brines in hydrologically closed basins that are responsible for basin-related ore deposits; (3) the global distribution of basin-related ore deposits in time and space; (4) the factors that influence the formation of metal-rich saline brines; (5) how climate influences the formation and distribution of basin-related ore deposits globally; and (6) how major geological events influence the global climate and the formation and distribution of basin-related ore deposits.

## 2. Description of Basin-Related Ore Deposits

Basin-related ore deposits are a diverse group of ores that are genetically related to basinal brines, and have no direct genetic association with igneous activity. These include Unconformity-type U

https://doi.org/10.5194/egusphere-2023-2091
Preprint. Discussion started: 29 January 2024


deposits, SEDEX and MVT Pb-Zn deposits, and Redbed Cu deposits (e.g., Hitzman et al., 2010; Leach et al., 2010), as well as vein type polymetallic deposits outside of basins but genetically related to basinal brines (Kyser, 2014; Zhang et al., 2023a, 2023b). These deposits are typically stratiform or strata-bound, although some discordant ores occur (e.g., Bradley and Leach, 2003; Zhang et al., 2019, 2022). Vein ore is often important in many deposits, and the ores consist of various metals such as Pb, Zn, Cu, As, Ag, Fe, and U (e.g., Selley et al., 2005; Kerrich et al., 2005, 2008; Farquhar et al., 2010). Comprehensive review articles are available for sediment-hosted Pb-Zn deposits (Leach et al., 2005), basin-related hydrothermal type U deposits (Cuney, 2010; Kyser, 2014), and sediment-hosted stratiform Cu deposits (Hitzman et al., 2010). Therefore, the author will not present a detailed description of the geological characteristics of basin-related ore deposits, but rather a brief summary and overview.

The presence of laminated metallic minerals that parallel bedding is commonly accepted as permissive evidence for exhalative ore (e.g., Goodfellow et al., 1993; Goodfellow and Lydon, 2007). However, this kind of explanation is unsatisfactory (detailed discussion in Leach et al., 2010). In addition to the laminated Pb-Zn deposits, there are many laminated deposits that did not form as exhalites, such as the strata-bound scheelite mineralization near Halls Creek in Western Australia (Todd Ririe, 1989), stratiform W-Sb-Au mineralization in South China (Gu et al., 2012), stratiform Mn-Fe deposits in North Europe (Bostrom et al., 1979), the Nuheting U deposit in China (Bonnetti et al., 2015), and partially the Bayan Obo REE deposit (e.g., Liu et al., 2004; Yang et al., 2017; Zhang et al., 2017). Previous researchers proposed that these deposits with ore textures that mimic synsedimentary textures were formed by replacement processes (e.g., Kelley et al., 2004a, b; Leach et al., 2005). This explanation is also unsatisfactory, as the highly selective mineral replacement after the deposition of host rocks without specific alteration is difficult to convince geologists.

The basins that host or are genetically related to ore deposits mainly occur in passive margins, continental rifts, and sag basins (e.g., Leach et al., 2010; Hitzman et al., 2010; Cuney, 2010). The tectonic setting of the basins determines the ore-hosting rock type, ore controls, as well as the survivability of the deposit during tectonic recycling (e.g., Goldfarb et al., 2010). The author did not

https://doi.org/10.5194/egusphere-2023-2091
Preprint. Discussion started: 29 January 2024


provide detailed descriptions of these tectonic settings; however, the similarity between them is the ubiquity of convergent sedimentary basins. In this paper, the author exemplified the SEDEX and MVT Pb-Zn deposits, sediment-hosted Cu deposits, and basin-related hydrothermal type U deposits, to find out their distribution characteristics in time and space, which could be used to test their major influencing factors.

### 2.1 SEDEX and MVT Pb-Zn deposits

The most common basin-related Pb-Zn deposits are SEDEX and MVT Pb-Zn deposits, hosted by a variety of carbonate and siliciclastic rocks (Leach et al., 2005). The major ore minerals are sulfides such as sphalerite, galena, and pyrite, while the nonsulfide minerals are mainly dolomite, calcite, barite, siderite, and chert (e.g., Cooke et al., 2000; Yardley, 2005). These deposits have formed in a variety of geologic and tectonic environments over the last two billion years, as documented by the compilation result of Leach et al. (2005), based on the World Minerals Geoscience Database Project (Sinclair et al., 1999).

### 2.2 Sediment-hosted Cu deposits

Sediment-hosted stratiform copper deposits comprise disseminated to veinlet copper and copper-iron sulfides in siliciclastic or dolomitic sedimentary rocks. Sulfides conform closely, but usually not exactly, with the stratification of host rocks (Brown, 1989, 1992, 1993, 1997). These deposits account for approximately 23% of the world's production and known reserves, and are also important sources of silver and cobalt (Hitzman et al., 2005). Some deposits contain other metals including lead, zinc, and uranium, and a few contain gold and platinum group elements. The basins that host the stratiform copper deposits can be marine or continental, and usually contain evaporites overlying redbeds or in isolated non-red units within the continental redbed sequences themselves (e.g., Cox et al., 2003; Hitzman et al., 2010). The compilation of sediment-hosted stratiform copper deposits was cited from the statistical work of Kirkham (1989) and Kirkham et al. (1994).

https://doi.org/10.5194/egusphere-2023-2091
Preprint. Discussion started: 29 January 2024


### 2.3 Hydrothermal type U deposits

The basin-related hydrothermal type U deposits include the sub-types of vein-type U deposits hosted by various lithologies, unconformity-related U deposits hosted by metamorphic rocks, collapse-breccia type deposits, and hydrothermal type U deposits hosted by Na- and/or K metasomatism alteration (Cuney, 2011, 2013, 2014, 2016; Cuney et al., 2012; Zhang et al., 2022). The hydrothermal U districts that the author has compiled include Proterozoic U deposits in the Nordic region, metasomatism type U deposits in Ukraine (Kirovogard-Smolino region, Krivoy Rog region) and the Russian Federation (Lake Ladoga and Onega districts, European Part), Proterozoic unconformity-related and vein type U deposits in Canada, Australia, India, Brazil, China, and Africa, such as the famous U deposits in Athabasca and Thelon basins, Cuddapah and Bhima U region, Singhbhum Cu-U belt, Pink Creek Inlier U region, Franceville U region in Gabon, and so on (Dahlkamp, 2009, 2010, 2016). In addition, the Phanerozoic vein-type U deposits account for a large portion, such as the Erzgebirge district in Germany, the La Crouzille district in France, the Holdita and Crucea districts in Romania, South China U Province, Streltsovsk district in the Russian Federation, the Spokane mountain area in the US, the Poços de Caldas Region in Brazil, and so on (Dahlkamp, 2009, 2010, 2016). The detailed statistics of U districts are in Appendix A.

## 3. Formation Processes of Ore-Forming Fluids of Basin-related Ore Deposits

Ore-forming fluids responsible for the formation of basin-related ore deposits are commonly metal-rich, hot, and of medium to high salinities (Kesler, 2005). The homogenization temperatures of fluid inclusions of ore-stage minerals from these deposits typically range from 50°C to 250°C, as high as 300°C; however, most temperatures are between 100 and 200°C, such as those of MVT Pb-Zn deposits, unconformity-related U deposits, vein type Pb-Zn and U deposits, and so on (e.g., Kesler and Reich, 2006; Stoffell et al., 2008; Richard et al., 2012; Zhang et al., 2017, 2019). Salinities commonly range from 10% to over 30% wt NaCl equiv (Basuki and Spooner, 2004; Leach et al., 2005). The geochemical composition of the paleo-ore-forming fluids is remarkably similar to the

https://doi.org/10.5194/egusphere-2023-2091
Preprint. Discussion started: 29 January 2024


compositions of present-day basin brines (Carpenter et al., 1974; Kesler et al., 1996; Viets et al., 1996), although there is a relatively large temperature difference between the developing basin brines and paleo-ore-forming fluids.

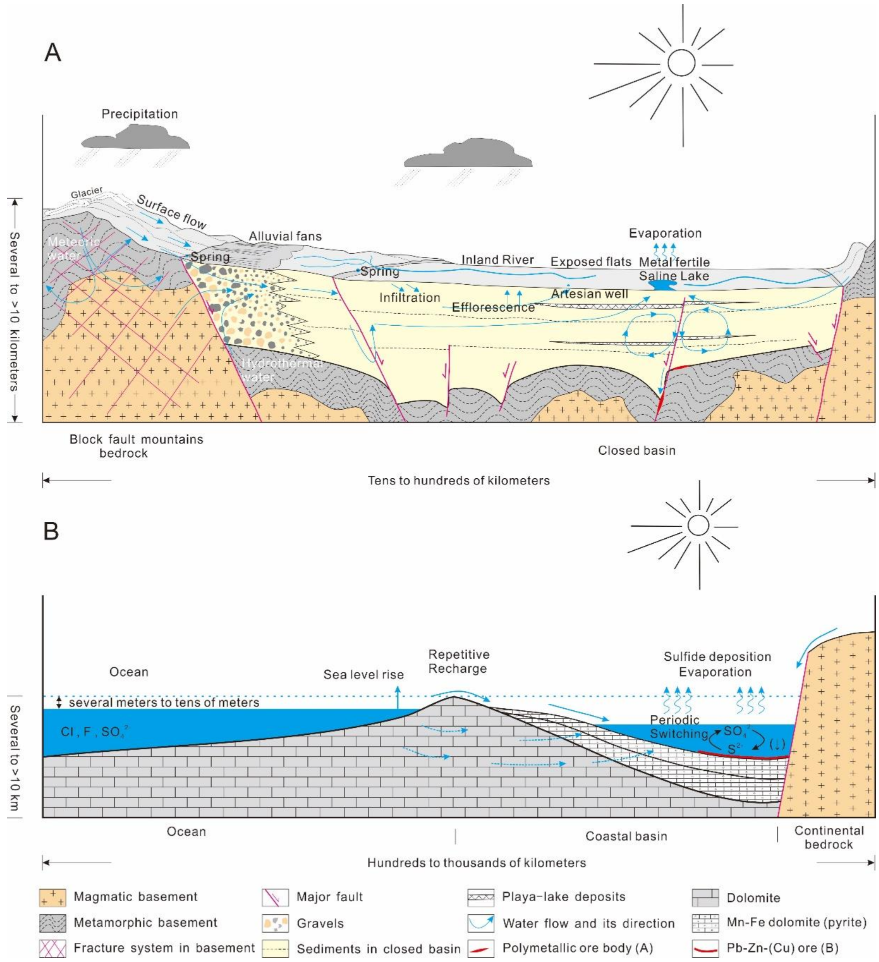


Fig.1 Sketch map showing the formation processes of metal fertile saline brines in continental closed basin (A, modified from Zhang et al., 2022) and coastal basin (B, modified from Large et al., 2002 and Zhang et al., 2022).

It is generally assumed, from mineralogical and geochemical considerations, that the paleo-ore-forming fluids were principally hot metalliferous basinal brines (Badham, 1981; Lydon, 1983;

https://doi.org/10.5194/egusphere-2023-2091
Preprint. Discussion started: 29 January 2024


Cooke et al., 2000). However, this does not mean that the initial ore-forming fluid reached high levels of trace metal compositions at high temperature conditions. There are three possibilities for the formation procedures of hot metalliferous basinal brines: I. the initial fluid was metal-rich and then heated to a high temperature; II. the initial fluid was heated to a high temperature first, and then obtained a large amount of trace metals from regional lithologies; III. the initial fluid obtained the trace metals and was heated simultaneously.

The author first discusses the possibility of surficial saline brines acting as ore-forming fluids. Many researchers have confirmed that the surficial saline brines in closed basins are metal-rich, such as the ephemeral Lake Merouane Chott in North Africa (U > 20 ppm, Cr > 100ppm, Cu > 200ppm, Co > 10 ppm, Pb > 2ppm, V > 2000ppm, and Zn > 200ppm; e.g., Hacini and Oelkers, 2010), various soda saline lakes in Mongolia (U > 20 ppm, Mo > 5 ppm; e.g., Volkova, 1998; Linhoff et al., 2011; Shvartsev et al., 2014; Zhang et al., 2022), and saline lakes on the Tibet Plateau (W > 5ppm, Mo > 5 ppm, REE > 10 ppm; Zheng et al., 1989). These metalliferous saline brines are the products of a complex system involving precipitation, weathering, precipitation-dissolution reactions, groundwater circulation and water-rock interactions, evaporations, and probably biological activity (Carroll and Bohacs, 1999). Such metal-rich saline brines usually exist in the form of saline lakes, and mainly develop in arid to semi-arid environments. The main influence on the formation of these brines is hydrological closure; that is, evaporation is the primary or only way for water to leave the converging area (Deocampo and Jones, 2014). The balance between water inflow and evaporation over time is the major factor causing ions to accumulate (Jones and Bodine, 1987) by exceeding the saturated solubility of various minerals, usually beginning with the alkaline-earth carbonates, then progressing to gypsum, and then to halite (Warren, 2014). In this enriching process, trace metals build up to an unusually high level (detailed examples in Zhang et al., 2022, 2023a, b). The mineralogical composition and order of salts precipitation in a surficial saline brine are controlled by the ionic make-up of the mother brine, which is commonly the surficial and underground runoff (Hardie and Eugster, 1970; Hardie et al., 1978).

The surficial saline brines have high salinities with total dissolved solids of more than 35 g/L but

https://doi.org/10.5194/egusphere-2023-2091
Preprint. Discussion started: 29 January 2024


commonly less than 400 g/L (Deocampo and Jones, 2014; Zhang et al., 2022). The high salinities mean higher density compared to fresh groundwater, which drives the surficial saline brines to circulate into the deep area and thus changes the salinities and trace metals concentrations of groundwater (Fig. 1A). During the circulation, these brines would be heated and pressurized, and obtain and deposit some specific metal ions, and alter the basement through water-rock chemical interactions (Hecht and Cuney, 2000; Mercadier et al., 2010, 2012, 2013; Kyser, 2014). Over time, the groundwater near saline lakes would eventually be transformed into metalliferous, pressurized, and hot salinized fluids.

The nearby sedimentary strata may become metalliferous fluid-hosting aquifers, such as the Mississippi Salt Dome (Kharaka and Thordsen, 1992; Kesler et al., 1996). These brines could be expelled from the aquifers during physical and/or chemical compaction and/or diagenesis, and migrate into structural conduits such as faults, creating opportunities for vein-type mineralization (Frape et al., 2014; Heinrich and Candela, 2014). If the basins are coastal, the formation of metal-fertile brines sourced from seawater requires (1) a steady influx of seawater, (2) multiple intervals of isolation from the ocean, (3) a saline-lake elevation lower than sea level, in addition to an arid, evaporative environment (Fig.1B; e.g., Messinian salinity crisis in the Mediterranean region, Krijgsman et al., 1999; Gillet et al., 2007).

In contrast, more researchers prefer Possibilities II and III, which suggest that the initial fluid obtained trace metals at high temperature conditions, such as the “Reflux brine model for Pb-Zn deposits in Passive Continental Margin” (Leach et al., 2005) and “Seawater extracting metals from redbeds model for sediment-hosted stratiform copper deposits” (e.g., Hitzman et al., 2005; Robb, 2005). The trace metals were extracted from the surrounding rocks, such as redbeds, marine sedimentary rocks, and wall rocks of regional faults (e.g., Hitzman et al., 2005; Kyser, 2014). Some of these models require the existence of evaporites. Direct dissolution of evaporites in the flow path of meteoric/marine waters has been the preferred source for dissolved salts (Goodfellow et al., 1993; Lydon, 1995; Emsbo, 2009), and then extract the trace metals from regional lithologies during groundwater circulation to become the metal-rich fluid (e.g., Hitzman et al., 2005; Kyser, 2014). It

https://doi.org/10.5194/egusphere-2023-2091
Preprint. Discussion started: 29 January 2024


is difficult to verify the authenticity of these models (Possibilities No. II and III) because the extraction of trace metals occurs several kilometers underground and is unobservable directly. However, the authenticity of these models can be indirectly verified by statistics of paleo-latitude of the basin-related ore deposits during their mineralization. For Possibility I, the initial ore-forming fluid formed in arid to semi-arid environments, which is dominantly controlled by the latitude. However, for Possibilities II and III, the formation of initial ore-forming fluid was independent of latitude, although some of these models need the existence of evaporites. The detailed latitude statistics of basin-related ore deposits are below.

## 4. Global Distribution of Metal-rich Saline Lakes and Its Major Controlling Factors

The current distribution of metal-rich saline lakes and their controlling factors could reveal the factors that control the global distribution pattern of basin-related metallogenesis. Climate plays a critical role in the formation of saline lakes; the amount of inflow to a hydrologically closed basin, mainly precipitation, must be closely balanced by evaporative loss, meaning that saline lakes are mainly found in semi-arid to arid environments (Deocampo and Jones, 2014). In the Quaternary, the saline lakes are mainly zonally distributed, as revealed by the global distribution pattern of Quaternary evaporites (Kottek et al., 2006; Warren, 2014). In terms of latitude, the saline lakes are dominantly located in the range of 5° to 50° in the Northern and Southern Hemispheres (Cooke and Warren, 1973; Smoot and Lowenstein, 1991). This zonal distribution pattern of saline lakes is the comprehensive result of many factors, including the zonal distribution of solar radiation over the surface of the Earth, the distribution of land masses and their elevations, and ocean and atmospheric circulation and interaction, among other causes (Mackenzie, 2003). These factors combine to control the global patterns of winds, the balance between precipitation and evaporation, and humidity, cloudiness, air pressure, and temperature (Kump et al., 2010). However, the primary factor is the zonal difference of solar radiation over the Earth. The high flux of solar radiation at the equator results in air rising in the equatorial zone and moving toward the poles, and cooler air from the poles moving toward the equator. The warm, moist, rising air forms large cumulus up into the high

https://doi.org/10.5194/egusphere-2023-2091
Preprint. Discussion started: 29 January 2024


troposphere, and is the source of precipitation in the equatorial zone. On the way to the poles, the dry air cools and begins to sink, forming the subtropical high pressure zone, which is commonly dry and rainless. This is the reason that saline lakes are commonly found in the low-mid latitudes (Fig.2). Then, the cooler air descends and moves toward the equator, creating the trade winds of both hemispheres, also known as the "Hadley cell" (Fig. 2). Due to the rotation of the Earth (termed the "Coriolis Effect"), the wind systems in the subtropical high pressure zone are prevailing westerlies. In contrast, very cold and dry air that forms in the poles moves toward the equator. On the way, the cold air uplifts the warm air in the lower latitudes. As warm air rises, it carries water vapor upward into the atmosphere, creating precipitation (Schneider and Londer, 1989). With consideration of temperature and associated evaporation, the arid to semi-arid zones are mainly located in the low and middle latitudes (Fig. 2). In addition, the distance to the ocean is another important factor; rainfall is much less in the interior of the continent than in coastal areas, which is caused by being far away from the water vapor source. The saline lakes are also located on the leeward slope of mountains, and may also unexpectedly appear on the west coast of the continent, where there is a middle latitude low pressure system towards the equator (Warren, 2014).

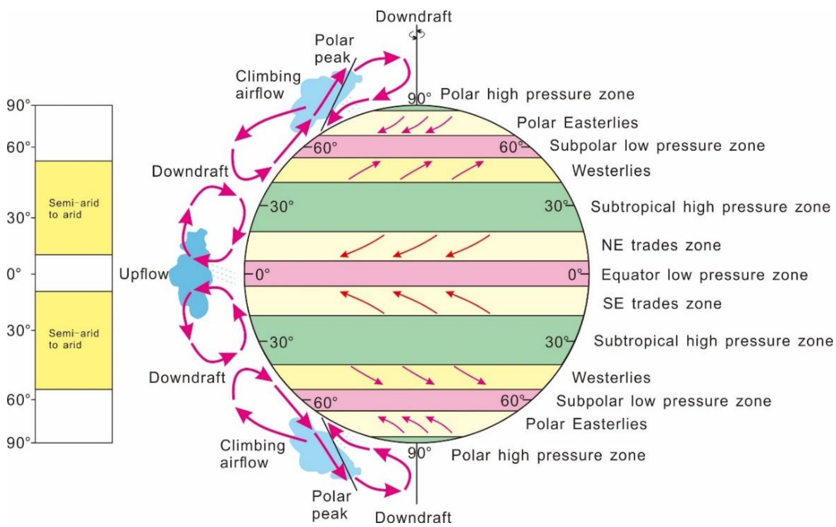


Fig.2 Distribution of modern climatic belts showing the Earth's atmosphere circulation cells across 90°N to 90°S. Belts of cool dry descending air around 15–45°N and S of the equator create the main arid zones of the world (e.g., Trewartha and Horn, 1980; Schneider and Londer, 1989; Darnell et al., 1992).

https://doi.org/10.5194/egusphere-2023-2091
Preprint. Discussion started: 29 January 2024


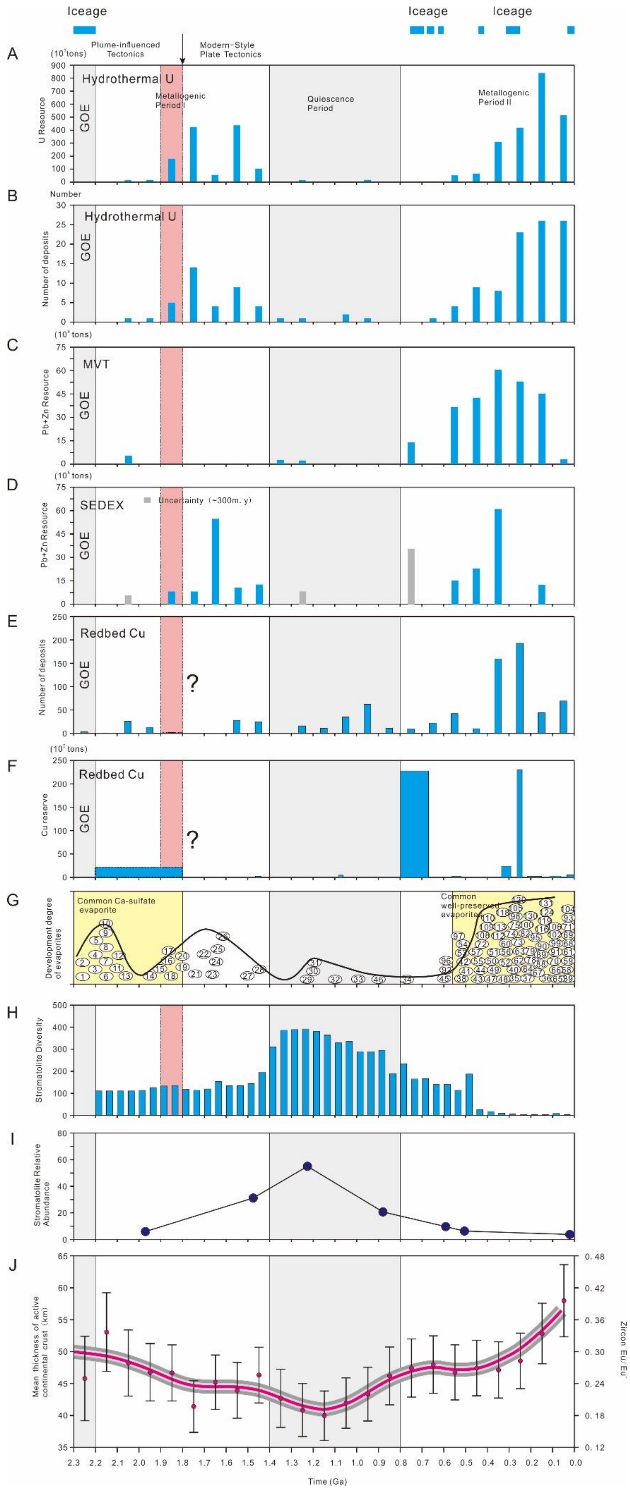

https://doi.org/10.5194/egusphere-2023-2091
Preprint. Discussion started: 29 January 2024


Fig.3 Occurrence (in terms of relative abundances) of basin related hydrothermal type U deposits (U resource for A, and Number of deposit for B), MVT (Pb+Zn resource, C, Leach et al., 2005) and SEDEX (Pb+Zn resource, D, Leach et al., 2005) Pb-Zn deposits, sediment-hosted stratiform Cu deposits (Number of deposits for E, and Cu reserve for F, Kirkham, 1989; Kirkham et al., 1994; Hitzman et al., 2010), saline giants (G, Bekker et al., 2006; Evans, 2006; Bekker and Holland, 2012; Ba˛bel and Schreiber, 2014), Stromatolite relative diversity (H, Awramik and Sprinkle, 1999) and abundance (I, Walter and Heys, 1985; Sheldon, 2013), and reconstructed thickness of active continental crust since 2.3Ga (J, Tang et al., 2021a, b). The basin-related mineral resources are mainly distributed in two stages which are 2.2-1.4 Ga, and 0.8-0.6 Ga, with one basin-related metallogenic gap period of 1.4-0.8 Ga. While the metallogenic gap period has witnessed the great prosperity of stromatolite in abundance and diversity. The global distribution pattern of basin-related ore deposits are showing similar shape with the saline giants, and reconstructed thickness of active continental crust since 2.3Ga.

The saline lakes that existed during geological history have disappeared, leaving evidence of their existence, such as evaporite salts and associated redbeds (Warren, 2010). Evaporites are believed to be important in the genesis of metal-fertile basin brines, as they are a key feature of basins hosting supergiant deposits. However, the exact genetic relationship between evaporites and ore deposits is controversial (e.g., Robb, 2005; Groves et al., 2010; Leach et al., 2010; Zhang et al., 2022). Ancient evaporites are varying combinations of gypsum or anhydrite, alkaline earth carbonates, and halite, with or without potash-bearing minerals such as sylvite, carnallite, and epsomite (e.g., Pope and Grotzinger, 2003; Bekker et al., 2006; Schro¨der et al., 2008). With the improvement of the availability of information in recent years, the global statistics of evaporites are becoming increasingly convincing. The author has compiled evaporite sediments of the world based on previous studies of Pope and Grotzinger (2003), Bekker et al. (2006), Schro¨der et al. (2008), Warren (2010, 2014), and others (Fig.3, 4, and 5).

https://doi.org/10.5194/egusphere-2023-2091
Preprint. Discussion started: 29 January 2024


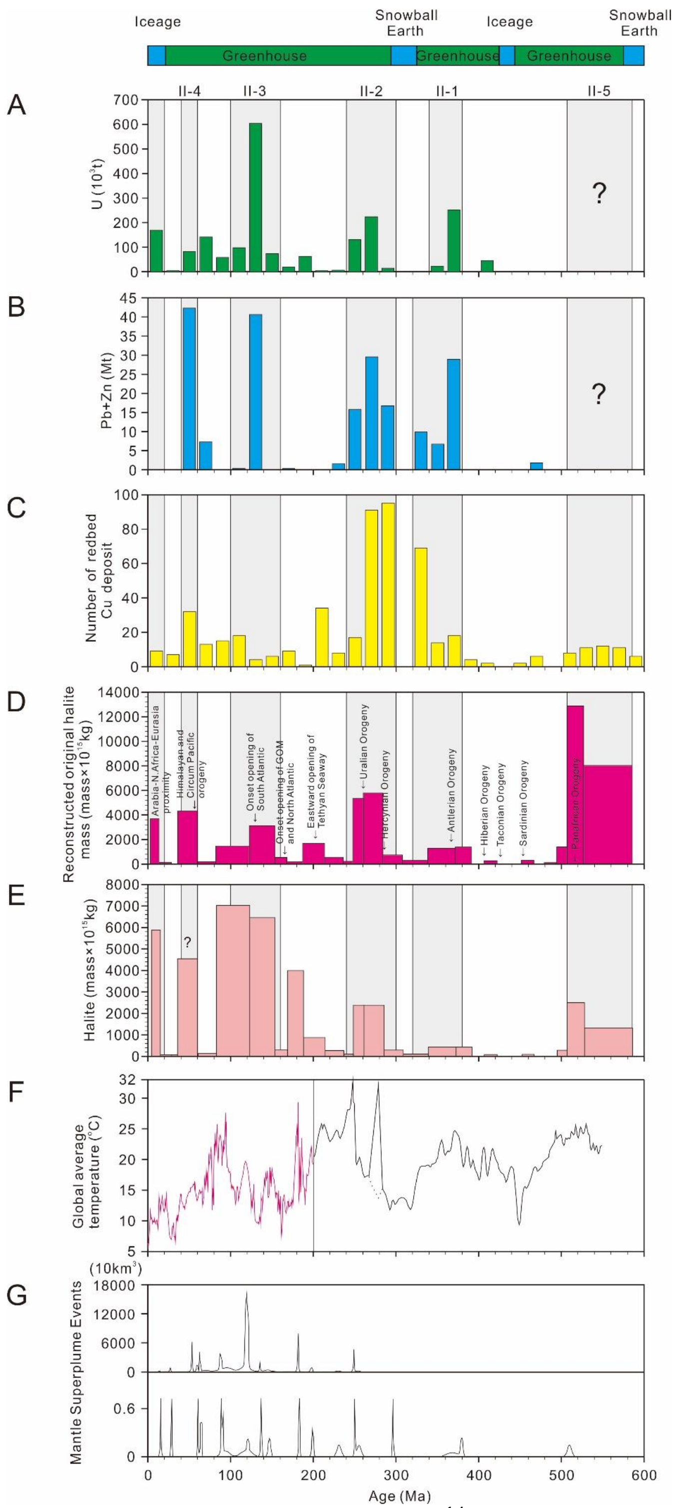

https://doi.org/10.5194/egusphere-2023-2091
Preprint. Discussion started: 29 January 2024


Fig.4 Temporal distribution (in terms of relative abundances) of basin related hydrothermal type U deposits (A, Dahlkamp, 2009, 2010, 2016; Zhang et al., 2022), MVT and SEDEX Pb-Zn deposits (B, Leach et al., 2005, 2010), sediment-hosted stratiform Cu deposits (C, Kirkham, 1989; Hitzman et al., 2005), saline deposits (D and E, Hay et al., 2006; Warren, 2010), global paleo-average temperature (Prokoph et al., 2008; Donnadieu et al., 2008; Ernst, 2014; Spray, 2020; Scotese et al., 2021), and large igneous provinces (Ernst and Buchan, 2001; Prokoph et al., 2013) since ~600Ma.

The compilation of evaporite sediments has shown that there are mainly two development stages (Fig.3). The first stage was about 2.3-1.4Ga and was represented by pseudomorphs after gypsum, anhydrite, and halite (Zharkov, 2005). The second stage is Phanerozoic and is represented by well-preserved gypsum, anhydrite, and halite. During most of the Phanerozoic, the Earth was in a greenhouse state, except for part of the Permo-Carboniferous. In the greenhouse times, there were no continental or polar ice sheets, and the planet's meridional temperature gradient was much less steep than it is at present (Warren, 2006, 2010). In this context, the Hadley-related circulation belts would be pushed away from the equator, global water recycling would be sped up, and many continental deserts would enter relatively humid environments than the Earth in the glacial age (Yan et al., 1998; Baker et al., 2001; Hesse et al., 2004). Therefore, saline lakes would be much more numerous and distributed more widely in the greenhouse stage than the Earth in the glacial stage. On the whole, the saline lakes during Phanerozoic were produced in the low to middle latitudes, as shown by the existence of evaporites (Fig.5). With estimates of the volume of salt being recycled back into the oceans added to the volumes of actual salt in various megahalite beds of the world, the original halite volume during the Phanerozoic can be reconstructed (Fig.4; Hay et al., 2006; Warren et al., 2010). This reconstructed original halite mass distribution can reveal the volumes of saline lakes during Phanerozoic generally. There are mainly seven periods of widely development of saline lakes on the Earth during Phanerozoic, which are 580-510Ma, 390-340Ma, 300-240Ma, 210-190Ma, 160-80Ma, 60-40Ma, and ~20Ma, respectively, corresponding to the greenhouse stages (Fig.4).

https://doi.org/10.5194/egusphere-2023-2091
Preprint. Discussion started: 29 January 2024


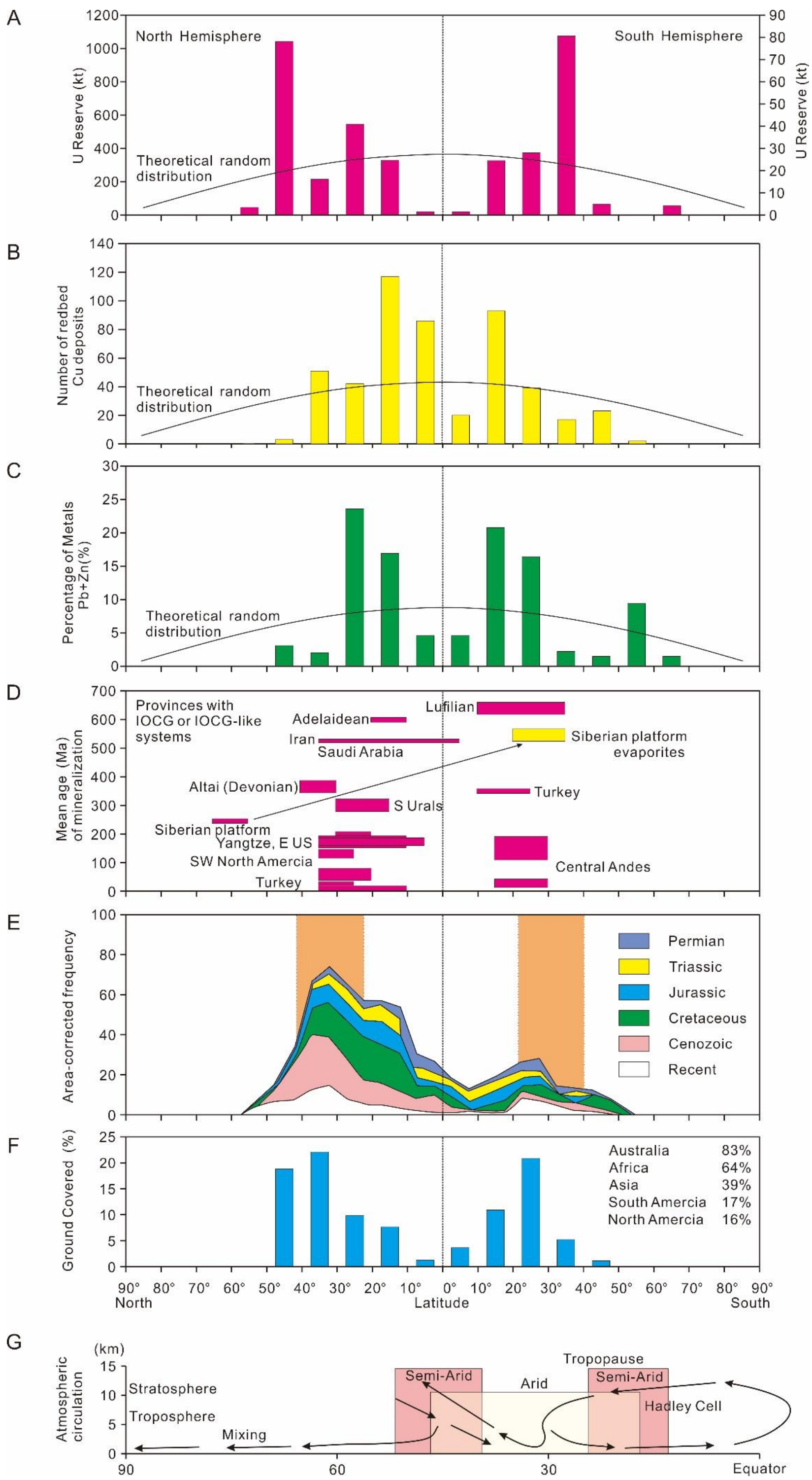


349

https://doi.org/10.5194/egusphere-2023-2091
Preprint. Discussion started: 29 January 2024


Fig.5 Paleo-latitude distribution (in terms of relative abundances) of basin related hydrothermal type U deposits (A, Dahlkamp, 2009, 2010, 2016; Zhang et al., 2022), sediment-hosted stratiform Cu deposits (B, Kirkham, 1989; Hitzman et al., 2005), MVT and SEDEX Pb-Zn deposits (C, Leach et al., 2005, 2010), IOCG deposits (D, Barton, 2014), Phanerozoic saline deposits (E, Hay et al., 2006; Warren, 2010), and Quaternary deserts (F, Prokoph et al., 2008; Donnadieu et al., 2008; Ernst, 2014; Spray, 2020; Scotese et al., 2021) since ~600Ma.

## 5. Uneven Distribution of Basin-Related Ore Deposits in Time and Space

The previous compilations of basin-related ore deposit types as a function of geological time by Meyer (1981, 1988), Veizer et al. (1989), Barley and Groves (1992), and Leach et al. (2005) have revealed that these deposits developed during particular periods of Earth's evolution, and the global pattern of basin-related mineral deposits is extremely uneven in time and space (Garnett and Bassett, 2005; Large et al., 2005; Cuney, 2010). With the improvement and increase of information on basin-related ore deposits, it is necessary to conduct a more comprehensive statistical analysis. Here, the author has compiled statistics for the world's major hydrothermal-type U ore deposits related to basins (Appendix A), the previous compilation of SEDEX and MVT Pb-Zn deposits during the Proterozoic and Phanerozoic (Leach et al., 2005; Zhang et al., 2022), sediment-hosted Cu deposits (Hitzman et al., 2005), and the world's major saline deposits (Appendix B) since the global oxidation event (GOE). The temporal and spatial distribution of these basin-related ore deposits is highlighted (Fig. 3, 4, and 5).

### 5.1 Metallogenic Peak of 1.8-1.5 Ga

The compilation results of basin-related ore deposits show that these types of ore deposits increased gradually in quantity and resource to a peak of about 1.8-1.5 Ga, with the onset of the Great Oxidation Event (Fig. 2). During this peak, a large number of basin-related ore deposits developed worldwide, such as the world-class unconformity-related U deposits in Canada (e.g., Athabasca basin, 1.8-1.7 Ga), Australia (e.g., Pink Creek Inlier U region, 1.8-1.7 Ga), and India (e.g.,

https://doi.org/10.5194/egusphere-2023-2091
Preprint. Discussion started: 29 January 2024


Singhbhum Cu-U belt, Cuddapah and Bhima U region, ~1760 Ma), world-class metasomatism type U deposits in Europe (e.g., Kirovogard-Smolino U region, Krivoy Rog U region, 1.8-1.7 Ga, 1750-1770 Ma; Lake Ladoga and Onega U districts, 1.8-1.7 Ga), China (e.g., metasomatism type U deposits North China Craton, 1740-1800 Ma), Australia (Mount Isa region, 1750-1730 Ma), and the famous vein type U deposits around the world (e.g., Beaverlodge area in Canada, Sierra Ancha/Apache Proterozoic Basin in Arizona, Central Ceará U Region in Brazil, Longshoushan U region in Northwest China; e.g., Dahlkamp, 2009, 2010, 2016). For the sediment-hosted Pb-Zn deposits, the SEDEX Pb-Zn deposits show a similar variation trend and reach a peak at 1.7-1.6 Ga, such as the world-class Pb–Zn deposits of eastern Australia (Mount Isa, Broken Hill, and McArthur River, Bodon, 1998; Chapman, 2004; Large et al., 2005), South Africa (Aggeneys and Gamsberg Pb-Zn districts, Rozendaal, 1980; Rozendaal and Stumpfl, 1984; Stalder and Rozendaal, 2004), India (Zawar Pb-Zn district, Bhattacharya and Bull, 2010), and China (Yanliao Pb-Zn region, Zhong et al., 2012; Duan et al., 2017). In contrast, during this period, the famous sediment-hosted stratiform Cu deposits were much less than the basin-related Pb-Zn and U deposits. The statistics of sediment-hosted stratiform Cu deposits are mainly based on the ages of ore-hosting rocks, and the distribution pattern of the sediment-hosted stratiform Cu deposits during 2.2-1.4 Ga is different from that of the basin-related Pb-Zn and U deposits. Post the Great Oxidation Event, the first famous supergiant stratiform Cu deposits were contained in the Paleoproterozoic Kodaro-Udokan basin of Siberia. The age of the ore-hosting sequence is poorly constrained, ranging from 2200 to 1800 Ma (Abramov, 2008), and the mineralization age is unknown (Volodin et al., 1994). The second famous ore-hosting sequence of stratiform Cu deposits is the Revett Formation, which hosts deposits such as Spar Lake in the NW United States. The Revett Formation is about 1460 Ma, constrained by the underlying 1468 Ma lower Belt sequence (Anderson and Davis, 1995) and the overlying 1454 Ma carbonate sequence (Evans et al., 2000).

## 5.2 Metallogenic Quiescence during 1.4-0.8 Ga

Irregular decline of basin-related ore deposits occurred during 1.5-1.4 Ga, and then the Earth entered a basin-related metallogenic quiescence period until about 0.8 Ga. This metallogenic quiescence

https://doi.org/10.5194/egusphere-2023-2091
Preprint. Discussion started: 29 January 2024


was also stressed by Bekker et al. (2010) to reflect a gap of Superior-type iron deposits and manganese ore deposits (Maynard, 2010). During this quiescence period, the global basin-related metallogeny was maintained at a low level, and a much smaller number of basin-related ore deposits were formed in this period in contrast to the period 1.8-1.5 Ga. For the hydrothermal type U deposits, most of the reported U mineralization ages during this period were from the Paleoproterozoic unconformity-related U deposits, and were interpreted to be the reformation age of the existing deposits or the new mineralization events that superimposed on the old deposits, such as the vein type U deposits in the Great Bear Batholith in Canada (e.g., ~1076Ma, Chi et al., 2018; Dahlkamp, 2016), unconformity-related U deposits in the Franceville region of Africa (e.g., 890-860Ma, Cuney and Mathieu, 2000), and vein type U deposits in the Kombolgie basin in Australia (e.g., ~1040Ma, Rawlings and Page, 1999; Polito et al., 2006a, b; Cuney and Kyser, 2008). The sediment-hosted stratiform Cu deposits were represented by the Mesoproterozoic Keweenaw basin of the Mid-Continent Rift of the USA (White Pine, Brown, 1971; White, 1971; Mauk et al., 1992). Moreover, the reported MVT and SEDEX Pb-Zn deposits were fewer during the quiescence period (Fig. 3).

### 5.3 Metallogenic Period of Phanerozoic

The quiescence period ended at about 0.8-0.7 Ga. From 0.8 to 0.5 Ga, the basin-related ore deposits began to increase in quantity and resource (Fig. 3), and the Earth entered a basin-related metallogenic period again. The second metallogenic period was mainly the Phanerozoic. Due to the lack of absolute values of resources of sediment-hosted stratiform Cu deposits, the author compiled the number of Cu deposits that differed from the basin-related Pb-Zn and U deposits, both of which were compiled in their resources (Fig. 4 and 5). The histogram of resource of basin-related U deposits and Pb-Zn deposits, and number of Cu deposits that formed within 600 Ma, referring to their formation or ore-hosting rock ages, show that these types of ore deposits are strikingly similar to each other (Fig. 4). The metallogenic peaks of basin-related U deposits are nearly coincident with the Pb-Zn deposits, and partially coincident with the stratiform Cu deposits. There are five metallogenic peaks (Fig. 4) that include ~380-340 Ma (II-1), ~300-240 Ma (II-2), ~160-100 Ma (II-3), 60-40 Ma (II-4), and one stratiform Cu metallogenic concentration period of ~580-500 Ma (II-

https://doi.org/10.5194/egusphere-2023-2091
Preprint. Discussion started: 29 January 2024


5).

During the metallogenic peak of II-1, the basin-related U deposits were represented by the Kokshetau and Kendyktas-Chuily-Betpak Dala U region of Kazakhstan, Eastern Karamazar-Northeastern Fergana U Region of Kyrgyzstan, and Schwarzach Valley U region of Germany (e.g., Dahlkamp, 2010). The Pb-Zn deposits were represented by the East Tennessee and Pine Point Pb-Zn district of the United States, and Lennard Shelf Pb-Zn region of Australia (e.g., Leach et al., 2005, 2010). The sediment-hosted stratiform Cu deposits are represented by the famous Cha-Sarysu Cu region of Kazakhstan, and numerous Cu deposits in Europe and the United States (e.g., Kirkham, 1989; Kirkham et al., 1994; Hitzman et al., 2010). The second metallogenic peak (II-2) was represented by the supergiant stratiform Cu deposit of Kupferschiefer in Europe, and the East Tennessee Pb-Zn region, Southeast Missouri Pb-Zn region, Tri-State Pb-Zn region, North Arkansas Pb-Zn region, and Upper Mississippi Valley Pb-Zn region of the United States, and numerous U regions in Europe (e.g., Dahlkamp, 2009, 2016; Hitzman et al., 2010; Leach et al., 2010). The metallogenic peak of II-3 and II-4 were represented by the Upper Silesia Pb-Zn region in Europe, Cevennes Pb-Zn region, Pine Point Pb-Zn region in the United States, South China metallogenic province, Streltsovsk U district, Elkon U district, Bureinsky U District in the Russian Federation, and numerous stratiform Cu deposits around the world (e.g., Dahlkamp, 2009, 2016; Hu et al., 2008, 2017; Hitzman et al., 2010). The temporal distributions of Phanerozoic hydrothermal type U deposits, SEDEX and MVT Pb-Zn deposits, and stratiform Cu deposits show a similar pattern with the Phanerozoic distribution of global evaporites (Warren, 2010; Fig.4).

The author has also compiled the paleo-latitudes of the Phanerozoic basin-related ore deposits during their mineralization (Fig. 5). The paleo-latitudes of basin-related U deposits, SEDEX and MVT Pb-Zn deposits, and stratiform Cu deposits are similar to each other. Most of the Phanerozoic basin-related ore deposits are formed at low to middle latitudes, with few deposits formed at middle-high latitudes (e.g., Barton and Johnson, 1996; Scotese et al., 1999; Soloviev, 2010a, b; Leach et al., 2010; Boucot et al., 2013). The formation latitudes of the basin-related ore deposits generally coincide with the broadly contemporaneous evaporitic settings (Fig. 2 and 5). Previous researchers have often emphasized the Earth's evolving tectonic setting and geochemical systems; many studies have proposed that the large-scale formation of basin-related ore deposits is related to global tectonic processes and patterns (orogenic processes, Wilson cycle, e.g., Nance et al., 1986; Larson, 1991; Barley and Groves, 1992; Barley et al., 1998; Kerrich et al., 2000, 2005; Goldfarb et al., 2005). However, the global tectonic evolution cannot explain the uneven distribution of basin-related ore deposits in time and space well. Admittedly, many basin-related ore deposits have been destroyed by subduction and erosion, or modified by post-ore metamorphism and tectonism, so that they are no longer recognizable (e.g., Veizer et al., 1989; Bradley, 2008). However, some basic distribution characteristics should still be retained; for example, if there were basin-related ore deposits formed at high latitudes (e.g., >70°), it is impossible to destroy them all; if there were a significant amount of basin-related ore deposits formed during 1.4-0.8 Ga, it is impossible that all the hydrothermal type U deposits, SEDEX and MVT Pb-Zn deposits, and stratiform Cu deposits showed one mineralization quiescence during this period (Fig.2).

# 6. Discussion

### 6.1 Another explanation for the genesis of basin related Pb-Zn deposits

The metal-fertile saline brines that are contemporaneous with evaporites are probably the initial ore-forming fluid of basin-related ore deposits (e.g., Zhang et al., 2022, 2023a, 2023b). This view comes from current research on saline lakes. The buildup of metals in basinal saline brines was mainly caused by the balance between water inflow and evaporation over time (Jones and Bodine, 1987). During the evaporation, the commonly enriched ions include $Na^+$, $K^+$, $Ca^{2+}$, $Mg^{2+}$, $Cl^-$, $HCO_3^-$, $SO_4^{2-}$ ($S^{2-}$ and/or $HS^-$), and sometimes $Li^+$ (e.g., Zheng, 1997; Dugamin et al., 2021). Due to the evaporation over time, some dissolved metals can accumulate by exceeding the saturated solubility of various minerals, usually beginning with alkaline-earth carbonates, then progressing to gypsum, and then to halite and sylvite (Warren, 2014). These chemical deposition processes generally limit the salinities of saline brines to not exceed 40%. In this enriching process, some trace metals build up to unusually high levels, such as U concentrations of Lake Shuiquanzi (China) reaching 35.0

https://doi.org/10.5194/egusphere-2023-2091
Preprint. Discussion started: 29 January 2024


mg/L, Pb and Zn concentrations of the central Mississippi Salt Dome Basin (US) reaching 100.0 mg/L and 250.0 mg/L, respectively (Hagni, 1983; Kharaka et al., 1987; Kharaka and Hanor, 2014), and Cu concentrations of Lake Merouane Chott (northern Africa) reaching 800.0 mg/L (Hacini and Oelkers, 2010), and so on.

The ores of basin-related Pb-Zn deposits (MVT and SEDEX) throughout the world are commonly fine-grained, banded, or colloform and dendritic in texture, which highly suggests sulfide deposition in an open space (McLimans et al., 1980; Leach and Sangster, 1993). The parallel bedding sulfides are assumed to be permissive evidence for exhalative ores (Leach et al., 2005). It is true that metal-rich exhalative fluids have been found in seafloor spreading centers, such as the Atlantis II Abyss of the Red Sea (Thisse et al., 1982, 1983; Barrett et al., 2021) and the Galapagos Spreading Center in the Eastern Pacific Ocean (Perfit et al., 1983, 1999). However, most of the Pb-Zn deposits classified as SEDEX lack unequivocal evidence of an exhalite in the ore or alteration component (Leach et al., 2005, 2010). In addition, the bedrocks of the Pb-Zn ores found in seafloor spreading centers include pillow lavas, pelagic sediments, and hyaloclastites. In contrast, most basin-related Pb-Zn deposits are thought to have been formed in extensional basins associated with orogeny, intracontinental and intracratonic failed rifts (Ervin and McGinnis, 1975), and continental marginal basins (Leach et al., 2005; Large et al., 2005). The bedrocks are commonly shoal and/or neritic carbonate rocks and continental clastic rocks (Leach et al., 2005). There are few basin-related Pb-Zn deposits thought to have been formed in ocean spreading centers. Therefore, researchers should look for another reasonable explanation. There is no denying that the exhalative process can result in the formation of laminated Pb-Zn ores. Here, the author proposes another simple explanation, referring to the studies of modern saline lakes.

What economic geologists who focus on basin-related ore deposits easily ignore is that condensed seawater and saline brines can be significantly enriched in metals and sulfates (e.g., Volkova, 1998; Hacini and Oelkers, 2010; Linhoff et al., 2011; Shvartsev et al., 2014). Previous studies of saline lakes have identified that many of them show vertical stratification of their water masses over extended periods (e.g., Lake Walker, Lake Mono, Lake Great Salt, Domagalski et al., 1990; Boehrer

https://doi.org/10.5194/egusphere-2023-2091
Preprint. Discussion started: 29 January 2024


and Schultze, 2008; Deocampo and Jones, 2014; Fig.6). This stratification includes density, temperature, dissolved substances, oxygen fugacity, and even living organisms. It can be caused by many factors, such as higher atmospheric temperatures during the warm season (e.g., Peeters et al., 2000) and external inflow of river water with lower density into saline lakes (e.g., Boehrer and Schultze, 2008). In some cases, stratification of saline lakes is temporarily destroyed by full or partial overturning, which may occur as a result of seasonal winds or seasonal temperature change (especially in the transition from the warm season to cold season; e.g., Steinhorn, 1985). The Dead Sea in the Middle East is a representative example of the occurrence of switching between stratification and full circulation in saline lakes; this switch occurs once a year, with stratification being weak in spring, autumn, and winter, but fully developed in summer (Steinhorn, 1985; Bartov et al., 2002; Arnon et al., 2019). The Jordan River was the water recharge source for the Dead Sea.

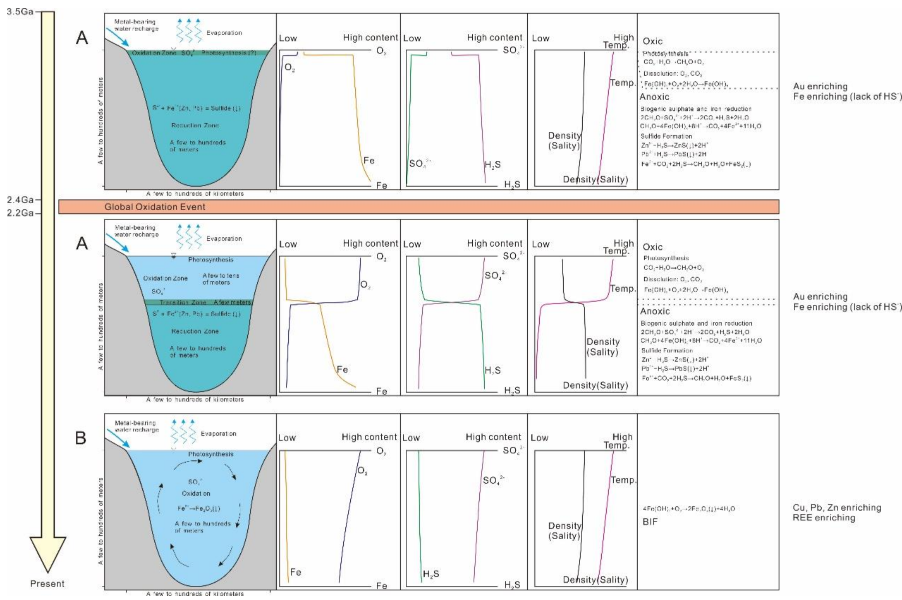


Fig. 6 Schematic diagrams showing redox status of saline lakes since the 3.5 Ga (A, appearance of photosynthetic algae), and 2.4-2.2 Ga (Global Oxidation Event, stratification of B and full overturn of C) to present (Boehrer and Schultze, 2008; Deocampo and Jones, 2014; Saleh et al., 2018; Arnon et al., 2019).

After the GOE, $SO_4^{2-}$ is a common ion in saline lakes, and the stratification of saline lakes would transform the $SO_4^{2-}$ into $S^{2-}$ in the deeper reducing layer, following which the enriched sulfurophiles (e.g., Pb, Zn, Fe) would be deposited as sulfides, including galena, sphalerite, and pyrite (Fig. 6; Domagalski et al., 1990; Stoffell et al., 2008; Deocampo and Jones, 2014). When the stratification is terminated (i.e., the saline lakes experience vertical circulation), the water mass becomes oxidizing, $SO_4^{2-}$ again becomes one of the major ions (Boehrer and Schultze, 2008), and sulfurophile metal ions start to become enriched again (Steinhorn, 1985; Boehrer and Schultze, 2008). The switching between stratification and full (or partial) overturn of saline lakes (condensed seawater) would form alternating-layered sedimentary structures of sulfurophile sulfides and other sediments. In this case, the laminated Pb-Zn ores would be formed (Schmalz, 1969; Fig. 6).

If the concentrations of S ($SO_4^{2-}$ + $S^{2-}$) are relatively low, or the concentrations of sulfurophile ions are much greater than those of S ($SO_4^{2-}$ + $S^{2-}$) ions, the stratification of saline lakes would allow for the enrichment of sulfurophile metal ions, commonly $Fe^{2+}$, in the deeper reducing layer. The full (or partial) overturn of saline lakes would lead to the oxidation of $Fe^{2+}$ to $Fe^{3+}$, which is then deposited as hematite. In this case, the switch between stratification and full (or partial) overturn may form the alternating-layered sedimentary structure of hematite and other sediments, which is likely the origin of the structure of partial banded iron formations (Fig. 6C; Gutzmer et al., 2006; Boehrer and Schultze, 2008; Deocampo and Jones, 2014). This is the reason that the SEDEX Pb-Zn deposits and BIF deposits have similar sedimentary textures.

The surficial saline brines and evaporated seawater were commonly located above regional faults, such as Lake Maharlou in the central Shiraz Basin of Iran (Fayazi et al., 2007), Lake Olduvai in Tanzania (Blumenschine et al., 2012), and various saline lakes on the Tibet Plateau (Zheng, 1997). Due to their high salinities, these brines have higher densities than those of fresh and brackish groundwater and seawater. Therefore, these saline brines migrate downward into the underlying or basal sequence of sedimentary basins. During the migration, the saline brines are heated and pressurized, in some cases, by high heat flow and/or igneous activity, and there is an exchange of elements between fluids and surrounding rocks, and/or metal deposition from metal-fertile saline

https://doi.org/10.5194/egusphere-2023-2091
Preprint. Discussion started: 29 January 2024


brines (Hoeve and Sibbald, 1978; Komninou and Sverjensky, 1996; Kyser, 2014; Chi et al., 2017). These saline brines may utilize fault systems within and connect to the basin to escape to other suitable regions and precipitate some specific minerals when they react with certain rocks. This is the reason that the researchers can observe Pb-Zn ores with vein-like texture (Fig. 1; Zhang et al., 2022). If the saline lakes are always in a non-stratified oxidation state, sulfurophile metal ions, such as $Pb^{2+}$, $Zn^{2+}$, $Cu^{2+}$, $Mo^{2+}$, and so on, are enriched.

**6.2 The factors that influence the formations of Ore-forming fluid**

The factor that controls the formation of initial ore-forming fluid also influences the formation of basin-related ore deposits (Zhang et al., 2022, 2023a, 2023b). The ancient metal-rich saline lakes have disappeared, but they have left evidence of their existence, such as evaporites, fossils, and residual metal-fertile brines (Ba̧bel and Schreiber, 2014). The metal-rich saline brines in hydrologically closed basins are controlled jointly by arid-semiarid climate, tectonic setting, and circulation processes underground (Carroll and Bohacs, 1999). However, the climatic setting is the dominant factor, even if seawater was the starting fluid (Deocampo and Jones, 2014). The distribution of global arid-to-semiarid zones is firstly controlled by the global atmospheric circulation model, which means the arid-to-semiarid zones are closely related to the latitudes (Fig. 2; Trewartha and Horn, 1980; Schneider and Londer, 1989).

Geologists working with continental saline lakes have reached a consensus that these lakes, as well as evaporites, form mostly in hot, arid to semi-arid zones within world-scale climatic regions known as the horse latitudes (Warren, 2010). The term "horse latitudes" encompasses the regions beneath the north and south Subtropical High atmospheric pressure belts (Oliver, 2005); see Warren (2010) for a detailed explanation of the formation of the horse latitudes. For marine saline brines, at particular times in the Earth's past, the hydrologies that facilitated the deposition of widespread sulfate or halite evaporites across large parts of ancient salt basins were tied to platform or basin-wide settings that have no same-scale modern counterparts (Fig. 5; Warren, 2010). The location of marine Phanerozoic evaporites in zones of appropriate adiabatic aridity and continentality extended

https://doi.org/10.5194/egusphere-2023-2091
Preprint. Discussion started: 29 January 2024


well into the equatorial belts; therefore, in the Earth's past, the equatorial belts could also have been the location of saline lakes (Ziegler et al., 2003). This is because evaporation rates of ocean waters were at their maximum if the seawater were drawn into isolated evaporitic depressions (Kendall et al., 2003; Warren, 2010). This is the reason that the paleo-latitudes of basin-related ore deposits range from 60° north to 60° south, and there are hardly any basin-related ore deposits formed at latitudes higher than 60° (Fig. 5). The paleo-latitudinal distribution of basin-related ore deposits should not be explained by the selective preservation of basin-related ore deposits.

The factors that influence global climate include $CO_2$ concentrations in the atmosphere (the primary driver of Phanerozoic climate, with large igneous provinces being the main source, according to Royer et al., 2004 and Royer, 2016), plate tectonics and continental weathering (which influence the long-term global temperature, Berner, 1994; van der Meer, 2017; Brune et al., 2017), the amount of solar radiation, biological influences (e.g., $C_4$ grasses can reduce the atmospheric $CO_2$ contents faster than $C_3$ plants, Lunt et al., 2007; Jiang, 2019), and ocean currents, which influence the global climatic pattern (Holland et al., 1986; Hoffman and Schrag, 2002; Huybers and Langmuir, 2009; Gnanaseelan and Deshpande, 2018). Of these factors, atmospheric $CO_2$ concentration might be the most important (Anagnostou et al., 2016; Wally, 2018; Scotese et al., 2021).

High concentrations of atmospheric $CO_2$ result in a greenhouse effect, accelerating evaporation globally (Linacre et al., 1970; Gilman, 1994). More importantly, these high concentrations result in greater volumes of precipitation (Walker et al., 1981; Lackner et al., 2012), making surface waters more acidic, leading to enhanced dissolution of calcium and silicates and accelerating the leaching of specific metals from rocks, thereby enhancing the degree of enrichment of trace metals in saline lakes under semi-arid climates (Almendinger, 1990; White and Buss, 2014). Greenhouse eustasy (with associated epeiric seaways) favors the formation of surface saline brine as well as platform evaporites (Warren, 2010).

Except for the planet-scale atmospheric circulation mainly caused by the varying intensity of solar irradiation from the equator to the poles, there are three interrelated factors which influence the broad scale distribution of the world's arid climate belts in time and their associated saline brines and evaporitic sediments (Warren, 2010). These three factors are also controlled by the latitudinal position of continental plates and variations in styles of plate-plate interaction. How these three factors influence the distribution of arid belts was discussed in Warren (2010). Meanwhile, the orogenic factor is also crucial for the development of arid to semi-arid regions. Likewise, orographic deserts are better developed at times when two continental plates collide or a transcontinental rift valley forms (Kendall et al., 2003; Warren, 2006). A rising mountain range, which is the direct result of tectonic activity, is a barrier to atmospheric circulation, especially if perpendicular to the incoming circulation (Sun et al., 2008). Tectonic activity is one dominant factor that influences the formation of hydrological closed basins which are home to metal-rich saline brines (Zhang et al., 2022, 2023a, 2023b). Therefore, in addition to climate, tectonic activity is the second prime factor that influences the formation and distribution of continental and marine saline brines (Warren, 2010).

The global tectonics are governed by the Wilson Cycle of plate–plate interactions, which encapsulates the notion that as new ocean basins open (rift of continents) via the formation of new seafloor, oceans close due to the processes of subduction of oceanic crust, and ultimately by continent–continent collision (Wilson, 1966; Nisbet and Fowler, 1983). Compilations of the time-related distribution of ancient evaporites suggest there are four plate tectonic situations where significant amounts of metal-rich saline brines could be produced at particular times in the past (Jackson et al., 2000; Warren, 2010). These four tectonic settings are: (1) rifting basins where continental plates are beginning to move apart, (2) foreland basins where continental plates are coming close to each other, (3) intracontinental or intraplate sagging (intracratonic basins), which are caused by the far-field effects of continental orogeny, (4) rapidly subsiding continental depressions in transform or strike-slip settings where plates are sliding horizontally past one-another (e.g., Kingston et al., 1983; Gasse and Fontes, 1989; Bosworth et al., 2005; Warren, 2006; Jordan et al., 2007). These saline brines occur in both continental and marine realms (Warren, 2010). The existence of metal-fertile saline brines is evidenced by the large volume of evaporites; see the detailed reasons and formation processes of surficial saline brines in different tectonic settings in Warren (2010). In summary, the factors that can affect global or regional climates indirectly affect

https://doi.org/10.5194/egusphere-2023-2091
Preprint. Discussion started: 29 January 2024


the formation of global or regional basin-related ore deposits.

### 6.3 How the major geological events influence the formation and distribution of basin related ore deposits globally?

Major geological events that can significantly influence climates include mantle super-plume events (or large igneous provinces), snowball Earth, and plate-plate tectonic events (Zhang et al., 2022, 2023a, 2023b). Mantle super-plume events create large volumes of igneous rocks (large igneous province, Coffin and Eldholm, 1994; Ernst and Buchan, 2001; Courtillot and Renne, 2003), triggering the input of large volumes of gas, including $CO_2$, into the ocean-atmosphere system (Prokoph et al., 2008, 2013). As a result, $CO_2$ concentrations in the atmosphere increase to high levels; for example, the Siberian large igneous province (ca. 251 Ma) is estimated to have released 0.7-4.8 × $10^7$ Tg $CO_2$, which could have raised the global temperature by 1.5-4.5 °C (Wignall, 2001; Berner, 2002; White and Saunders, 2005; Tang et al., 2013). Mantle super-plume events thus influence both atmosphere and ocean chemistry (Coltice et al., 2007; Ernst and Youbi, 2017). Furthermore, the increase in global temperature during mantle super-plume events would increase the rates of rainfall and evaporation, as well as the rate of weathering of silicate minerals, giving rise to bursts of metal-fertile saline brines and evaporites (Fig. 4). In addition, snowball Earth events could also result in a burst of global metallogenesis. Such an event dramatically slows the normal consumption of $CO_2$ through chemical weathering of silicate rocks. However, shifting tectonic plates would continue to generate volcanoes and supply the atmosphere with $CO_2$ (Hoffman et al., 1998; Hoffman and Schrag, 2000, 2002). In this situation, $CO_2$ could accumulate to an extremely high level (roughly 350 to 1000 times the present-day concentration of $CO_2$ in the atmosphere; Hoffman and Schrag, 2000; Higgins and Schrag, 2003; Le Hir et al., 2009). The heat-trapping capacity of $CO_2$ would warm the planet and begin to melt the ice that wrapped the planet. The thaw would take only a short time (a few hundred years), after which Earth would enter a brutal greenhouse stage (Allen and Hoffman, 2005; Font et al., 2010). Surface temperatures would soar to >50 °C, driving an intense cycle of evaporation and rainfall (Hoffman and Schrag, 2000). Torrents of carbonic-acid rain would erode exposed rocks, with the weathered metal ions being transported

https://doi.org/10.5194/egusphere-2023-2091
Preprint. Discussion started: 29 January 2024


into the oceans and (locally) lakes. In this case, there would most likely be more numerous and larger metal-bearing brine bodies on Earth's surface compared to the present. This explains the global burst of basin-related ore deposits in the period 295-260 Ma (e.g., Hein and Lehmann, 2009; Dolníček et al., 2009, 2014), following the snowball Earth event of the early Permian.

During Icehouse times (not Snowball Earth times), the oceanic eustatic response to rapidly waxing and waning polar ice sheets is excessively high amplitude and too short in time to allow continental (or periplatform) margin biogenic buildups to grow into continuous barriers (more than 100m of sea level oscillation every 100,000 years, Fischer, 1981; Warren, 2010). In contrast, the less than 5-10m of sea level change every 100,000 years during Greenhouse times are much more beneficial to the formation of barriers of platform-edge reefs and shoals (Fischer, 1981; Warren, 2010). These barriers are the key to the periodical hydrographic disconnection of back-barrier lagoons (periplatform) from the open ocean. This facilitated the creation of metal-fertile saline brines that originated from seawater, and therefore the formation of related SEDEX and MVT Pb-Zn deposits, stratiform Cu deposits, and so on (Warren, 2006, 2010).

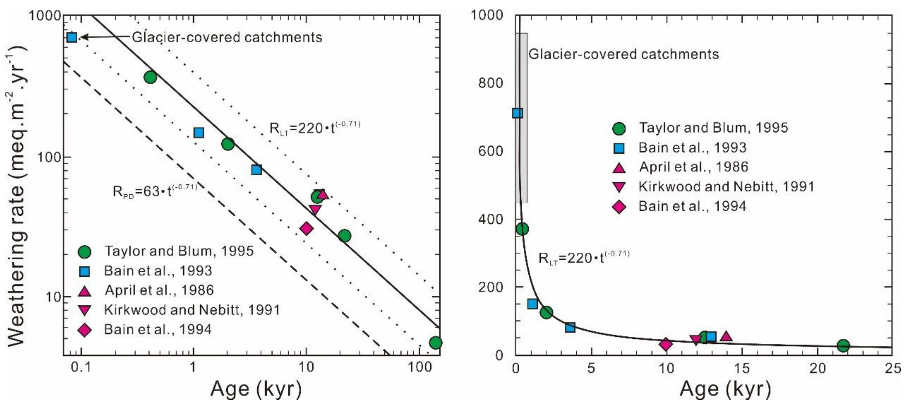


Fig.7 A Log-log plot of base cation weathering rates vs. soil age (Blum, 1997). Data points are long-term weathering rates (RLT) from the references listed on the figure. The dark solid line is a power-law curve fit to the data from Taylor and Blum (1995, R = 0.99). Light dotted lines bracket curve fit to data and represent estimated maximum uncertainties of a factor of two in weathering rates. Question mark indicates two points from Bain et al. (1993) that are suspect on the basis of high Zr

https://doi.org/10.5194/egusphere-2023-2091
Preprint. Discussion started: 29 January 2024


contents of parent materials. Dashed line represents present-day weathering rates (RPD) calculated from solid curve (see text). The shaded area represents the range of fluxes in glacier-covered catchments compiled by Sharp et al. (1995) and are plotted at an arbitrary age. Fig.7 B Linear plot of the same data and power law function as in Fig. 7A, but with the age axis truncated at 25 thousand years.

For the mantle Super-plume event (or Large Igneous Provinces), Snowball Earth, and Plate-Plate tectonic events, there is one collective result: these geological events can produce a large area of exposed fresh bedrocks. Especially for the aftermath of Snowball Earth Events, chemical weathering rates (or metal and base cation releasing rates) should be at their peak, as all the continents are exposed with fresh bedrock (Fig. 7; Allen and Hoffman, 2005; Font et al., 2010). Because the weathering rates for all of the base cations decrease with increasing soil age, such as the weathering rates of soil age of 0.4 thousand years being at least two orders of magnitude higher than the soils with age of 138 thousand years (Fig. 7; e.g., Bain et al., 1993; Sharp et al., 1995; Taylor and Blum, 1995). When the soil age is relatively large, such as bigger than 138kyr, the weathering rate would be relatively low and stable (e.g., 1-5 meg/m$^2$.yr.; Blum, 1997). Actually, there are many factors other than soil age that influence the chemical weathering rates, including human activities, precipitation, temperature, vegetation, relief, silicate rock mineralogy, uplift rate, and glacial history (Raymo and Ruddiman, 1992; Richter et al., 1992; Blum, 1997). However, it is extremely difficult to confidently isolate the influence of the various factors affecting weathering rates. On the whole, the relation between soil age and silicate weathering rates suggests one well-defined power law relation for young soils (≤138 thousand years old), and the chemical weathering rates are significantly accelerated in fresh bedrock outcropping environments (Fig. 7; Bain et al., 1993; Sharp et al., 1995; Taylor and Blum, 1995). Therefore, the releasing rate of metals of continents is the fastest following Snowball Earth Events, and the accumulation rate of metals elements in saline lakes is the fastest, with consideration of the Greenhouse Effect of Snowball Earth Events.

In contrast to the Snowball Earth Event, Plate-Plate Tectonic Events, particularly plate convergence, can result in the rapid uplifting of mountainous areas, which undergo high rates of mechanical

https://doi.org/10.5194/egusphere-2023-2091
Preprint. Discussion started: 29 January 2024


denudation, often predominantly by mass wasting (Derry and France-Lanord, 1997). In addition, mountainous areas are more likely to experience earthquakes and mass failures, as well as, for example, heavy rains and snow melts, all of which facilitate erosion. Mechanical erosion processes periodically regenerate fresh mineral surfaces and expose them to the agents of chemical weathering (Berner and Berner, 1997; Taylor and Blum, 1995). Furthermore, one of the consequences of tectonic uplift is that mountain ranges are often raised to elevations that can support alpine glaciation. The available data on chemical weathering rates of silicate catchments containing active alpine glaciers has shown that they are elevated by at least an order of magnitude compared to nonglaciated catchments, although the exact magnitude of this increase is difficult to estimate (Hallet et al., 1996; Blum, 1997). Both glaciation and rapid uplift are accompanied by rapid physical denudation, which exposes fresh bedrock minerals to the agents of chemical weathering. This means that the rapid uplifting of mountains caused by plate convergence can quickly release dissolved metals into nearby hydrological basins. Other indirect outcomes of uplift are the changes in mean annual temperatures that accompany high elevation, and changes in precipitation patterns owing to orographic effects (e.g., rain shadow effect, An et al., 2014; Caves, 2016). Therefore, metal-rich saline lakes are likely to be produced in this geological context.

The Large Igneous Provinces are massive crustal emplacements of predominantly iron- and magnesium-rich (mafic) rock that formed by processes other than normal seafloor spreading (Coffin and Eldholm, 2005). They are the dominant form of near-surface magmatism on the terrestrial planets, with areal extents greater than 0.1 million km$^2$ (Ernst and Jowitt, 2013). These occurrences on the continents, such as the continental flood basalt provinces and volcanic passive margins well preserved in the Mesozoic and Cenozoic periods, created a cover of fresh bedrocks. In this situation, the large igneous provinces could also rapidly release base and metal cations into regional hydrological closed basins. These are the reasons that the Snowball Earth events, large igneous provinces, and plate-plate tectonic events are commonly related to global and regional basin-related ore deposits in time and space (e.g., Ernst and Jowitt, 2013; Zhang et al., 2022).

Global tectonism controls the distribution of lithologic assemblages (both supracrustal rocks and

https://doi.org/10.5194/egusphere-2023-2091
Preprint. Discussion started: 29 January 2024


intrusive rocks), styles of deformation, and the grade, duration, and location of metamorphic events. Rock assemblages that form in specific plate tectonic settings and which are available for weathering exert control on the initial chemistry of water flowing into closed basins and, therefore, influence subsequent brine chemistry (Deocampo and Jones, 2014; Zhang et al., 2022). In addition, the geology of watersheds (drainage divides) is commonly affected by tectonic processes, which directly affect the topography and lithologic assemblages (Pietras et al., 2003; Singh and Jain, 2009; Sangma and Balamurugan, 2017). As a consequence, certain patterns of major ions and enriched metals correspond to particular tectonic settings around the world (Deocampo and Jones, 2014). For example, calc-alkaline volcanic activity has dominated East Africa since the Miocene and has produced widespread sodium carbonate water (Jones et al., 1977; Cerling, 1996). In contrast, the northern plains of North America are underlain by Paleozoic to Mesozoic evaporitic sedimentary rocks and Quaternary till, which have helped to generate strongly sulfatic waters (Last, 1999). Trace-metal compositions of brines, such as the brines of Inner Mongolia, are enriched in U–Mo, whereas brines in the Tien Shan mountains and northern Qinghai-Tibet Plateau are enriched in Cu–Cr and Co–Mn, respectively (Zhang et al., 2022). These differences suggest that heterogeneity in the evolution and nature of continental crust may be an additional large-scale influence on basin-related mineralization (O'Nions and Oxburgh, 1988; Rudnick and Gao, 2014; Tang et al., 2016).

Another important role of tectonism is to provide the geological and structural setting for metal-bearing brines, including the generation of fractures or fold-related structures that can act as fluid conduits and points/zones of flow convergence (e.g., Sibson, 1985, 1987; Cox et al., 1991). This would favor the convergence of large volumes of ore-forming fluids in a relatively small space (several kilometers) over a relatively short time (<1Ma; Cox and Knackstedt, 1999; Skinner, 1997), thus creating the opportunity for mineralization to occur (Cox et al., 2001).

From a metallogenic viewpoint, the emergence of basin-related ore deposits in the rock record between 2.02 Ga and 1.85 Ga (Hitzman et al., 2010; Leach et al., 2010) shows that these deposits are unevenly distributed in two periods: 2.1-1.4 Ga (Period I) and 0.8 Ga to present (Period II), with few scattered between these two periods and barely before the Great Oxygenation Event (GOE; Fig.

https://doi.org/10.5194/egusphere-2023-2091
Preprint. Discussion started: 29 January 2024


3 and 6). The Period I occurred following the GOE, which is very significant due to the major changes of the atmosphere, especially the rise of oxygen contents in the atmosphere at around 2.2-2.4 Ga (Catling, 2014). Before the GOE, the surficial water bodies were mainly in a reducing state, and sulfur existed in the form of $S^{2-}$ (e.g., Roscoe, 1969; Prasad and Roscoe, 1996; Williford et al., 2011). The existence of $S^{2-}$ limited the contents of sulfophilic elements (e.g., Cu, Zn, Pb, Fe) in the surficial water bodies. The Fe, S, Zn, Pb and Cu contents in the crust are ~58000 ppm, 200-500 ppm, 60-95 ppm, 10-16 ppm, and ~55 ppm, respectively (Liu et al., 1984). The solubility product of galena is $1\times10^{-29}$, of chalcopyrite is $25\times10^{-36}$, of sphalerite is $8\times10^{-26}$, and of pyrite is $4\times10^{-19}$ (the chemical reaction equations are as follows; Liu et al., 1984). This means that $S^{2-}$ would consume the $Pb^{2+}$ and $Zn^{2+}$ first. In addition, the abundance of sulfur is much higher than that of Pb and Zn. In this situation, it is difficult to accumulate Zn, Pb, and Cu (sulphophile elements) but can accumulate Fe in surficial water bodies.

$Cu^{2+}+Fe^{2+}+2S^{2-}=CuFeS_2$ (↓, $Ksp=25\times10^{-36}$)

$Pb^{2+}+S^{2-}=PbS$ (↓, $Ksp=1\times10^{-29}$)

$Zn^{2+}+S^{2-}=ZnS$ (↓, $Ksp=8\times10^{-26}$)

$Fe^{2+}+S^{2-}+S=FeS_2$ (↓, $Ksp=4\times10^{-19}$)

The solubility of uranium in surficial water is primarily controlled by its oxidation state. Generally, U is more soluble in oxidizing, alkaline, and carbonate-rich water than in acidic, reducing water (Cuney, 2010). This is due primarily to the tendency of $U^{6+}$ to form strong complexes in oxidizing fluids, regardless of the temperature. Before the GOE, Earth's surficial waters were dominantly reducing and acidic, both of which restricted the uranium content in surficial brines at that time (e.g., Fig.6A; Cuney and Kyser, 2008; Kyser, 2014). Therefore, there were barely any basin-related Pb-Zn, Cu, and U deposits before the GOE.

After the GOE, the relatively high oxygen content resulted in the oxidation of surficial waters, and sulfur existed in the form of $SO_4^{2-}$, which was different from the time before the GOE (e.g., Roscoe, 1969; Prasad and Roscoe, 1996; Williford et al., 2011). In this environment, some metals in the surficial saline brines were significantly enriched to an extreme high level, such as Cu (~800 ppm), Zn (lack of $S^{2-}$, locally up to 250 ppm), Pb (lack of $S^{2-}$, locally up to ~100 ppm), and so on (Hagni,

https://doi.org/10.5194/egusphere-2023-2091
Preprint. Discussion started: 29 January 2024


1983; Kharaka et al., 1987; Hacini and Oelkers, 2010; Kharaka and Hanor, 2014; Zhang et al., 2022). This means that metal-fertile saline brines were present on the Earth's surface since this time point, which was the prerequisite for the formation of basin-related Pb-Zn, and Cu deposits. In addition, after the GOE, the surficial brines had the ability to render greater solubilities of uranium by several orders of magnitude (over tens of ppm), particularly when phosphate and carbonate were present (Cuney, 2010; Kyser, 2014). Therefore, basin-related U deposits began to emerge.

The period of 1.9-1.8 Ga was the transformational period from plume-influence tectonics to modern-style plate tectonics (e.g., de Wit, 1998; Goldfarb et al., 2001a, b; Condie, 2002a, 2002b, 2014), and Cordilleran-style tectonics began to dominate Earth by 1.7 Ga (Goldfarb et al., 2010). The start-up of modern-style plate tectonics and the widespread development of evaporite sediments meant the extensive development of hydrological closed basins covered by arid-semi arid climates similar to the Phanerozoic (e.g., Condie, 2005; Warren, 2006, 2010). This is the main reason that the period of 1.8-1.5 Ga was the peak period of basin-related mineralization and characterized by a global basin-related U and Pb-Zn metallogeny (Fig. 3; e.g., Rozendaal, 1980; Rozendaal and Stumpfl, 1984; Bodon, 1998; Chapman, 2004; Stalder and Rozendaal, 2004; Large et al., 2005; Dahlkamp, 2009, 2010, 2016). For the famous U and Pb-Zn districts, contemporaneous saline deposits (direct evidence of the existence of metal-fertile saline brines) were developed in their region, such as the Lower Proterozoic saline giants in Australia, Proterozoic redbeds and saline giants in Canada, Lower Proterozoic saline giants in Papaghni Group of India, Lower Proterozoic redbeds in North China Cratons, and Lower Proterozoic evaporites in Europe (detailed comparison in Appendix A and B, e.g., Pirajno and Grey, 2002; Pope and Grotzinger, 2003; Bekker et al., 2006; Evans, 2006; Aspler and Chiarenzelli, 2002; Walker et al., 1977). Basin-related mineralization could last for tens of millions to hundreds of millions of years within the evolving basins (Brown, 2009; Hitzman et al., 2010), because as long as it was covered by semi-arid climatic environments, there would be (metal-rich oxidizing) saline brines existing in the hydrological closed basins, as well as basin-related mineralization.

In contrast to Period I, the distribution of evaporites and evolution of paleoclimate of the Earth is

https://doi.org/10.5194/egusphere-2023-2091
Preprint. Discussion started: 29 January 2024


relatively well understood (e.g., Prokoph et al., 2013; Godderis et al., 2014; Wang et al., 2020; Scotese et al., 2021), and there is a greater degree of confidence that the semi-arid sediments accompanied the basin-related ore deposits during Period II, which is mainly the Phanerozoic Eon (a detailed comparison is shown in Fig.4 and 5). There are many famous basin-related mineral regions during Period II, such as the Central Massif of France (U-W, 290-260Ma), Bohemian Massif of the Czech Republic (U-W, 290-260Ma), Pyrenees Peninsula (U-W, 290-260Ma), stratiform red-bed hosted Cu–Ag ores of the Permian Kupferschiefer in Poland and Germany, Devonian to Permian and Cretaceous to Paleogene SEDEX and MVT Pb-Zn deposits in the USA, and South China Polymetallic Province (Leach et al., 2005; Zhang et al., 2022). During the mineralization period of these basin-related deposits, they were generally located in semi-arid to arid zones of low to middle latitudes, and accompanied by the development of evaporites (detailed locations are in Zhang et al., 2022).

### 6.4 One Warm, Humid and Flat Era during 1.4-0.8 Ga

The statistical results of basin-related ore deposits show one quiescence period during 1.4-0.8 Ga (Fig. 3). This mineralization gap has been addressed by Meyer (1981, 1988), and is now referred to as the "Boring Billion". During this quiescence period, the saline giants were much less than in Metallogenic Periods I and II, which means the surficial metal-fertile saline brines were also much less than in both periods. There are several possibilities for the cause of this Metallogenic Quiescence Period: I. there were few hydrologically closed basins; II. the climate zoning was weak, and the arid-semi arid climatic zones or "horse latitudes" during this period were relatively small; III. both I and II.

https://doi.org/10.5194/egusphere-2023-2091
Preprint. Discussion started: 29 January 2024


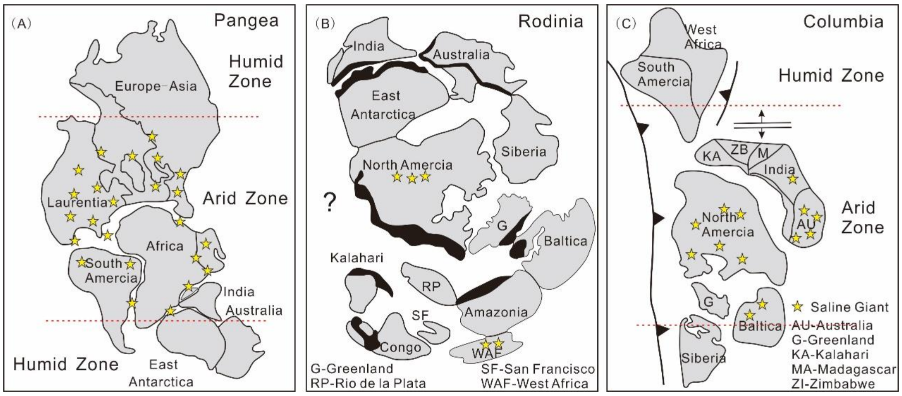


Fig.8 Three supercontinents and the major saline giants in Earth's history: (A) Pangea formed 300-250Ma ago (Rogers et al., 1995); (B) Rodinia formed ~1.0 Ga ago (Dalziel, 1997; Dalziel et al., 2000); and (C) Columbia formed ~1.8Ga ago (Rogers and Santosh, 2002).

For Possibility I, Tang et al. (2021a) proposed that the Earth was in an Orogenic Quiescence Period in its middle age, using a recently calibrated zircon-based crustal thickness proxy (Tang et al., 2021b). The zircon-based crustal thickness proxy uses pressure-sensitive Eu systematics during magmatic differentiation, which is recorded as Eu anomalies in crystallizing zircons (see Tang et al., 2021a, b for details). The reconstructed thickness of active continental crust averaged 50 to 60 km in Metallogenic Periods I and II (Fig. 3J). In contrast, the average thickness of continental crust was smaller than 45 km and even close to 40 km during the metallogenic quiescence period. This thin continental crust suggests that the continents were likely flat and lacked hydrological closed continental basins during the metallogenic quiescence period.

For Possibility No. II, much less saline deposits were reported during the metallogenic quiescence period than Metallogenic Periods I and II (Fig.3 and 8; e.g., Kozary et al., 1968; Boucot et al., 2013). The metallogenic quiescence period witnessed the breakup of the Nuna supercontinent (1.6-1.2 Ga) and the subsequent amalgamation of the Rodinia supercontinent during 1.2 to 0.9 Ga (e.g., Zhao et al., 2002; Roberts, 2013; Cawood et al., 2016). Published evidence suggests that the breakup of Nuna was limited and transitioned to Rodinia with only minor reconfiguration (Bradley, 2008; Cawood and Hawkesworth, 2014; Cawood, 2020). The Rodinia supercontinent consisted of most of

https://doi.org/10.5194/egusphere-2023-2091
Preprint. Discussion started: 29 January 2024


the continents and was characterized by multiple Grenvillian continent–continent collisions (Bradley, 2008). These collision belts are generally located inboard of the supercontinental boundaries (Hoffman, 1991; Condie and Rosen, 1994; Pelechaty, 1996; Frost et al., 1998; Rainbird et al., 1998). Geodynamically, the mainlands were at low to mid latitudes during this period (Robb and Hawkesworth, 2020). In this context, the Earth was probably in a warm and humid greenhouse stage during this gap, which ended with glaciations of ~850-630 Ma, despite a 7-14% reduction in solar output compared to modern during this interval (Fiorella and Sheldon, 2017). Elevated greenhouse gas concentrations have been invoked to explain the warmth of this period, such as high contents of $CO_2$ (10-300 × preindustrial $CO_2$ level, ~280ppmv., Kah and Riding, 2007; Sheldon, 2006; Kanzaki and Murakami, 2015) and/or $CH_4$ (~28-140ppmv., Fiorella and Sheldon, 2017). CIA and Eu/Eu∗ values of the Mesoproterozoic argillites from India and North America signify the intensity of secular weathering similar to CIA values for the Orinoco, Nile, and Amazon (Bose et al., 2008). These sedimentary researches also suggest that the Earth was generally in a hot, wet climate and the mainlands were experiencing aggressive chemical weathering during the basin-related metallogenic gap, since Proterozoic rivers had less sediment residence times due to a lack of vegetation cover and hydrological closed basins (Bose et al., 2008). This warm and humid climate was also supported by the fact that Grenvillian-aged zircon grains are everywhere, which means the sediments during this period were laid down by a colossal river system that emanated from the same Grenvillian mountain chain (Rainbird and Young, 2009). Such river systems may have covered a large part of the supercontinent Rodinia (Rainbird and Young, 2009). In this context, there were barely any hydrological closed basins.

The climatic conditions can also be roughly estimated by the life on Earth. During the period of the Precambrian, stromatolites were the most prominent and widespread life forms, as suggested by the widely preserved Precambrian benthic microbial carbonates (Walter, 1994). Several ecological factors combine to permit stromatolite formation and preservation, regardless of geologic age (Pratt, 1982). These include sufficient light and oxygen, and favorable water temperature and chemistry (Peters et al., 2017). The constraints of oxygen concentrations during the Proterozoic were poor, but were estimated to be within 1-10% of today's value (e.g., Buick et al., 1995; Canfield, 2014). The

https://doi.org/10.5194/egusphere-2023-2091
Preprint. Discussion started: 29 January 2024


Sun was about 85% of its present value at 2.2 Ga, and was gradually getting brighter to 95% at the Late Precambrian. Therefore, the light and oxygen can be regarded as stable factors. The water temperature and chemistry are the remaining major factors, which could influence the stromatolites' abundance and diversity.

Two categories of abundance data have been compiled for the stromatolites since GOE (Walter, 1994). Morphotype diversity data counts the number of stromatolite form taxa through time. Forms are based on macroscopic features such as external shape and internal lamina arrangement (Awramik, 1971; Walter and Heys, 1985; Awramik and Sprinkle, 1999; Semikhatov and Raaben, 2000). Stromatolites increased in abundance from the Paleoproterozoic to ~1450Ma ago, at the beginning of the basin-related metallogenic gap, and then rapidly increased to a peak between ~1350Ma and 1100Ma ago. An irregular decline from the peak occurred between ~900 and ~700Ma ago, corresponding to the global glaciation of the Cryogenian and also the end of the basin-related metallogenic quiescence period. In addition, the stromatolites diversity shows similar variation characteristics to the stromatolites abundance (Fig.3; Walter and Heys, 1985; Sheldon, 2013), with the stromatolite diversity increasing rapidly at about ~1.4 Ga and reaching a peak at about ~1350Ma. After the peak, the stromatolite diversity declined gradually to 550 Ma ago. The stromatolite diversity of the basin-related quiescence period was generally at least two times that of metallogenic period I (Fig.3). After the Precambrian biological explosion, the stromatolites were restricted to locations where the activity of metazoans was limited, so the stromatolites abundance and diversity of the Phanerozoic were not used to reflect the climate conditions (Awramik and Sprinkle, 1999). The peak of stromatolites diversity and abundance during 1.4-0.8 Ga suggests that there should have been widely developed shallow marine environments on the continents at middle and low latitudes. The environments were unfavorable for the formation of saline brines on the continents and their margins (Fig.8). Therefore, this Metallogenic Quiescence Period was probably caused by the combination of the lack of hydrological closed basins and a relatively warm and humid climate during 1.4-0.8 Ga.

## 7. Conclusion

https://doi.org/10.5194/egusphere-2023-2091
Preprint. Discussion started: 29 January 2024


For the basin-related ore deposits, the ore-forming fluids were probably metal-rich saline brines formed in hydrologically closed basins. These saline brines usually exist in the form of saline lakes and mainly develop in arid to semi-arid environments. The main influence on the formation of these brines is evaporation, which is the primary or only way for water to leave the convergent area. Therefore, climate is an important factor influencing global metallogeny.

The statistical results of basin-related mineral deposits worldwide show that there are two metallogenic periods after the great oxidation event: 2.1-1.4Ga (Period I) and 0.8Ga to present (Period II), with a few scattered between these two periods (the metallogenic gap period). In addition, Metallogenic Period II has five metallogenic peaks: ~380-340Ma (II-1), ~300-240Ma (II-2), ~160-100Ma (II-3), 60-40Ma (II-4), and one stratiform Cu metallogenic concentration period of ~580-500Ma (II-5). These two metallogenic periods and five metallogenic peaks are coupled with the widespread development of saline deposits in time and space. The metallogenic quiescence period corresponded to the scarcity of saline deposits, and was probably caused by the combination of the lack of hydrologically closed basins and arid to semi-arid environments during 1.4-0.8 Ga.

## Acknowledgement

The authors thank Dr. Junxian Wang for his helpful comments.

## Author contributions

Chuang Zhang wrote the paper and drafted the figures.

## Competing interests

The author has declared that there isn't any competing interests.

## Financial support

This research has been supported by the Uranium Exploration Projects (Grant No. 22045004) of China National Nuclear Corporation.

## Reference

Abramov, B.N.: Petrochemistry of the Paleoproterozoic Udokan copper-bearing sedimentary complex. Lithol. Miner. Resour., 43, 37-43, doi: 10.1134/S0024490208010033, 2008.

Abrantes, Jr.F.R., Nogueira, A.C.R., de Andrade, L.S., Bandeira, J., Soares, J.L., Medeiros, R.S.P.: Register of increasing continentalization and palaeoenvironmental changes in the west-central Pangaea during the Permian-Triassic, Parnaíba Basin, Northern Brazil. J. South Am. Earth Sci., 93, 294-312, doi: 10.1016/j.jsames.2019.05.006, 2019.

Allen, P.A., and Hoffman, P.F.: Extreme winds and waves in the aftermath of a Neoproterozoic glaciation. Nature, 433 (7022), 123–127, doi: 10.1038/nature03176, 2005.

Almendinger, J.E.: Groundwater control of closed–basin lake levels under steady-state conditions. J. Hydrol., 112 (3-4), 293–318, doi: 10.1016/0022-1694(90)90020-X, 1990.

An, Z.S., Sun, Y.B., Chang, H., Zhang, P.Z., Liu, X.D., Cai, Y.J., Jin, Z.D., Qiang, X.K., Zhou, W.J., Li, L., Shi, Z.G., Tan, L.C., Li, X.Q., Zhang, X.B., Jin, Z.: Late Cenozoic Climate Change in Monsoon-Arid Asia and Global Changes. In: An, Z.S. (Ed.), Late Cenozoic Climate Change in Asia - Loess, Monsoon and Monsoon-arid Environment Evolution. Springer, Netherlands, pp. 491–582, doi: 10.1007/978-94-007-7817-7_6, 2014.

Anagnostou, E., John, E.H., Edgar, K.M., Foster, G.L., Ridgwell, A., Inglis, G.N., Pancost, R.D., Lunt, D.J., Pearson, P.N.: Changing atmospheric $CO_2$ concentration was the primary driver of early Cenozoic climate. Nature, 533 (7603), 380–384, doi: 10.1038/nature17423, 2016.

Anderson, H.E., Davis, D.W.: U-Pb geochronology of the Moyie sills, Purcell Supergroup, southeastern British Columbia: Implications for the Mesoproterozoic geologic history of the Purcell (Belt) basin. Can. J. Earth Sci., v. 32, p. 1180–1193, doi: 10.1139/e95-097, 1995.

https://doi.org/10.5194/egusphere-2023-2091
Preprint. Discussion started: 29 January 2024



Anfort, S.J., Bachu, S., Bentley, L.R.: Regional-scale hydrogeology of the Upper Devonian–Lower Cretaceous sedimentary succession, south-central Alberta basin, Canada. AAPG Bulletin, 85, 637-660, doi: 10.1016/S0927-0248(00)00249-X, 2001.

Arnon, A., Brenner, S., Selker, S.J., Gertman, I., Lensky, N.G.: Seasnonal dynamics of internal waves governed by stratification stability and wind: Analysis of highresolution observations from the Dead Sea. Limnol. Oceanogr., 9999, 1–19, doi: 10.1002/lno.11156, 2019.

Arthurton, R.S., Hemingway, J.E.: The St. Bees Evaporites-A carbonate-evaporite formation of Upper Permian age in West Cumberland, England. Proc. Yorks. geol. SOC., 38, 565, doi: 10.1144/pygs.38.4.565, 1972.

Aspler, L.B., Chiarenzelli, J.R.: Mixed siliciclastic-carbonate storm-dominated ramp in a rejuvenated Palaeoproterozoic intracratonic basin: Upper Hurwitz Group, Nunavut, Canada. In: Altermann, W., Corcoran, P.L. (eds.) Precambrian Sedimentary Environments: A Modern Approach to Ancient Depositional Systems. Spec. Public. Int. Assoc. Sedimentol., 33, 293–321. UK: Blackwell Science, 2002.

Awramik, S.M.: Precambrian columnar stromatolite diversity: reflection of metazoan appearance. Science, 174, 825–827, doi: 10.1126/science.174.4011.825, 1971.

Awramik, S.M., Sprinkle, J.: Proterozoic stromatolites: the first marine evolutionary biota. Hist. Biol., 13, 241–253, doi: 10.1080/08912969909386584, 1999.

Bąbel, M., Schreiber, B.C.: Geochemistry of evaporites and evolution of Seawater. In: Holland, H.D., Turekian, K.K. (Eds.) Treatise on Geochemistry 9, Elsevier, Oxford, pp. 484–548, doi: 10.1016/B978-0-08-095975-7.00718-X, 2014.

Badham, J.P.N.: Shale-hosted Pb-Zn deposits: Products of exhalation of formation waters? T. Ins. Mini. Metallur., sec. B, 90, B70–B76, 1981.

Bain, D.C., Mellor, A., Robertson-Rintoul, M.S.E., Buckland, S.T.: Variations in weathering processes and rates with time in a chronosequence of soils from Glen Feshie, Scotland. Geoderma, 57(3), 275-293, doi: 10.1016/0016-7061(93)90010-I, 1993.

Balkwill, R.H.: Evolution of Sverdrup Basin, Arctic Canada. AAPG Bulletin, 62, 1004-1028, doi: 10.1306/C1EA4F86-16C9-11D7-8645000102C1865D, 1978.

Barley, M.E., Groves, D.I.: Supercontinent cycles and distribution of metal deposits through time. Geology, 20, 291–94, doi: 10.1130/0091-7613(1992)020<0291:SCATDO>2.3.CO;2, 1992.

Barley, M.E., Krapez, B., Groves, D.I., Kerrich, R.: The late Archaean bonanza: metallogenic and environmental consequences of the interaction between mantle plumes, lithospheric tectonics and global cyclicity. Precambrian Res., 91, 65–90, doi: 10.1016/S0301-9268(98)00039-4, 1998.

Barrett, T.J., Jarvis, I., Hannington, M.D., Thirlwall, M.F.: Chemical characteristics of modern deep-sea metalliferous sediments in closed versus open basins, with emphasis on rare-earth elements and Nd isotopes. Earth-Sci. Rev., 222, 103801, doi: 10.1016/j.earscirev.2021.103801, 2021.

Barth, S.R.: Stable isotope geochemistry of sediment-hosted groundwater from a Late Paleozoic–Early Mesozoic section in central Europe. J. Hydrol., 235, 72-87, doi: 10.1016/S0022-1694(00)00264-X, 2000.

Barton, M.D.: Iron Oxide(–Cu–Au–REE–P–Ag–U–Co) Systems. In: Holland, H.D., Turekian, K.K. (Eds.) Treatise on Geochemistry 13, 515–536. Elsevier, Oxford, doi: 10.1016/B978-0-08-095975-7.01123-2, 2014.

Barton, M.D., Johnson, D.A.: Evaporitic source model for igneous-related Fe oxide–(REE–Cu–Au–U) mineralization. Geology, 24, 259–262, doi: 10.1130/0091-7613(1996)0242.3.CO;2, 1996.

Bartov, Y., Stein, M., Enzel, Y., Agnon, A., Reches, Z.: Lake Levels and Sequence Stratigraphy of Lake Lisan, the Late Pleistocene Precursor of the Dead Sea. Quatern. Res., 57, 9-21, doi: 10.1006/qres.2001.2284, 2002.

Basuki, N.I., Spooner, E.T.C.: A review of fluid inclusion temperatures and salinities in Mississippi Valley-type Zn-Pb deposits: Identifying thresholds for metal transport. Explor. Mining Geol., v. 11, p. 1–17, doi: 10.2113/11.1-4.1, 2004.

Bekker, A., Holland, H.D.: Oxygen overshoot and recovery during the early Paleoproterozoic. Earth Planet. Sci. Lett., 317–318, 295–304, doi: 10.1016/j.epsl.2011.12.012, 2012.

https://doi.org/10.5194/egusphere-2023-2091
Preprint. Discussion started: 29 January 2024


Bekker, A., Karhu, J.A., Kaufman, A.J.: Carbon isotope record for the onset of the Lomagundi carbon isotope excursion in the Great Lakes area, North America. Precambrian Res., 148, 145–180, doi: 10.1016/j.precamres.2006.03.008, 2006.

Bekker, A., Slack, F.J., Planavsky, N., Krapez, B., Hofmann, A., Konhauser, O.K., Rouxel, J.O.: Iron Formation: The Sedimentary Product of a Complex Interplay among Mantle, Tectonic, Oceanic, and Biospheric Processes. Econ. Geol., 105, 467-508, doi: 10.2113/gsecongeo.105.3.467, 2010.

Bell, C.M., Suarez, M.: The depositional environments and tectonic development of a Mesozoic intra-arc basin, Atacama Region, Chile. Geol. Mag., 130, 417-430, doi: 10.1017/S0016756800020501, 1993.

Benison, K.C., Goldstein, R.H., Wopenka, B., Burruss, R.C., Pasteris, J.D.: Extremely acid Permian lakes and ground waters in North America. Nature, 392, 911-914, doi: 10.1038/31917, 1998.

Berner, R.A.: GEOCARB II: A revised model of atmospheric $CO_2$ over Phanerozoic time. Am. J. Sci. 294 (1), 56–91, doi: 10.2475/ajs.294.1.56, 1994.

Berner, R.A.: Examination of hypothesis for the Permo-Triassic boundary extinction by carbon cycle modeling. P. Nati. Acad. Sci. USA 99, 4172–4177, doi: 10.1073/pnas.032095199, 2002.

Berner, R.A., Berner, E.K.: Silicate weathering and climate. In Ruddiman et al. (eds) Tectonic uplift and climate change. Springer, Boston, MA, 353-365, doi: 10.1007/978-1-4615-5935-1_15, 1997.

Bhattacharya, H.N., Bull, S.: Tectono-sedimentary setting of the Paleoproterozoic Zawar Pb–Zn deposits, Rajasthan, India. Precambrian Res., 177, 323-338, doi: 10.1016/j.precamres.2010.01.004, 2010.

Blum, J.D.: The effect of late Cenozoic glaciation and tectonic uplift on silicate weathering rates and the marine 87Sr/86Sr record. In Ruddiman et al. (eds) Tectonic uplift and climate change. Springer, Boston, MA, 259-288, doi: 10.1007/978-1-4615-5935-1_11, 1997.

Blumenschine, R.J., Masao, F.T., Stollhofen, H., Stanistreet, I.G., Bamford, M.K., Albert, R.M., Njau, J.K., Prassack, K.A.: Landscape distribution of Oldowan stone artifact assemblages across the fault compartments of the eastern Olduvai Lake Basin during early lowermost Bed II times. J. Hum. Evol. 63 (2), 384–394, doi: 10.1016/j.jhevol.2011.05.003, 2012.

https://doi.org/10.5194/egusphere-2023-2091
Preprint. Discussion started: 29 January 2024


Bodon, S.B.: Paragenetic relationships and their implications for ore genesis at the Cannington Ag-Pb-Zn deposit, Mt. Isa inlier, Queensland, Australia. Econ. Geol., 93, 1463–1489, doi: 10.2113/gsecongeo.93.8.1463, 1998.

Boehrer, B., Schultze, M.: Stratification of lakes. Rev. Geophys. 46, 2006RG000210, 1–27, doi: 10.1029/2006rg000210, 2008.

Bose, K.P., Sarkar, S., Mukhopadhyay, S., Saha, B., Eriksson, P.: Precambrian basin-margin fan deposits: Mesoproterozoic Bagalkot Group, India. Precambrian Res., 162, 264-283, doi: 10.1016/j.precamres.2007.07.022, 2008.

Bostrom, K., Rydell, H., Joensuu, O.: Langban-An Exhalative Sedimentary Deposits? Econ. Geol., 74, 1002-1011, doi: 10.2113/gsecongeo.74.5.1002, 1979.

Bosworth, W., Huchon, P., McClay, K.: The Red Sea and Gulf of Aden Basins. J. Afr. Earth Sci., 43, 334–378, doi: 10.1016/j.jafrearsci.2005.07.020, 2005.

Boucot, A.J., Xu, C., Scotese, C.R.: Phanerozoic Paleoclimate: An Atlas of Lithologic Indicators of Climate. SEPM Concepts in Sedimentology and Paleontology, (Print-on-Demand Version), 11, 478. Soc. Sediment. Geol, Tulsa, OK, doi: 10.2110/sepmcsp.11, 2013.

Bourquin, S., Bercovici, A., López-Gómez, J., Diez, J.B., Broutin, J., Ronchi, A., Durand, M., Arché, A., Linol, B., Amour, F.: The Permian–Triassic transition and the onset of Mesozoic sedimentation at the northwestern peri-Tethyan domain scale: Palaeogeographic maps and geodynamic implications. Palaeogeogr. Palaeocl., 299, 265-280, doi: 10.1016/j.palaeo.2010.11.007, 2011.

Bradley, D.C.: Passive margins through earth history. Earth-Sci. Rev., 91(1-4), 1-26, doi: 10.1016/j.earscirev.2008.08.001, 2008.

Bradley, D.C., Leach, D.L.: Tectonic controls of Mississippi Valley-type lead-zinc mineralization in orogenic forelands. Miner. Deposita, 38, 652-667, doi: 10.1007/s00126-003-0355-2, 2003.

Brasier, A.T., Fallick, A.E., Prave, A.R., Melezhik, V.A., Lepland, A., FAR-DEEP Scientists: Coastal sabkha dolomites and calcitised sulphates preserving the Lomagundi-Jatuli carbon isotope signal. Precambrian Res., 189, 193–211, doi: 10.1016/j.precamres.2011.05.011, 2011.

Brown, A.C.: Zoning in the White Pine copper deposit, Ontonogan County, Michigan. Econ. Geol., 66, 543–573, doi: 10.2113/gsecongeo.66.4.543, 1971.

https://doi.org/10.5194/egusphere-2023-2091
Preprint. Discussion started: 29 January 2024


Brown, A.C.: Sediment-hosted copper deposits: Deposit-type name and related terminology. Geol. Assoc. Can. Spec. Paper, 36, p. 39–52, doi: 10.1016/0926-9851(92)90063-g, 1989.

Brown, A.C.: Sediment-hosted stratiform copper deposits. Geosci. Can., 19, 125–141, 1992.

Brown, A.C.: Sediment-hosted stratiform copper deposits. Geol. Assoc. Can. Geosci. Reprint Ser., 6, 99–116, doi: 10.1007/978-94-011-3925-012, 1993.

Brown, A.C.: World-class sediment-hosted stratiform copper deposits: Characteristics, genetic concepts and metallotects. Aust. J. Earth Sci., 44, 317–328, doi: 101080/08120099708728315, 1997.

Brown, A.C.: A process-based approach to estimating the copper derived from red beds in the sediment-hosted stratiform copper deposit model. Econ. Geol., 104, 857–868, doi: 10.2113/gsecongeo.104.6.857, 2009.

Brune, S., Williams, S.E., Müller, R.D.: Potential links between continental rifting, CO2 degassing and climate change through time. Nat. Geosci., 10 (12), 941–946, doi: 10.1038/s41561-017-0003-6, 2017.

Burke, K.: Atlantic evaporites formed by evaporation of water spilled from Pacific, Tethyan, and Southern oceans. Geology, 3, 613-617, doi: 10.1130/0091-7613(1975)3<613:aefbeo>2.0.co;2, 1975.

Cameron, E.M.: Evidence from early Proterozoic anhydrite for sulphur isotopic partitioning in Precambrian oceans. Nature, 304, 54–56, doi: 10.1038/304054a0, 1983.

Carpenter, A.B., Trout, M.L., Pickett, E.E.: Preliminary report on the origin and chemical evolution of lead- and zinc-rich brines in central Mississippi. Econ. Geol., 69, 1191–1206, doi: 10.2113/gsecongeo.69.8.1191, 1974.

Carroll, A.R., Bohacs, K.M.: Stratigraphic classification of ancient lakes: Balancing tectonic and climatic controls. Geology, 27 (2), 99-102, doi: 10.1130/0091-7613(1999)0272.3.CO;2, 1999.

Catling, D.C.: The great oxidation event transition. In: Holland, H.D., Turekian, K. K. (Eds.), Treatise on Geochemistry 7, Elsevier, Oxford, pp. 177–193, doi: 10.1016/b978-0-08-095975-7.01307-3, 2014.

Caves, J.K.: The Cenozoic climatic and tectonic history of Asia. A dissertation submitted to Stanford University for the degree of Doctor of Philosophy, 2016.

https://doi.org/10.5194/egusphere-2023-2091
Preprint. Discussion started: 29 January 2024


Cawood, P.A.: Earth Matters: A tempo to our planet's evolution. Geology, 48(5), 525-526, doi: 10.1130/focus052020.1, 2020.

Cawood, P.A., Hawkesworth. C.J.: Earth's middle age. Geology, 42(6), 503-506, doi: 10.1130/g35402.1, 2014.

Cawood, P.A., Strachan, R.A., Pisarevsky, S.A., Gladkochub, D.P., Murphy, J.B.: Linking collisional and accretionary orogens during Rodinia assembly and breakup: Implications for models of supercontinent cycles. Earth Planet. Sci. Lett., 449, 118-126, doi: 10.1016/j.epsl.2016.05.049, 2016.

Cerling, T.E.: Pore water chemistry of an alkaline lake: Lake Turkana. In: Johnson, C., Odada, E.O. (Eds.), The Limnology, Climatology, and Paleoclimatology of the East African Lakes. Gordon and Breach Science, Amsterdam, pp. 225–240, doi: 10.1201/9780203748978-12, 1996.

Chapman, L.H.: Geology and mineralization styles of the George Fisher Zn-Pb-Ag deposit, Mount Isa, Australia. Econ. Geol., 99, 233–256, doi: 10.2113/gsecongeo.99.2.233, 2004.

Chen, J., Liu, D.Y., Peng, P.A., Chen, N., Hou, X.L., Zhang, B.S., Xiao, Z.Y.: Iodine-129 chronological study of brines from an Ordovician paleokarst reservoir in the Lunnan oilfield, Tarim Basin. Appl. Geochem., 65, 14-21, doi: 10.1016/j.apgeochem.2015.10.012, 2016.

Chi, G., Haid, T., Quirt, D., Fayek, M., Blamey, N., Chu, H.: Petrography, fluid inclusion analysis and geochronology of the End uranium deposit, Kiggavik, Nunavut. Canada. Miner. Deposita, 52 (2), 211–232, doi: 10.1007/s00126-016-0657-9, 2017.

Chi, G., Li, Z.H., Chu, H., Bethume, K.M., Quirt, D.H., Ledru, P., Normand, C., Card, C., Bosman, S., Davis, W.J., Potter, E.G.: A Shallow-Burial Mineralization Model for the Unconformity-Related Uranium Deposits in the Athabasca Basin. Econ. Geol., 113, 1209-1217, doi: 10.5382/gecongeo.2018.4588, 2018.

Cody, R.D., Anderson, R.R., McKay, R.M.: Geology of the Fort Dodge Formation (Upper Jurassic) Webster County, Iowa. Iowa Geological Survey Bureau Guide book Series No.19, 74 p., doi: 10.17077/2160-5270.1271, 1997.

Coffin, M.F., Eldholm, O.: Large igneous provinces: crustal structure, dimensions, and external consequences. Rev. Geophys., 32 (1), 1, doi: 10.1029/93RG02508, 1994.

https://doi.org/10.5194/egusphere-2023-2091
Preprint. Discussion started: 29 January 2024


Coffin, M.F., Eldholm, O.: Large Igneous Provinces. Encyclopedia of geology, 315-323, doi: 10.1016/b0-12-369396-9/00455-X, 2005.

Coltice, N., Phillips, B.R., Bertrand, H., Ricard, Y., Rey, P.: Global warming of the mantle at the origin of flood basalts over supercontinents. Geology, 35 (5), 391., doi: 10.1130/G23240A.1., 2007.

Condie, K.C.: The supercontinent cycle: Are there two patterns of cyclicity? J. Afr. Earth Sci., 35, 179–183, doi: 10.1016/s0899-5362(02)00005-2, 2002a.

Condie, K.C.: Continental growth during a 1.9-Ga superplume event. J. Geodyn., 34, 249–264, doi: 10.1016/s0264-3707(02)00023-6, 2002b.

Condie, K.C.: Earth as an evolving planetary system. Amsterdam, Elsevier, 447 p, doi: 10.1016/b978-012088392-9/50001-3, 2005.

Condie, K.C.: Growth of continental crust: a balance between preservation and recycling. Miner. Mag., 78, 623-637, doi: 10.1180/minmag.2014.078.311, 2014.

Cooke, D.R., Bull, S.W., Large, R.R., McGoldrick, P.J.: The importance of oxidized brines for the formation of Australian Proterozoic stratiform sediment-hosted Pb-Zn (Sedex) deposits. Econ. Geol., 95, 1-18, doi: 10.2113/gsecongeo.95.1.1, 2000.

Courtillot, V.E., Renne, P.R.: On the ages of flood basalt events. C.R. Geosci., 335 (1), 113–140, doi: 10.1016/s1631-0713(03)00006-3, 2003.

Cox, D.P., Lindsey, D.A., Singer, D.A., Diggles, M.F.: Sediment hosted copper deposits of the world: Deposit models and database. USGS Open-File Report 03-107, 50 p, doi: 10.3133/ofr2003107, 2003.

Cox, S.F., Braun, J., Knackstedt, M.A.: Principles of structural control on permeability and fluid flow in hydrothermal systems. Rev. Econ. Geol. 14, 1–24, doi: 10.5382/rev14.01, 2001.

Cox, S.F., Knackstedt, M.A.: Ore genesis in fracture–controlled hydrothermal systems: percolation theory approaches. PACRIM'99, doi: 10.5382/rev.21.02, 1999.

Cox, S.F., Wall, V.J., Etheridge, M.A., Potter, T.F.: Deformational and metamorphic processes in the formation of mesothermal vein–hosted gold deposits – examples from the Lachlan fold belt in central Victoria. Australia. Ore Geol. Rev., 6 (5), 391–423, doi: 10.1016/0169-1368(91)90038-9, 1991.

https://doi.org/10.5194/egusphere-2023-2091
Preprint. Discussion started: 29 January 2024


Cuney, M.: Evolution of uranium fractionation processes through time: driving the secular variation of uranium deposit types. Econ. Geol., 105 (3), 553–569, doi: 102113/gsecongeo.105.3.553, 2010.

Cuney, M.: Uranium and thorium: The extreme diversity of the resources of the world's energy minerals. In: Sinding-Larsen, R., Wellmer, F.-W. (Eds.), NonRenewable Resource Issues: Geoscientific and Societal Challenges, International Year of Planet Earth, Springer, 91-129, doi: 10.1007/978-90-481-8679-2_6, 2011.

Cuney, M.: Uranium and thorium resources and sustainability of nuclear energy. In: Burns, P., Sigmon, G. (Eds.), Uranium: Cradle to Grave. Mineral. Assoc. Can., Short Course Ser. 43, 15, 417–438, doi: 10.3749/9780921294689.ch15, 2013.

Cuney, M.: Felsic magmatism and uranium deposits. Bulletin De La Societe Geologique De France, 185, 75-92. Bruneton, doi: 10.2113/gssgfbull.185.2.75, 2014.

Cuney, M.: Geology of uranium deposits. In "Uranium for Nuclear Power. Resources, Mining and Transformation to Fuel". Edt. Ian Hore Lacy. Elsevier. 488, doi: 10.1016/b978-0-08-100307-7.00002-8, 2016.

Cuney, M., Emetz, A., Mercadier, J., Mykchaylov, V., Shunko, V., Yuslenko, A.: Uranium deposits associated with Na-metasomatism from central Ukraine: A review of some of the major deposits and genetic constraints. Ore Geol. Rev., 44, 82–106, doi: 10.1016/j.oregeorev.2011.09.007, 2012.

Cuney, M., Kyser, K.: Recent and not–So–Recent developments in uranium deposits and implications for exploration. Quebec, Mineral. Assoc. Can. Short course ser., 39, 161–223, doi: 10.2113/gsecongeo.104.4.600, 2008.

Cuney, M., Mathieu, R.: Extreme light rare earth element mobilization by diagenetic fluids in the geological environment of the Oklo natural reactor zones, Franceville basin, Gabon. Geology, 28, 743-746, doi: 10.1130/0091-7613(200002830743:elreem>2.3.co;2, 2000.

Dahlkamp, F.J. (Ed.): Uranium Deposits of the World (Asia). Springer Berlin Heidelberg, Berlin, Heidelberg, doi: 10.1007/978-3-540-78558-3_19, 2009.

Dahlkamp, F.J. (Ed.): Uranium Deposits of the World (USA and Latin America). Springer, Berlin, Heidelberg, doi: 101007/978-3-540-78943-7, 2010.

https://doi.org/10.5194/egusphere-2023-2091
Preprint. Discussion started: 29 January 2024


Dahlkamp, F.J. (Ed.): Uranium Deposits of the World (Europe). Springer, Berlin, Heidelberg. 2016.

Dalziel, I.W.D.: Neoproterozoic–Paleozoic geography and tectonics: review, hypothesis, environmental speculation. GSA Bulletin, 108, 16–42. , doi: 10.1130/0016-7606(1997)109<0016:onpgat>2.3.co;2, 1997.

Dalziel, I.W.D., Mosher, S., Gahagan, L.M.: Laurentia–Kalahari collision and the assembly of Rodinia. J. Geol., 108, 499–513, doi: 10.1086/314418, 2000.

Darnell, W.L., Staylor, W.F., Gupta, S.K., Ritchey, N.A., Wilber, A.C.: Seasonal variation of surface radiation budget derived from international satellite cloud climatology project C1 data. J. Geophys. Res., 97, 15741-15760, doi: 10.1029/92jd00675, 1992.

Davis, A.D., Rahn, P.H.: Karstic gypsum problems at waste water stabilization sites in the Black Hills of South Dakota. Carbonate Evaporite, 12, 73-80, doi: 101007/bf03175804, 1997.

de Wit, M.J.: On Archean granites, greenstones, cratons and tectonics: Does the evidence demand a verdict? Precambrian Res., 91, 181-227, doi: 10.1016/s0301-9268/98100043-6, 1998.

Dean, W.E., Johnson, K.S.: Anhydrite deposits of the United States and characteristics of anhydrite important for storage of radioactive wastes. USGS Professional Paper, 1794, 132 p, doi: 10.3133/b1794, 1989.

Deocampo, D.M., Jones, B.F.: Geochemistry of Saline Lakes. In: Holland, H.D., Turekian, K.K. (Eds.), Treatise on Geochemistry 7, Elsevier, Oxford, pp. 437–469, doi: 10.1016/b978-0-08-095975-7.00515-5, 2014.

Derry, L.A., France-Lanord, C.: Himalayan weathering and erosion fluxes: climate and tectonic controls. In Ruddiman et al. (eds) Tectonic uplift and climate change. Springer, Boston, MA, 289-312, doi: 10.1007/978-1-4615-5935-1 12, 1997.

Diaz, G.C.: The Cenozoic saline deposits of the Chilean Andes Between 18"00' and 27*00' South Lattitude. In Bahlburg, H., Breitkreuz, Ch., Giese, P., (Eds.) Lecture Notes in Earth Sciences, 17, 137-151, doi: 101007/bfb0045179, 1988.

Doelling, H.H.: Geology of Salt Valley anticline and Arches National Parle, Grand County, Utah. Utah Geol. Miner. Sur. Bulletin, 122, 58, doi: 10.3133/b863, 1988.

https://doi.org/10.5194/egusphere-2023-2091
Preprint. Discussion started: 29 January 2024


Dolníˇcek, Z., Fojt, B., Prochaska, W., Kuˇcera, J., Sulovský, P.: Origin of the Z´ alesí U-Ni–Co–As–Ag/Bi deposit, Bohemian Massif, Czech Republic: fluid inclusion and stable isotope constraints. Miner. Deposita, 44 (1), 81–97, doi: 101007/s00126-008-0202-6, 2009.

Dolníˇcek, Z., Ren´ e, M., Hermannova, ´S., Prochaska, W.: Origin of the Okrouhl´ a Radounˇ episyenite-hosted uranium deposit, Bohemian Massif, Czech Republic: fluid inclusion and stable isotope constraints. Miner. Deposita, 49 (4), 409–425, doi: 10.1007/s00126-013-0500-5, 2014.

Domagalski, J.L., Eugster, H.P., Jones, B.F.: Trace metal geochemistry of Walker, Mono, and Great Salt Lakes. In: Spencer, R.J., Chou, I.M. (Eds.), Fluid–Mineral Interactions: A Tribute to H.P. Eugster, Special Public., 2, 315–354. San Antonio, TX: Geochemical Society, doi: 10.1016/0016-7037(89)90163-4, 1990.

Donnadieu, Y., Godderis, Y., Bouttes, N.: Exploring the climate impact of the continental vegetation on the Mesozoic atmospheric CO2 and climate history. Clim. Past, 4, 2012–11045, doi: 10.5194/cp-5-85-2009, 2008.

Duan, X.X., Zeng, Q.D., Wang, Y.B., Zhou, L.L., Chen, B.: Genesis of the Pb− Zn deposits of the Qingchengzi ore field, eastern Liaoning, China: Constraints from carbonate LA− ICPMS trace element analysis and C–O–S–Pb isotopes. Ore Geol. Rev., 89, 752-771, doi: 10.1016/j.oregeorev.2017.07.012, 2017.

Dugamin, E.J.M., Richard, A., Cathelineau, M., Boiron, M-C., Despinois, F., Brisset, A.: Groundwater in sedimentary basins as potential lithium resource: a global prospective study. Sci. Rep., 11, 21091, doi: 10.1038/s41598-021-99912-7, 2021.

Elliott, W.C., Aronson, L.J.: The timing and extent of illite formation in Ordovician K-bentonites at the Cincinnati Arch, the Nashville Dome and north-eastern Illionis basin. Basin Res., 5, 125-135, doi: 10.1111/j.1365-2117.1993.tb00061.x, 1993.

El-Tabakh, M., Grey, K., Pirajno, F., Schreiber, B.C.: Pseudomorphs after evaporitic minerals interbedded with 2.2 Ga stromatolites of the Yerrida Basin, Western Australia: origin and significance. Geology, 27, 871–874, doi: 10.1130/0091-7613(1999)027<0871:PAEMIW>2.3.CO;2, 1999.

https://doi.org/10.5194/egusphere-2023-2091
Preprint. Discussion started: 29 January 2024


El-Tabakh, M., Mory, A., Schreiber, B.C., Yasin, R.: Anhydrite cements after dolomitization of shallow marine Silurian carbonates of the Gascoyne Platform, Southern Carnarvon Basin, Western Australia. Sediment. Geol., 164, 75-87, doi: 10.1016/j.sedgeo.2003.09.003, 2004.

Engle, M.A., Reyes, F.R., Varonka, M.S., Orem, W.H., Ma, L., Ianno, A.J., Schell, T.M., Xu, P., Carroll, K.C.: Geochemistry of formation waters from the Wolfcamp and "Cline" shales: Insights into brine origin, reservoir connectivity, and fluid flow in the Permian Basin, USA. Chem. Geol., 425, 76-92, doi: 10.1016/j.chemgeo.2016.01.025, 2016.

Ernst, R.E.: Large Igneous Provinces. Cambridge University Press, Cambridge, UK, p. 653, doi: 10.1017/cbo9781139025300, 2014.

Ernst, R.E., Buchan, K.L.: Large mafic magmatic events through time and links to mantle-plume heads. Geol. Soc. Am. Spec. Pap. 352, 483–575, doi: 10.1130/0-8137-2352-3.483, 2001.

Ernst, R.E., Jowitt, S.M.: Large igneous provinces (LIPs) and metallogeny. Soc. Econ. Geol. Spec. Public., 17, 17-51, doi: 105382/sp17.02, 2013.

Ernst, R.E., Youbi, N.: How Large Igneous Provinces affect global climate, sometimes cause mass extinctions, and represent natural markers in the geological record. Palaeogeogr. Palaeocl. 478, 30–52, doi: 10.1016/j.palaeo.2017.03.014, 2017.

Ervin, C.P., McGinnis, D.L.: Reelfoot Rift: Reactivated Precursor to the Mississippi Embayment. GSA Bulletin, 86, 1287-1295, doi: 10.1130/0016-7606(1975)86<1287:rrrptt>2.0.co;2, 1975.

Evans, D.A.D.: Proterozoic low orbital obliquity and axial-dipolar geomagnetic field from evaporite palaeolatitudes. Nature, 444, 51–55, doi: 10.1038/nature05203, 2006.

Evans, K.V., Aleinikoff, J.N., Obradovich, J.D., and Fanning, C.M.: SHRIMP U-Pb geochronology of volcanic rocks, Belt Supergroup, western Montana: Evidence for rapid deposition of sedimentary strata. Can. J. Earth Sci., 37, 1287–1300, doi: 10.1139/e00-036, 2000.

Farquhar, J., Wu, N.P., Canfield, E.D., Oduro, H.: Connections between Sulfur Cycle Evolution, Sulfur Isotopes, Sediments, and Base Metal Sulfide Deposits. Econ. Geol., 105, 509-533, doi: 10.2113/gsecongeo.105.3.509, 2010.

Farquhar, J., Zerkle, A.J., Bekker, A.: Geologic and Geochemical Constraints on Earth's Early Atmosphere. In: Holland, H.D., Turekian, K.K. (Eds.), Treatise on Geochemistry 6, Elsevier, Oxford, pp. 91–129, doi: 10.1016/6978-0-08-095975-7.01304-8, 2014.

https://doi.org/10.5194/egusphere-2023-2091
Preprint. Discussion started: 29 January 2024


Fayazi, F., Lak, R., Nakhaei, M.: Hydrogeochemistry and evolution of Maharlou saline lake, Southwest of Iran. Carbonate. Evaporite., 22, 33–42, doi: 10.1007/bf03175844, 2007.

Fiorella, P.R., Sheldon, D.N.: Equable end Mesoproterozoic climate in the absence of high CO2. Geology, 45, 231-234, doi: 10.1130/g38682.1, 2017.

Fischer, A.G.: Climatic oscillations in the biosphere. In: Nitecki, M. (Ed.), Biotic crises in ecological and evolutionary time. Academic Press, New York, pp. 103–131, doi: 10.1016/b978-0-12-519640-6.50012-0, 1981.

Font, E., N´ed´elec, A., Trindade, R.I.F., Moreau, C.: Fast or slow melting of the Marinoan snowball Earth? The cap dolostone record. Palaeogeogr. Palaeocl. 295 (1-2), 215–225, doi: 101016/j.palaeo.2010.05.039, 2010.

Forbes, J., Nance, R.: Stratigraphy, sedimentology, and structural geology of gypsum caves in southeast New Mexico. Carbonate Evaporite, 12, 64-72, doi: 10.1007/bf03175803, 1997.

Frape, S.K., Blyth, A., Stotler, R.L., Rusheeniemi, T., Blomqvist, R., Mcnutt, R.H., Gascoyne, M.: Deep fluids in the continents. In: Holland, H.D., Turekian, K.K. (Eds.), Treatise on Geochemistry 7, Elsevier, Oxford, pp. 518–561, doi: 10.1016/b978-0-08-095975-7.00517-9, 2014.

Galamay, R.A., Bukowski, K., Zinchuk, M.I., Meng, F.W.: The Temperature of Halite Crystallization in the Badenian Saline Basins, in the Context of Paleoclimate Reconstruction of the Carpathian Area. Minerals, 11, 831, doi: 10.3390/min11080831, 2021.

Garnett, R.H.T., Bassett, N.C.: Placer Deposits. Econ. Geol., 100, 813-843, doi: 105382/av100.25, 2005.

Gasse, F., Fontes, J.C.: Palaeoenvironments and palaeohydrology of a tropical closed lake (Lake Asal, Djibouti) since 10,000 yr B.P. Palaeogeogr. Palaeocl. 69, 67–102, doi: 10.1016/0031-0182(89)90156-9, 1989.

Gaupp, R., Gast, R., Forster, C.: Late Permian Playa Lake Deposits of the Southern Permian Basin (Central Europe). AAPG Studies Geol., 46, 75-86, doi: 10.1306/st46706c5, 2000.

Gillet, H., Lericolais, G., R´ehault, J.-P.: Messinian event in the black sea: Evidence of a Messinian erosional surface. Mar. Geol. 244 (1-4), 142–165, doi: 10.1016/j.margeo.2007.06.004, 2007.

https://doi.org/10.5194/egusphere-2023-2091
Preprint. Discussion started: 29 January 2024


Gilman, K.: Hydrology and Wetland Conservation. Wiley, Chichester. Walker, J.C.G., Hays, P.B., Kasting, J.F., 1981. A negative feedback mechanism for the long–term stabilization of Earth's surface temperature. J. Geophys. Res., 86, 9776–9782, doi: 10.1029/jc086ic10p09776, 1994.

Gnanaseelan, C., Deshpande, A.: Equatorial Indian Ocean subsurface current variability in an Ocean General Circulation Model. Clim. Dynam., 50 (5-6), 1705–1717, doi: 10.1007/s00382-017-3716-8, 2018.

Godderis, Y., Donnadieu, Y., Le Hir, G., Lefebvre, V., Nardin, E.: The role of palaeogeography in the Phanerozoic history of atmospheric $CO_2$ and climate. Earth-Sci. Rev., 128, 122-138, doi: 10.1016/j.earscirew.2013.11.004, 2014.

Goldberg, T., Poulton, W.S., Strauss, H.: Sulphur and oxygen isotope signatures of late Neoproterozoic to early Cambrian sulphate, Yangtze Platform, China: Diagenetic constraints and seawater evolution. Precambrian Res., 137, 223-241, doi: 10.1016/j.precamres.2005.03.003, 2005.

Goldfarb, J.R., Bradley, D., Leach, D.L.: Secular Variation in Economic Geology. Econ. Geol., 105, 459-465, doi: 10.2113/gsecongeo.105.3.459, 2010.

Goldfarb, R.J., Groves, D.I., and Gardoll, S.: Orogenic gold and geologic time: A global synthesis. Ore Geol. Rev., 18, 1–75, doi: 10.1016/s0169-1368(01)00016-6, 2001a.

Goldfarb, R.J.: Rotund versus skinny orogens: Well-nourished or malnourished gold? Geology, 29, 539–542, doi: 10.1130/0091-7613(2001)02<0539:rvsown>2.0.co;2, 2001b.

Goldfarb, R.J., Baker, T., Dube, B., Groves, D.I., Hart, C.J., Gosselin, P.: Distribution, character, and genesis of gold deposits in metamorphic terranes. Econ. Geol., 100, 407–450, doi: 10.5382/av100.14, 2005.

Goodfellow, W.D., and Lydon, J.W.: Sedimentary-exhalative (SEDEX) deposits. Geol. Assoc. Can., Mineral Deposits Division, Spec. Public., 5, 163-183, doi: 10.4095/207970, 2007.

Goodfellow, W.D., Lydon, J.W., Turner, R.J.W.: Geology and genesis of stratiform sediment-hosted (SEDEX) zinc-lead-silver sulphide deposits. Geol. Assoc. Can. Spec. Paper, 40, 201-251, 1993.

https://doi.org/10.5194/egusphere-2023-2091
Preprint. Discussion started: 29 January 2024


Groves, D.I., Condie, K.C., Goldfarb, R.J., Hronsky, J.M.A., Vielreicher, R.M.: Secular changes in global tectonic processes and their influence on the temporal distribution of gold–bearing mineral deposits. Econ. Geol., 100, 203–224, doi: 10.2113/gsecongeo.100.2.203, 2005a.

Groves, D.I., Vielreicher, R.M., Goldfarb, R.J. and Condie, K.C.: Controls on the heterogeneous distribution of mineral deposits through time, in Mc Donald, I. et al., eds., Mineral deposits and earth evolution. Geol. Soc., London, Spec. Public., 248, 71–101, doi: 10.1144/aslsp.2005.248.01.04, 2005b.

Groves, I.D., Bierlein, P.F., Meinert, D.L., Hitzman, W.M.: Iron Oxide Copper-Gold (IOCG) Deposits through Earth History: Implications for Origin, Lithospheric Setting, and Distinction from Other Epigenetic Iron Oxide Deposits. Econ. Geol., 105, 641-654, doi: 10.2113/gsecongeo.105.3.641, 2010.

Gu, A.L., Eastoe, C.J.: The Origins of Sulfate in Cenozoic Non-Marine Evaporites in the Basin and-Range Province, Southwestern North America. Geosciences, 11, 455, doi: 10.3390/geosciences11110455, 2021.

Gu, X.X., Zhang, Y.M., Schulz, O., Vavtar, F., Liu, J.M., Zheng, M.H., Zheng, L.: The Woxi W–Sb–Au deposit in Hunan, South China: An example of Late Proterozoic sedimentary exhalative (SEDEX) mineralization. J. Asian Earth Sci., 57, 54-75, doi: 10.1016/j.jseaes.2012.06.006, 2012.

Guo, P., Liu, C.Y., Gibert, L., Huang, L., Zhang, D.W., Dai, J.: How to find high-quality petroleum source rocks in saline lacustrine basins: A case study from the Cenozoic Qaidam Basin, NW China. Marine Petrol. Geol., 111, 603-623, doi: 10.1016/j.marpetgeo.2019.08.050, 2020.

Guo, P., Liu, C.Y., Huang, L., Yu, M.L., Wang, P., Zhang, G.Q.: Palaeohydrological evolution of the late Cenozoic saline lake in the Qaidam Basin, NE Tibetan Plateau: Tectonic vs. climatic control. Global Planet. Change, 165, 44-61, doi: 10.1016/j.gloplacha.2018.03.012, 2018.

Gutzmer, J., Mukhopadhyay, J., Beukes, N.J., Pack, A., Hayashi, K., Sharp, Z.D.: Oxygen isotope composition of hematite and genesis of high–grade BIF–hosted iron ores. Geol. Soc. Am. Mem., 198, 257–268, doi: 10.1130/2006.1198(15), 2006.

Guzman, E.J.: Sedimentary volumes in Gulf Coastal Plain of the United States and Mexico. GSA Bulletin, 63, 1201-1220, doi: 10.1130/0016-7606(1952)63[1201:svigcp]2.0.co;2, 1962.

https://doi.org/10.5194/egusphere-2023-2091
Preprint. Discussion started: 29 January 2024


Hacini, M., Oelkers, E.H.: Geochemistry and behavior of trace elements during the complete evaporation of the Merouane Chott Ephemeral Lake: Southeast Algeria. Aquat. Geochem., 17 (1), 51–70, doi: 10.1007/s10498-010-9106-z, 2010.

Hagni, R.D.: Ore microscopy, paragenetic sequence, trace element content, and fluid inclusion studies of the copper–lead–zinc deposits of the Southeast Missouri lead district. In: Kisvarsanyi, G., Grant, S.K., Pratt, W.P., Koenig, J.W. (Eds.) Proceedings of International Conference on Mississippi Valley Type Lead–Zinc Deposits: Rolla, University of Missouri–Rolla Press, 243–256, doi: 10.5382/mono.03.18, 1983.

Hallet, B., Hunter, L., Bogen, J.: Rates of erosion and sediment evacuation by glaciers: A review of field data and their implications. Global Planet. Change, 12(1-4), 213-235, doi: 10.1016/0921-8181(95)00021-6, 1996.

Hanor, J. S., McIntosh, J. C.: Diverse origins and timing of formation of basinal brines in the Gulf of Mexico sedimentary basin. Geofluids, 7, 227-237, doi: 10.1111/1468-81232007.00177.x, 2007.

Hardie, L.A., Smoot, J.P., Eugster, H.P.: Saline lakes and their deposits: a sedimentological approach. Modern and Ancient Lake Sediments. Wiley, 7–41, doi: 10.1002/9781444303698.ch2, 1978.

Hardie, L.A., Eugster, H.P.: The evolution of closed-basin brines. Spec. Public. Miner. Soc. Am., 3, 273–290, doi: 10.2475/ajs.279.6.609, 1970.

Hay, W.W., Migdisov, A., Balukhovsky, A.N., Wold, C.N., Flögel, S., and Söding, E.: Evaporites and the salinity of the ocean during the Phanerozoic: Implications for climate, ocean circulation and life. Palaeogeogr., Palaeocl., 240, 3-46, doi: 10.1016/,palaeo.2006.03.044, 2006.

Hecht, L., Cuney. M.: Hydrothermal alteration of monazite in the Precambrian crystalline basement of the Athabasca Basin (Saskatchewan, Canada): Implications for the formation of unconformity-related uranium deposits. Miner. Deposita, 35, 791–795, doi: 10.1007/s001260050280, 2000.

Hein, D., Lehmann, B.: The Roˇzna´ uranium deposit (Bohemian Massif, Czech Republic): shear zone-hosted, late Variscan and post-Variscan hydrothermal mineralization. Miner. Deposita, 44, 99–128, doi: 10.1007/s00126-008-018-0, 2009.

https://doi.org/10.5194/egusphere-2023-2091
Preprint. Discussion started: 29 January 2024


Heinrich, C.A., Candela, P.A.: Fluids and ore formation in the Earth's Crust. In: Holland, H.D., Turekian, K.K. (Eds.), Treatise on Geochemistry 13, Elsevier, Oxford, pp. 1–28, doi: 10.1016/b978-0-08-095975-7.01101-3, 2014.

Higgins, A.J., Schrag, P.D.: Aftermath of a snowball Earth. Geochem., Geophy., Geosy., 4, 1–20, doi: 10.1029/2002ac000403, 2003.

Hite, R.J., Lohman, S.W.: Geologic appraisal of Paradox basin salt deposits for waste emplacement. USGS Open-File Report 4339-6, 75 p, doi: 103133/ofr73114, 1973.

Hitzman, M., Kirkham, R., Broughton, D., Thorson, J., Selley, D.: The Sediment-Hosted Stratiform Copper Ore System. Econ. Geol., 100, 609-642, doi: 10.5382/av100.19, 2005.

Hitzman, W.M., Selley, D., Bull, S.: Formation of Sedimentary Rock-Hosted Stratiform Copper Deposits through Earth History. Econ. Geol., 105, 627-639, doi: 10.2113/gsecongeo.105.3.627, 2010.

Hoeve, J., Sibbald, T.I.I.: On the genesis of Rabbit Lake and other unconformity–type uranium deposits in northern Saskatchewan, Canada. Econ. Geol., 73, 1450–1473, doi: 10.2113/gsecongeo.73.8.1450, 1978.

Hoffman, P.F., Kaufman, A.J., Halverson, G.P., Schrag, D.P.: A Neoproterozoic Snowball Earth. A Neoproterozoic snowball Earth. Science 281 (5381), 1342–1346, doi: 10.1126/science.281.5381.1342, 1998.

Hoffman, P.F., Schrag, D.P.: Snowball Earth. Sci. Am., 282 (1), 68–75, doi: 10.1038/scientificamerican0100-68, 2000.

Hoffman, P.F., Schrag, D.P.: The snowball Earth hypothesis: testing the limits of global change. Terra Nova, 14 (3), 129–155, doi: 10.1046/.1365-3121.200200408.x, 2002.

Holland, H.D.: The Chemical Evolution of the Atmosphere and the Oceans. Princeton University Press, doi: 101126/science226.4672.332, 1984.

Holland, H.D.: Sedimentary mineral deposits and the evolution of Earth's near-surface environments. Econ. Geol., 100, 1489-1509, doi: 10.2113/asecongeo.100.8.1489, 2005.

Holland, H.D., Lazar, B., McCaffrey, M.: Evolution of the atmosphere and oceans. Nature, 320 (6057), 27–33, doi: 10.1038/320027a0, 1986.

https://doi.org/10.5194/egusphere-2023-2091
Preprint. Discussion started: 29 January 2024


Horita, J., Weinberg, A., Das, N., Holland, D.H.: Brine Inclusions in Halite and the Origin of the Middle Devonian Prairie Evaporites of Western Canada. J. Sediment. Res., 66, 956-964, doi: 10,1306/d4268450-2b26-11d7-8648000102c1865d, 1996.

Hu, R.-Z., Bi, X.-W., Zhou, M.-F., Peng, J.-T., Su, W.-C., Liu, S., Qi, H.-W.: Uranium metallogenesis in South China and its relationship to crustal extension during the Cretaceous to Tertiary. Econ. Geol. 103 (3), 583–598, doi: 102113/gsecongeo.103.3.583, 2008.

Hu, R.-Z., Chen, W.T., Xu, D.-R., Zhou, M.-F.: Reviews and new metallogenic models of mineral deposits in South China: An introduction. J. Asian Earth Sci., 137, 1–8, doi: 10.1016/j.jseaes.2017.02.035, 2017.

Huang, J.G.: Saltness and Geologic background of the Cambrian Strata in the Sichuan Basin in the Upper Yangtz Area. Sediment. Geol. Tethyan Geol., 13(5), 44-56 (in Chinese with English abstract), 1993.

Hutchinson, R.W., Engels, G.G.: Tectonic Significance of Regional Geology and Evaporite Lithofacies in Northeastern Ethiopia. Philos. Trans. A. Math. Phys. Eng. Sci., 267, 313-329, doi: 10.1098/rsta.1970.0038, 1970.

Huybers, P., Langmuir, C.: Feedback between deglaciation, volcanism, and atmospheric CO2. Earth. Planet. Sci. Lett. 286 (3-4), 479–491, doi: 10.1016/j.epsl.2009.07.014, 2009.

Iturralde-Vinent, M.A.: Meso-Cenozoic Caribbean Paleogeography: Implications for the Historical Biogeography of the Region. Int. Geol. Rev., 48, 791-827, doi: 10.2747/0020-6814.48.9.791, 2006.

Jackson, M.P.A., Cramez, C., Fonck, J.M.: Role of subaerial volcanic rocks and mantle plumes in creation of South Atlantic margins: implications for salt tectonics and source rocks. Mar. Petrol. Geol., 17, 477–498, doi: 10.1016/s0264-8172(00)00006-4, 2000.

Jiang, S., Henriksen, S., Wang, H., Lu, Y.C., Ren, J.Y., Cai, D.S., Feng, Y.L., Weimer, P.: Sequence-stratigraphic architectures and sand-body distribution in Cenozoic rifted lacustrine basins, east China. AAPG Bulletin, 97, 1447-1475, doi: 101306/03041312026, 2013.

Jiang, W.Q.: Global C3 and C4 plant evolution and its response to climate and CO2 change since the last glacial maximum. Beijing, A doctoral dissertation submitted to University of Chinese Academy of Sciences, doi: 10.46427/gold2020.1691, 2019.

https://doi.org/10.5194/egusphere-2023-2091
Preprint. Discussion started: 29 January 2024


Johnson, K.S.: Hydrogeology and karst of the Blaine gypsum dolomite aquifer, southwestern Oklahoma. Oklahoma Geol. Sur. Spec. Public., 90-5, 31 p, doi: 10.1306/83d9230-16:7-11d7-8645000102:1865d, 1990.

Johnson, K.S.: Evaporite karst in the Permian Blaine Formation and associated strata in western Oklahoma, USA. In Back, W., Heman, J.S., and Paloc, H. (eds.), Hydrogeology of selected karst regions: International Association Hydrogeologists, Verlag Heinz Heisse Publishing Co., Hannover, Germany, 13, 405-420, 1992.

Johnson, S.K.: Evaporite karst in the United States. Carbonate Evaporite, 12, 2-14, doi: 10.1007/bf03175797, 1997.

Jones, B.F., Bodine, M.W.Jr.: Normative salt characterization of natural waters. In: Fritz, P., Frape, S.K. (Eds.) Saline Water and Gases in Crystalline Rocks. Geol. Assoc. Can. Spec. Pap. 33, 5–18, doi: 10.1002/gj.3350240317, 1987.

Jones, B.F., Eugster, H.P., Rettig, S.L.: Hydrochemistry of the Lake Magadi basin, Kenya. Geochim. Cosmochim. Ac., 41 (1), 53–72, doi: 10.1016/0016-7037(77)90186-7, 1977.

Jordan, T.E., Mpodozis, C., Munoz, N., Blanco, N., Pananont, P., Gardeweg, M.: Cenozoic subsurface stratigraphy and structure of the Salar de Atacama Basin, northern Chile. J. South Am. Earth Sci., 23, 122–146, doi: 10.1016/j.jsames.2006.09.024, 2007.

Kah, L.C., Bartley, J.K., Teal, D.A.: Chemostratigraphy of the Late Mesoproterozoic Atar Group, Taoudeni Basin, Mauritania: Muted isotopic variability, facies correlation, and global isotopic trends. Precambrian Res., 200–203, 82–103, doi: 10.1016/j.precamres.2012.01.011, 2012.

Kah, L.C., Lyons, T.W., Chesley, J.T.: Geochemistry of a 1.2 Ga carbonate-evaporite succession, northern Baffin and Bylot Islands: Implications for Mesoproterozoic marine evolution. Precambrian Res., 111, 203–234, doi: 10.1016/S0301-9268(01)00161-9, 2001.

Kah, L.C., Riding, R.: Mesoproterozoic carbon dioxide levels inferred from calcified cyanobacteria. Geology, 35, 799–802, doi: 10.1130/g23680a.1, 2007.

Kanzaki, Y., Murakami, T.: Estimates of atmospheric CO2 in the Neoarchean–Paleoproterozoic from paleosols. Geochim. Cosmochim. Ac., 159, 190–219, doi: 10.1016/j.gca.2015.03.011, 2015.

https://doi.org/10.5194/egusphere-2023-2091
Preprint. Discussion started: 29 January 2024


Kasedde, H., Kirabira, B.J., Babler, U.M., Tilliander, A., Jonsson, S.: Characterization of brines and evaporites of Lake Katwe, Uganda. J. Afr. Earth Sci., 91, 55-65, doi: 10.1016/j.jafrearsci.2013.12.004, 2014.

Kelley, K.D., Dumoulin, J.A., and Jennings, S.: The Anarraaq Zn-Pb-Ag and barite deposit, northern Alaska: Evidence for replacement of carbonate by barite and sulfides. Econ. Geol., 99, 1577-1591, doi: 10.2113/gsecongeo.99.7.1577, 2004a.

Kelley, K.D., Leach, D.L., Johnson, C.A., Clark, J.L., Fayek, M., Slack, J.F., Anderson, V.M., Ayuso, R.A., Ridley, W.I.: Textural, compositional, and sulfur isotope variations of sulfide minerals in the Red Dog Zn-Pb-Ag deposits, Brooks Range, Alaska: Implications for ore formation. Econ. Geol., 99, 1509–1533, doi: 10.2113/gsecongeo.99.7.1509, 2004b.

Kendall, G.C.S.C., Lake, P., Weathers III, H.D., Lakshmi, V., Althausen, J., Alsharan, A.S.: Evidence of rain shadow in the geologic record: repeated evaporite accumulation at extensional and compressional plate margins. In: Alsharan, A.S., Wood, W.W., Goudie, A.S., Fowler, A., Abdellatif, E.M. (Eds.), Desertification in the Third Millennium: Lisse, Netherlands, Swets and Zeitlinger, 45–52, doi: 10.1201/noe9058095718.ch5, 2003.

Kennedy, M.: The Undoolya sequence: Late Proterozoic salt influenced deposition, Amadeus Basin, central Australia. Aust. J. Earth Sci., 40, 217-228, doi: 10.1080/08120099308728076, 1993.

Kerrich, R., Goldfarb, R., Groves, D., Garwin, S.: The geodynamics of world–class gold deposits: characteristics, space–time distributions, and origins. Rev. Econ. Geol., 13, 501–551, doi: 10.5382/rev.13.15, 2000.

Kerrich, R., Goldfarb, R.J., Cline, J., Leach, D.: Metallogenic provinces of North America in a superplume-supercontinent framework. Arizona Geol. Soc. Digest, 22, 1–18, 2008.

Kerrich, R., Goldfarb, R.J., Richards, J.P.: Metallogenic provinces in an evolving dynamic framework. Econ. Geol. 100, 1097–1136, doi: 10.5382/av100.33, 2005.

Kesler, S.E., Martini, A.M., Appold, M.S., W alter, L.M., Huston, T .J., and Furman, F.C.: Na-Cl-Br systematic of fluid inclusions from Mississippi Valley-type deposits, Appalachian basin: Constraints on solute origin and migration paths. Geochim. Cosmochim. Ac., 60, 225–233, doi: 10.1016/0016-7037(95)00390-8, 1996.

https://doi.org/10.5194/egusphere-2023-2091
Preprint. Discussion started: 29 January 2024


Kesler, S.E., Reich, M.H.: Precambrian Mississippi Valley–type deposits: relation to changes in composition of the hydrosphere and atmosphere. Geol. Soc. Am. Mem., 198, 185–204, doi: 10.1130/2006.1198(11), 2006.

Kesler, S.E.: Ore-Forming Fluids. Elements, 1, 13-18, doi: 10.2113/gselements.1.1.13, 2005.

Ketzer, J. M., Iglesias, R., Einloft, S., Dullius, J., Ligabue, R., de Lima, V.: Water–rock–CO2 interactions in saline aquifers aimed for carbon dioxide storage: Experimental and numerical modeling studies of the Rio Bonito Formation (Permian), southern Brazil. Appl. Geochem., 24, 760-767, doi: 10.1016/j.apgeochem.2009.01.001, 2009.

Kharaka, Y.K., Hanor, J.S.: Deep fluids in sedimentary basins. In: Holland, H.D., Turekian, K.K. (Eds.) Treatise on Geochemistry 7, 472–508. Oxford: Elsevier, doi: 10.1016/b978-0-08-095975-7.00516-7, 2014.

Kharaka, Y.K., Maest, A.S., Carothers, W.W., Law, L.M., Lamothe, P.J., Fries, T.L.: Geochemistry of metalrich brines from central Mississippi Salt Dome Basin, USA. Appl. Geochem., 2 (5-6), 543–561, doi: 10.1016/0883-2927(87)90008-4, 1987.

Kharaka, Y.K., Thordsen, J.J.: Stable isotope geochemistry and origin of water in sedimentary basins. In: Clauer, N., and Chaudhuri, S. (Eds.) Isotope Signatures and Sedimentary Records, Berlin, Springer, pp. 411–466, doi: 10.1007/bfb0009873, 1992.

Kiersnowski, H., Paul, J., Marek, T.M., Smith, D.B.: Facies, Paleogeography, and Sedimentary History of the Southern Permian Basin in Europe. Springer Berlin Heidelberg, 119-136, doi: 10.1007/978-3-642-78590-0_7, 1995.

Kiipli, E., Kiipli, T., Kallaste, T.: Reconstruction of currents in the Mid-Ordovician–Early Silurian central Baltic Basin using geochemical and mineralogical indicators. Geology, 37, 271-274, doi: 10.1130/g25075a.1, 2009.

Kingston, D.R., Dishroon, C.P., Williams, P.A.: Global Basin Classification System. AAPG Bulletin, 67, 2175-2193, doi: 10.1306/ad460936-16f7-11d7-8645000102c1865d, 1983.

Kirkham, R.V.: Distribution, settings, and genesis of sediment-hosted stratiform copper deposits: Geol. Assoc. Can. Spec. Paper 36, p 3–38, 1989.

https://doi.org/10.5194/egusphere-2023-2091
Preprint. Discussion started: 29 January 2024


Kirkham, R.V., Carriere, J.J., Laramee, R.M., and Garson, D.F.: Global distribution of sediment-hosted stratiform copper deposits and occurrences. GSC Open File 2915b, 256 p, doi: 10.4095/207806, 1994.

Kirkland, D.W., Evans, R.: Origin of castiles on Gypsum Plain of Texas and New Mexico, in Dickerson, P.W., Hoffer, J.M. ,(eds.) Trans-Pecos region, southeastern New Mexico and west Texas. New Mexico Geol. Soc. 31st Field Confer., 173-178, doi: 10.56577/ffc-31.173, 1980.

Klingspor, A.M.: Middle Devonian Muskeg Evaporites of Western Canada. AAPG Bulletin, 53, 927-948, doi: 10.1306/5d25c80b-16c1-11d7-8645000102c1865d, 1969.

Knauth, L.P.: Temperature and salinity history of the Precambrian ocean: Implications for the course of microbial evolution. Palaeogeogr. Palaeocl., v. 219, p. 53-69, doi: 10.1016/b978-0-444-52019-7.50007-3, 2004.

Komninou, A., Sverjensky, D.A.: Geochemical Modeling of the Formation of an Unconformity-Type Uranium Deposit. Econ. Geol., 91 (3), 590–606, doi: 10.2113/gsecongeo.91.3.590, 1996.

Kovalevych, V.M.: Phanerozoic evolution of ocean water composition. Geochem. Int., 25, 20-27, doi: 10.1130/dnag-cot-pen.1, 1988.

Kovalevych, V.M.: Galogenez i khimicheskaya evolutsia okeana v fanerozoye. Naukova Dumka, Kiev., 1990.

Kovalevych, V.M., Zang, L.W., Peryt, T.M., Khmelevska, O.V., Halas, S., Iwasinska-Budzyk, I., Boult, P.J., Heithersay, P.S.: Deposition and chemical composition of early Cambrian salt in the eastern Officer Basin, South Australia. Aust. J. Earth Sci., 53, 577-593, doi: 101080/08120090600686736, 2006.

Kowalewska, A., Cohen, A.S.: Reconstruction of paleoenvironments of the Great Salt Lake Basin during the late Cenozoic. J. Paleolimnol., 20, 381-407, doi: 10.1023/A:1008053505320, 1998.

Kozary, M.T., Dunlap, J.C., Mumphrey, W.E.: Incidence of saline deposits in geological time. Geol. Soc. Am. Spec. Pap., 88, 45-57, doi: 10.1130/SPE88-p43, 1968.

Krijgsman, W., Langereis, C.G., Zachariasse, W.J., Boccaletti, M., Moratti, G., Gelati, R., Iaccarino, S., Papani, G., Villa, G.: Late Neogene evolution of the Taza-Guercif basin (Rifian Corridor, Morocco) and implications for the Messinian salinity crisis. Mar. Geol., 153 (1-4), 147–160, doi: 10.1016/S0025-3227(98)00084-X, 1999.

https://doi.org/10.5194/egusphere-2023-2091
Preprint. Discussion started: 29 January 2024


Kyser, K.: Uranium ore deposits. In: Holland, H.D., Turekian, K.K. (Eds.) Treatise on Geochemistry 13, 489–510. Oxford: Elsevier, doi: 10.1016/B978-0-08-095975-7.01122-0, 2014.

Lackner, K.S., Brennan, S., Matter, J.M., Park, A.-H., Wright, A., van der Zwaan, B.: The urgency of the development of CO2 capture from ambient air. P. Nati. Acad. Sci. USA 109 (33), 13156–13162, doi: 10.1073/pnas.1108765109, 2012.

Land, L.S., Prezbindowski, D.R.: The origin and evolution of saline formation water, Lower Cretaceous carbonates, southcentral Texas, U.S.A. J. Hydrol., 54, 51–74, doi: 10.1016/0022-1694(81)90152-9, 1981.

Large, R.R., Bull, S.W., McGoldrick, P.J., Derrick, G., Carr, G., Walters, S.: Stratiform and strata-bound Zn-Pb-Ag deposits of the Proterozoic sedimentary basins of northern Australia. Econ. Geol., 100, 931-963, doi: 10.5382/av100.28, 2005.

Large, R.R., Bull, S.W., Yang, J., Cooke, D.R., Garven, G., McGoldrick, P.J., and Selley, D.: Controls on the formation of giant stratiform sediment-hosted Zn-Pb-Ag deposits with particular reference to the north Australian Proterozoic. University of Tasmania, Centre for Special Ore Deposit and Exploration (CODES) Studies Publication 4, p. 107-149, 2002.

Larson, R.L.: Geological consequences of superplumes. Geology, 19, 963–6, doi: 10.1130/0091-7613(1991)019<0963:GCOS>2.3.CO;2, 1991.

Last, W.M.: Geolimnology of the Great Plains of western Canada. In: Lemmen, D.S., Vance, R.E. (Eds.) Holocene Climate and Environmental Change in the Palliser Triangle. A Geoscientific Context for Evaluating the Impacts of Climate Change on the Southern Canadian Prairies, Geol. Surv. Can. Bull. 534, 23–55, doi: 10.4095/211045, 1999.

Le Hir, G., Donnadieu, Y., Godd´eris, Y., Pierrehumbert, R.T., Halverson, G.P., Macouin, M., N´ ed´elec, A., Ramstein, G.: The snowball earth aftermath: exploring the limits of continental weathering processes. Earth. Planet. Sci. Lett., 277 (3-4), 453–463, doi: 10.1016/j.epsl-2008.11.010, 2009.

Leach, D. L., Apodaca, L. E., Repetski, J. E., Powell, J. W., Rowan E. L.: Evidence for hot Mississippi Valley-type brines in the Reelfoot Rift complex, south-central United States, in Late Pennsylvanian-Early Permian. U.S. Geol. Surv. Professional Paper 1577, 43 pp, doi: 10.3133/pp1577, 1997.

https://doi.org/10.5194/egusphere-2023-2091
Preprint. Discussion started: 29 January 2024


Leach, D.L., Sangster, D.F.: Mississippi Valley-type lead-zinc deposits. Geol. Assoc. Can. Spec. Paper 40, p. 289–314, doi: 104095/207988, 1993.

Leach, L.D., Bradley, C.D., Huston, D., Pisarevsky, A.S., Taylor, D.R., Gardoll, J.S.: Sediment-Hosted Lead-Zinc Deposits in Earth History. Econ. Geol., 105, 593-625, doi: 10.2113/gsecongeo.105.3.593, 2010.

Leach, L.D., Sangster, F.D., Kelley, D.K., Large, R.R., Garven, G., Allen, R.C., Gutzmer, J., Walters, S.: Sediment–hosted lead–zinc deposits: A global perspective. Econ. Geol., 100, 561–607, doi: 10.5382/av100.18, 2005.

Li, B.P., Liu, L., Zhao, J.X., Chen, X.C., Feng, Y.X., Han, G.H., Zhu, J.X.: Chemical fingerprinting of whitewares from Nanwa site of the Chinese Erlitou state. Nuclear Instruments Method Phys. Res. B, 266, 2614–2622, doi: 10.1016/j.nimb.2008.03.202, 2008a.

Li, Y.L., Wang, C.S., Li, Y.T.: Characteristics of the Jurassic saline deposits and its significance to hydrocarbon accumulation in Qiangtang Basin of Tibet area. Ac. Petrol. Sin., 29, 173-178, 2008b.

Li, M., Barnes, L.H.: Orbitally Forced Sphalerite Growth in the Upper Mississippi Valley District. Geochem. Perspect. Lett., 12, 18-22, doi: 10.7185/geochemlet.1929, 2019.

Bonnetti, C., Cuney, M., Malartre, F., Michels, R., Liu, X.D., Peng, Y.B.: The Nuheting deposit, Erlian Basin, NE China: Synsedimentary to diagenetic uranium mineralization. Ore Geol. Rev., 69, 118-139, doi: 10.1016/j.oregeorev.2015.02.010, 2015.

Liang, G.H., Xu X.W.: Potash Deformation and Enrichment Modes in Vientiane Sag, Laos. Earth Sci., 47, 136-148, doi: 10.1016/j.jseaes.2012.11.036, 2022.

Linacre, E.T., Hicks, B.B., Sainty, G.R., Grauze, G.: The evaporation from a swamp. Agricult. Meteorol., 7, 375–386, doi: 10.1016/0002-1571(70)90033-6, 1970.

Linhoff, B.S., Bennett, P.C., Puntsag, T., Gerel, O.: Geochemical evolution of uraniferous soda lakes in eastern Mongolia. Environ. Earth Sci., 62 (1), 171–183, doi: 10.1007/s12665-010-0512-8, 2011.

Liu, C.L., Wang, L.C., Yan, M.D., Zhao, Y.J., Cao, Y.T., Fang, X.M., Shen, L.J., Wu, C.H., Lv, F.L., Ding, T.: The Mesozoic-Cenozoic tectonic settings, paleogeography and evaporitic

https://doi.org/10.5194/egusphere-2023-2091
Preprint. Discussion started: 29 January 2024


sedimentation of Tethyan blocks within China: Implications for potash formation. Ore Geol. Rev., 102, 406-425, doi: 10.1016/j.oregeorev.2018.09.002, 2018.

Liu, Y.L., Yang, G., Chen, J.F., Du, A.D., Xie, Z.: Re-Os dating of pyrite from Giant Bayan Obo REE-Nb-Fe deposit. Chinese Sci. Bull., 49, 2627-2631, doi: 10.1360/04wd0185, 2004.

Liu, Y.J., Cao, L.M., Li, Z.L., Wang, H.N., Chu, T.Q., Zhang, J.R.: Geochemistry of Elements. Beijing, Science Press, pp. 460, 1984.

Lüders, V., Plessen, B., Romer, R.L., Weise, S.M., Banks, D.A., Hoth, P., Dulski, P., Schettler, G.: Chemistry and isotopic composition of Rotliegend and Upper Carboniferous formation waters from the North German Basin. Chem. Geol., 276, 198-208, doi: 10.1016/j.chemgeo.2010.06.006, 2010.

Lunt, D.J., Ross, I., Hopley, P.J., Valdes, P.J.: Modelling Late Oligocene C4 grasses and climate. Palaeogeogr. Palaeocl. 251 (2), 239–253, doi: 10.1016/j.palaeo.2007.04.004, 2007.

Lydon, J.W.: Chemical parameters controlling the origin and deposition of sediment-hosted stratiform lead-zinc deposits. Mineralogical Association of Canada Short Course Handbook, 9, 175–250, doi: 10.5382/av75.06, 1983.

Marjoribanks, R.W., Black, L.P.: Geology and Geochronology of the Arunta Complex, north of Ormiston Gorge, central Australia. J. Geol. Soc. Austr., 21, 291-299, doi: 10.1080/00167617408728852, 1974.

Mauk, J.L., and Hieshima, G.B.: Organic matter and copper mineralization at White Pine, Michigan, U.S.A. Chem. Geol., 99, 189-211, doi: 10.1016/0009-2541(92)90038-7, 1992.

Maynard, B.J.: The Chemistry of Manganese Ores through Time: A Signal of Increasing Diversity of Earth-Surface Environments. Econ. Geol., 105, 535-552, doi: 10.2113/gsecongeo.105.3.535, 2010.

McGrain, P., Helton, W.L.: Gypsum and anhydrite in the St Louis Limestone in northwestern Kentucky. Kentucky Geological Survey, Series X. Information Circular 13, 26 p, 1964.

McLaughlin, D.H.: Evaporite Deposits of Bogota Area, Cordillera Oriental, Colombia. AAPG Bulletin, 56, 2240-2259, doi: 10.1306/819A41FE-16C5-11D7-8645000102C1865D, 1972.

McLimans, R.K., Barnes, H.L., Ohmoto, H.: Sphalerite stratigraphy of the Upper Mississippi Valley zinc-lead district. Econ. Geol., 75, 351–361, doi: 10.2113/gsecongeo.75.3.351, 1980.

https://doi.org/10.5194/egusphere-2023-2091
Preprint. Discussion started: 29 January 2024


Melezhik, V.A., Fallick, A.F., Rychanchik, D.V., Kuznetsov, A.B.: Palaeoproterozoic evaporites in Fennoscandia: Implications for seawater sulphate, the rise of atmospheric oxygen and local amplification of the d13C excursion. Terra Nova, 17, 141–148, doi: 10.1111/j.1365-3121.2005.00600.x, 2005.

Meng, F.W., Zhang, Z.L., Yan, X.Q., Ni, P., Liu, W.H., Fan, F., Xie, G.W.: Stromatolites in Middle Ordovician carbonate–evaporite sequences and their carbon and sulfur isotopes stratigraphy, Ordos Basin, northwestern China. Carbonate Evaporite., 34, 11–20, doi: 10.1007/s13146-017-0367-0, 2019.

Mercadier J., Richard A., Cathelineau M.: Boron and magnesium-rich marine brines at the origin of giant unconformity-related uranium deposits: d11B evidence from Mg-tourmalines. Geology, 40, 231–234, doi: 10.1130/G32509.1, 2012.

Mercadier J., Skirrow, G.R., Cross, J.A.: Uranium and Gold deposits in the Pine Creek Orogen (North Australian Craton): A link at 1.8 Ga? Precambrian Res., 238, 111-119, doi: 10.1016/j.precamres.2013.10.001, 2013.

Mercadier, J., Richard, A., Boiron, M.-C., Cathelineau, M., Cuney, M.: Migrations of brines in the basement rocks of the Athabasca Basin through microfracture networks (P-Patch U deposits Canada). Lithos, 115, 121–136, doi: 10.1016/j.lithos.2009.11.010, 2010.

Meyer, C.: Ore-forming processes in geologic history. Econ. Geol., 75, 6–41, doi: 10.5382/av75.02, 1981.

Meyer, C.: Ore deposits as guides to the geologic history of the Earth. An. Rev. Earth Planet. Sci., 16, 147–71, doi: 10.1146/annurev.ea.16.050188.001051, 1988.

Mitchell, A.H.G., Garson, M.S.: Mineral deposits and global tectonic settings. New York, Academic Press, 410 p, doi: 10.1029/EO065i011p00098-02, 1981.

Mpodozis, C., Arriagada, C., Basso, M., Roperch, P., Cobbold, P., Reich, M.: Late Mesozoic to Paleogene stratigraphy of the Salar de Atacama Basin, Antofagasta, Northern Chile: Implications for the tectonic evolution of the Central Andes. Tectonophysics, 399, 125-154, doi: 10.1016/j.tecto.2004.12.019, 2005.

https://doi.org/10.5194/egusphere-2023-2091
Preprint. Discussion started: 29 January 2024


Mu¨ller, W. D., Hsu¨. J.K.: Event stratigraphy and paleoceanography in the fortuna basin (Southeast Spain): A scenaria for the Messinian salinity crisis. Paleoceanography, 2, 679-696, doi: 10.1029/PA002i006p00679, 1987.

Muir, M.D.: Facies models for Australian Precambrian evaporites. In: Peryt, T.M. (ed.) Evaporite Basins. Lecture Notes in Earth Sciences, 13, 5–21. Berlin-Heidelberg: Springer, 1987.

Nance, R.D., Worsley, T.R., Moody, J.B.: Post Archean biogeochemical cycles and long-term episodicity in tectonic processes. Geology, 14, 514–18, doi: 10.1130/0091-7613(1986)142.0.CO;2, 1986.

Neal, T.J., Johnson, K.S.: McCauley Sinks: A compound breccia pipe in evaporite karst, Holbrook basin, Arizona, U.S.A. Carbonates and Evaporites, 17, 98-106, doi: 10.1007/BF03176474, 2002.

Nemcok, M., Gayer, R.: Modelling palaeostress magnitude and age in extensional basins: a case study from the Mesozoic Bristol Channel Basin, U.K. J. Structural Geol., 18, 1301-1314, doi: 10.1016/S0191-8141(96)00048-X, 1996.

Nisbet, E.G., Fowler, C.M.R.: Model for Archean plate tectonics. Geology, 11, 376–379, doi: 10.1130/0091-7613(1983)11<376:MFAPT>2.0.CO;2, 1983.

O'Nions, R.K., Oxburgh, E.R.: Helium, volatile fluxes, and the development of continental crust. Earth. Planet. Sci. Lett., 90 (3), 331–347, doi: 10.1016/0012-821x(88)90134-3, 1988.

Oliver, J.E.: Encyclopedia of world climatology. Springer, Dordrecht. 854 pp, doi: 101007/1-4020-3266-8, 2005.

Palmer, M.R., Helvacı, C., Fallick, A.E.: Sulphur, sulphate oxygen and strontium isotope composition of Cenozoic Turkish evaporites. Chem. Geol., 209, 341–356, doi: 10.1016/j.chemgeo.2004.06.027, 2004.

Peeters, F., Kipfer, R., Achermann, D., Hofer, M., AeschbachHertig, W., Beyerle, U., Imboden, D.M., Rozanski, K., Fro¨hlich, K.: Analysis of deep-water exchange in the Caspian Sea based on environmental tracers. Deep Sea Res. Part I 47(4), 621–654, doi: 10.1016/s0967-0637(99)00066-7, 2000.

https://doi.org/10.5194/egusphere-2023-2091
Preprint. Discussion started: 29 January 2024


Pe-Piper, G., Piper, D.J.W., Zhang, Y.Y., Chavez, I.: Diagenetic barite and sphalerite in middle Mesozoic sandstones, Scotian Basin, as tracers for basin hydrology. AAPG Bulletin, 99, 1281-1313, doi: 10.1306/02171514067, 2015.

Perfit M R, Ridley W I, Jonasson I R.: Geologic, petrologic and geochemical relationships between magmatism and massive sulfide mineralization along the eastern Galapagos Spreading Center. Reviews in Econ. Geol., 8, 75-100, doi: 10.5382/rev08.04, 1999.

Perfit, M.R., Fornari, D.J., Malahoff, A., and Embley, R.W.: Geochemical studies of abyssal lavas recovered by DSRV ALVIN from the eastern Galapagos Rift - Inca Transform - Ecuador Rift: III: Trace elements abundances and petrogenesis. J. Geophys. Res., 88, 10551–10572, doi: 10.1029/jb088ib12p10551, 1983.

Perfit, M.R., Ridley, W.I., Jonasson, I.R.: Geologic, petrologic and geochemical relationships between magmatism and massive sulfide mineralization along the eastern Galapagos Spreading Center. Rev. Econ. Geol., 8, 75-100, doi: 9781629490151, 1997.

Pietras, J.T., Carroll, A.R., Rhodes, M.K.: Lake basin response to tectonic drainage diversion: Eocene Green River Formation. Wyoming. J. Paleolimnol. 30, 115–125, doi: 10.1130/0091-7613(2002)030<0167:siropa>2.0.co;2, 2003.

Pirajno, F., Grey, K.: Chert in the Palaeoproterozoic Bartle Member, Killara Formation, Yerrida Basin, Western Australia: A rift-related playa lake and thermal spring environment? Precambrian Res., 113, 169–192, doi: 10.1016/s0301-9268(01)00196-6, 2002.

Polito, P.A., Kyser, T.K., Jackson, M.J.: The role of sandstone diagenesis and aquifer evolution in the formation of uranium and zinc-lead deposits, southern McArthur Basin, Northern Territory, Australia. Econ. Geol. 101, 1189-1209, doi: 10.2113/qsecongeo.101.6.1189, 2006b.

Polito, P.A., Kyser, T.K., Southgate, P.N., Jackson, M.J.: Sandstone diagenesis and aquifer evolution in the Mt Isa Basin: the isotopic and fluid inclusion history of fluid flow in the Mt Isa Basin. Econ. Geol., 101, 1159-1188, doi: 10.2113/gsecongeo.101.6.1159, 2006a.

Pope, M.C., Grotzinger, J.P.: Paleoproterozoic Stark Formation, Athapuscow basin, northwest Canada: Record of cratonic-scale salinity crisis. J. Sediment. Res., 73, 280–295, doi: 10.1306/091302730280, 2003.

https://doi.org/10.5194/egusphere-2023-2091
Preprint. Discussion started: 29 January 2024


Prasad, N., Roscoe, S.M.: Evidence of anoxic to oxic atmosphere change during 2.45-2.22 Ga from lower and upper sub-Huronian paleosols Canada. Catena, 27, 105–121, doi: 10.1016/0341-8162(96)00003-3, 1996.

Pre´at, A., Bouton, P., Thie´blemont, D., Prian, J-P., Ndounze, S.S., Delpomdor, F.: Paleoproterozoic high d13C dolomites from the Lastoursville and Franceville basins (SE Gabon): Stratigraphic and synsedimentary subsidence implications. Precambrian Res., 189, 212–228, doi: 10.1016/j.precamres.2011.05.013, 2011.

Preiss, W.V.: The systematics of South Australian Precarnbrian and Cambrian stromatolites. I. Trans. R. Soc. S. Austr., 96, 67-100, 1972.

Prokoph, A., El Bilali, H., Ernst, R.: Periodicities in the emplacement of large igneous provinces through the Phanerozoic: Relations to ocean chemistry and marine biodiversity evolution. Geosci. Front., 4 (3), 263–276, doi: 10.1016/gsf2012.08.001, 2013.

Prokoph, A., Shields, G.A., Veizer, J.: Compilation and time-series analysis of a marine carbonate d18O, d13C, 87Sr/86Sr and d34S database through Earth history. Earth-Sci. Rev. 87, 113-133, doi: 10.1016/j.earscirev.2007.12.003, 2008.

Puigdefabregas, C., Souquet, P.: Tecto-Sedimentary Cycles and Depositional Sequences of the Mesozoic and Tertiary from the Pyrenees. Tectonophysics, 129, 173-203, doi: 101016/0040-1951(86)90251-9, 1986.

Rahn, P.H., Davis, A.D.: Gypsum foundation problems in the Black Hills area, South Dakota. Environ. Eng. Geosci., 2, 213-223, doi: 10.2113/gseegeosci.II.2.213, 1996.

Ramseyer, K., Amthor, J.E., Matter, A., Pettke, T., Wille, M., Fallick, A.E.: Primary silica precipitate at the Precambrian/Cambrian boundary in the South Oman Salt Basin, Sultanate of Oman. Mar. Petrol. Geol., 39, 187-197, doi: 10.1016/j.marpetgeo.2012.08.006, 2013.

Ravenhurst, C.R., Reynolds, P.H., Zentilli, M., Krueger, H.W., Blenkinsop, J.: Formation of Carboniferous Pb-Zn and Barite Mineralization from Basin-Derived Fluids, Nova Scotia, Canada. Econ. Geol., 84, 1471-1488, doi: 10.2113/gsecongeo.84.6.1471, 1989.

Rawlings, D.J., Page, R.W.: Geology, geochronology and emplacement structures associated with the Jimbu Microgranite, McArthur Basin, Northern Territory. Precambrian Res., 94, 225-250, doi: 10.1016/s0301-9268(98)00116-8, 1999.

https://doi.org/10.5194/egusphere-2023-2091
Preprint. Discussion started: 29 January 2024


Raymo, M.E., Ruddiman, W.F.: Tectonic forcing of late Cenozoic climate. Nature, 359(6391), 117-122. 10.1038/359117a0, 1992.

Regenspurg, S., Feldbusch, E., Norden, B., Tichomirowa, M.: Fluid-rock interactions in a geothermal Rotliegend/Permo-Carboniferous reservoir (North German Basin). Appl. Geochem., 69, 12-27, doi: 10.1016/j.apgeochem.2016.03.010, 2016.

Retallack, G.J.: Laterization and bauxitization events. Econ. Geol., 105, 655–667, doi: 10.2113/gsecongeo.105.3.655, 2010.

Reuschel, M., Melezhik, V.A., Whitehoused, M.J., Lepland, A., Fallick, A.E., Strauss, H.: Isotopic evidence for a sizeable seawater sulfate reservoir at 2.1 Ga. Precambrian Res., 192–195, 78–88, doi: 10.1016/j.precamres.2011.10.013, 2012.

Richard, A., Boulvais, P., Mercadier, J., Boiron, M.-C., Cathelineau, M., Cuney, M., France-Lanord, C.: From evaporated seawater to uranium–mineralizing brines: Isotopic and trace element study of quartzdolomite veins in the Athabasca system. Geochim. Cosmochim. Ac. 113, 38–59, doi: 10.1016/j.gca.2013.08.008, 2013.

Richard, A., Kendrick, M.A., Cathelineau, M.: Noble gases (Ar, Kr, Xe) and halogens (Cl, Br, I) in fluid inclusions from the Athabasca Basin (Canada): Implications for unconformity–related U deposits. Precambrian Res. 247, 110–125, doi: 10.1016/j.precamres.2014.03.020, 2014.

Richard, A., Rozsypal, C., Mercadier, J., Banks, D.A., Cuney, M., Boiron, M.-C., Cathelineau, M.: Giant uranium deposits formed from exceptionally uranium–rich acidic brines. Nat. Geosci., 5, 142–146, doi: 10.1038/ngeo1338, 2012.

Richter, F.M., Rowley, D.B., DePaolo, D.J.: Sr isotope evolution of seawater: the role of tectonics. Earth Planet. Sci. Lett., 109(1-2), 11-23, doi: 10.1016/0012-821x(92)90070-c, 1992.

Robb, L., Hawkesworth, C.: Plate Tectonics and Metallogeny. Encyclopedia of Geology (Second Edition), 643-662, doi: 10.1016/b978-0-12-409548-9.12535-7, 2020.

Robb, L.J.: Introduction to Ore-Forming Processes. Blcakwell Publishing Company, Oxford, 311–345, doi: 10.1144/1467-7873/05-073, 2005.

Roberts, N.M.W.: The boring billion?–Lid tectonics, continental growth and environmental change associated with the Columbia supercontinent. Geosci. Frontiers, 4(6), 681-691, doi: 10.1016/j.gsf.2013.05.004, 2013.

https://doi.org/10.5194/egusphere-2023-2091
Preprint. Discussion started: 29 January 2024


Rogers, J.J.W., Santosh, M.: Configuration of Columbia, a Mesoproterozoic Supercontinent. Gondwana Res., 5, 5–22, doi: 10.1016/s1342-937x(05)70883-2, 2002.

Rogers, J.J.W., Unrug, R., Sultan, M.: Tectonic assembly of Gondwana. J. Geodyn., 19, 1–34, doi: 10.1016/0264-3707(94)00007-7, 1995.

Rona, P.: Global plate motion and mineral resources, in Strangway, D.W., ed., The continental crust and its mineral deposits. Geol. Assoc. Can. Spec. Paper, 20, 607–622, doi: 10.1126/science212.4498.1020.a, 1980.

Roscher, M., Schneider, J.W.: Permo-Carboniferous climate: Early Pennsylvanian to Late Permian climate development of central Europe in a regional and global context. Geol. Soc., London, Spec. Public., 265, 95-136, doi: 10.1144/gsl.sp.2006.265.01.05, 2006.

Roscoe, S.M.: Huronian rocks and uraniferous conglomerates in the Canadian Shield. Geol. Sur. Can. Paper, 68-40, 205, doi: 10.4095/102290, 1969.

Rowen, E.L., Engle, M.A., Kraemer, T.F., Schroeder, K.T., Hammack, R.W., Doughten, M.W.: Geochemical and isotopic evolution of water produced from Middle Devonian Marcellus shale gas wells, Appalachian basin, Pennsylvania. AAPG Bulletin, 99, 181-206, doi: 10.1306/07071413146, 2015.

Royer, D.: Climate Sensitivity in the Geological Past. Annu. Rev. Earth. Planet. Sci., 44, 277–293, doi: 101146/annurev-earth-100815-024150, 2016.

Royer, D.L., Berner, R.A., Montanez, I.P., Tabor, N.J., Beerling, D.J.: CO2 as a primary driver of Phanerozoic climate. GSA Today, 14 (3), 4–10, doi: 10.1130/1052-5173(2004)014<4:caapdo>2.0.co;2, 2004.

Rozendaal, A.: The Gamsberg zinc deposit, South Africa: A banded stratiform base-metal sulfide ore deposit. In Ridge, J.D., ed., Proceedings of the Quadrennial IAGOD Symposium, 5: Stuttgart, E. Schweizerbart'sche Verlagsbuchhandlung (Naegele u. Obermiller), 619–633, doi: 10.5382/econgeo.4725, 1980.

Rozendaal, A., Stumpfl, E.F.: Mineral chemistry and genesis of Gamsberg zinc deposit, South Africa. T. Ins. Mining Metall., sec. B, 93, B161–B175, doi: 10.1201/9781003077503-82, 1984.

Rudnick, R.L., Gao, S.: Composition of the continental crust. In: Holland, H.D., Turekian, K.K. (Eds.) Treatise on Geochemistry 4, 1–45. Oxford: Elsevier, doi: 10.1016/b978-0-08-095975-7.00301-6, 2014.

Saleh, A., Hamzehpour, A., Mehdinia, A., Bastami, D.K., Mazaheri, S.: Hydrochemistry and nutrient distribution in southern deep-water basin of the Caspian Sea. Mar. Pollut. Bull. 127, 406–411, doi: 10.1016/j.marpolbul.2017.12.013, 2018.

Sanchez, J.A., Coloma, P., Perez, A.: Sedimentary processes related to the groundwater flows from the Mesozoic Carbonate Aquifer of the Iberian Chain in the Tertiary Ebro Basin, northeast Spain. Sediment. Geol., 129, 201-213, doi: 101016/s0037-0738(99)00016-0, 1999.

Sando, W.J.: Madison Limestone (Mississippian) paleokarst: a geologic synthesis, in James, N.P., Choquette, P.W. (eds.) Paleokarst. Springer-Verlag, New York, p. 256-277, doi: 10.1007/978-1-4612-3748-8_13, 1988.

Sangma, F., Balamurugan, G.: Morphometric Analysis of Kakoi River Watershed for Study of Neotectonic Activity Using Geospatial Technology. Int. J. Geosci., 8, 1384–1403, doi: 10,4236/ijg.2017.811081, 2017.

Sangster, D.F.: Mississippi Valley-type and sedex lead-zinc deposits: A comparative examination. Ins. Mining Metall. T., 99, sec. B, B21-B42, doi: 10.4095/207988, 1990.

Sawkins, F.J.: Metal Deposits in Relation to Plate Tectonics. Berlin, Springer-Verlag, Berlin, 325 p, doi: 10.1017/s0016756800030892, 1984.

Sawkins, F.J.: Metal Deposits in Relation to Plate Tectonics. Springer-Verlag, 461, doi: 10.1007/978-3-662-08681-0_11, 1990.

Schenk, P.E., Matsumoto, R., von Bitter, P.: Loch Macumber (early Carboniferous) of Atlantic Canada. J. Paleolimnol., 11, 151-172, doi: 10.1007/bf00686863, 1994a.

Schenk, P.E., von Bitter, P., Matsumoto, R.: Deep basin/Deep water carbonate evaporite deposition of a Saline Giant: Loch Macumber (Visean), Atlantic Canada. Carbonate Evaporite, 9, 187-210, doi: 10.1007/bf03175230, 1994b.

Schmalz, R.F.: Deep water evaporite deposits: a genetic model. AAPG Bull., 53, 798-823, doi: 10.1306/5d257fd-16c1-11d7-8645000102c1865d, 1969.

https://doi.org/10.5194/egusphere-2023-2091
Preprint. Discussion started: 29 January 2024


Schneider, S.H., Londer, R.: The Coevolution of Climate and Lift. Sierra Club Books, San Francisco. 56-154, doi: 10.1017/s0084255900046295, 1989.

Schro¨der, S., Bekker, A., Beukes, N.J., Strauss, H., and van Niekerk, H.S.: Rise in seawater sulphate concentration associated with the Paleoproterozoic positive carbon isotope excursion: Evidence from sulphate evaporites in the 2.2–2.1 Gyr shallow-marine Lucknow Formation, South Africa. Terra Nova, 20, 108–117, doi: 10.1111/j.1365-3121.2008.00795.x, 2008.

Schubel, K.A., Lowenstein, T. K.: Criteria for the Recognition of Shallow-Perennial-Saline Lake Halites based on Recent Sediments from the Qaidam Basin, Western China. J. Sediment. Res., 67, 74-87, doi: 10.1306/d42684fa-2b26-11d7-8648000102c1865d, 1997.

Scotese, C.R., Boucot, A.J., McKerrow, W.S.: Gondwanan paleogeography and paleoclimatology, in Gondwana 10: Event Stratigraphy. J. Afr. Earth Sci., 28, 99–114, doi: 10.1016/s0899-5362(98)00084-0, 1999.

Scotese, C.R., Song, H.J., Mills, B.J.W., van der Meer, D.G.: Phanerozoic paleotemperatures: The earth's changing climate during the last 540 million years. Earth Sci. Rev. https://doi.org/10.1016/j.earscirev.2021.103503, 2021.

Selley, D., Broughton, D., Scott, R., Hitzman, M., Barra, F.: A New Look at the Geology of the Zambian Copperbelt. Econ. Geol., 100, 965-1000, doi: 10.5382/av100.29, 2005.

Semikhatov, M.A., Raaben, M.E.: Proterozoic stromatolite taxonomy and biostratigraphy. In: Riding, R., Awramik, S.M. (Eds.), Microbial Sediments. Springer-Verlag, Heidelberg, pp. 295– 306, doi: 10.1007/978-3-662-04036-2_32, 2000.

Sharp, M., Tranter, M., Brown, G.H., Skidmore, M.: Rates of chemical denudation and CO2 drawdown in a glacier-covered alpine catchment. Geology, 23(1), 61-64, doi: 10.1130/0091-7613(1995)023<0061:rocdac>2.3.co;2, 1995.

Sheldon, D.N.: Causes and consequences of low atmospheric pCO2 in the Late Mesoproterozoic. Chem. Geol., 362, 224-231, doi: 10.1016/j.chemgeo.2013.09.006, 2013.

Sheldon, N.D.: Precambrian paleosols and atmospheric CO2 levels. Precambrian Res., 147, 148–155, doi: 10.1016/j.precamres.2006.02.004, 2006.

https://doi.org/10.5194/egusphere-2023-2091
Preprint. Discussion started: 29 January 2024


Shvartsev, S.L., Kolpakova, M.N., Isupov, V.P., Vladimirov, A.G., Ariunbileg, S.: Geochemistry and chemical evolution of saline lakes of Western Mongolia. Geochem. Int., 52, 388–403, doi: 10.1134/s0016702914030070, 2014.

Sibson, R.H.: A note on fault reactivation. J. Struct. Geol., 7, 751–754, doi: 10.1016/0191-8141(85)90150-6, 1985.

Sibson, R.H.: Earthquake rupturing as a mineralizing agent in hydrothermal systems. Geology, 15, 701–704, doi: 10.1130/0091-7613(1987)15<701:eraama>2.0.co;2, 1987.

Sinclair W.D., Chorlton L.B., Laramee R.M., Eckstrand O.R., Kirkham R.V., Dunne K.P.E., and Good D.J.: World minerals geoscience databaseproject: Digital databases of generalized world geology and mineral deposits for mineral exploration and research, in Stanley C.L., et al, eds., Mineral deposits: Processes to Processing: Rotterdam, Balkema, p. 1435–1437, doi: 10.4095/214766, 1999.

Singh, T., Jain, V.: Tectonic constraints on watershed development on frontal ridges: Mohand Ridge, NW Himalaya, India. Geomorphology, 106, 231–241, doi: 10.1016/j.geomorph.2008.11.001, 2009.

Skinner, B.J.: Hydrothermal mineral deposits–what we do and don't know. In: Barnes, H.L., (Ed.) Geochemistry of hydrothermal ore deposits (3rd ed.). New York, Wiley, 1–26, doi: 101126/science.159.3813.418, 1997.

Slack, J.F., Cannon, W.F.: Extraterrestrial demise of banded iron formations 1.85 billion years ago. Geology, 37, 1011–1014, doi: 10.1130/g30259a.1, 2009.

Smoot, P.J.: Sedimentary facies and depositional environments of early Mesozoic Newark Supergroup basins, eastern North America. Palaeogeogr. Palaeocl., 84, 369-423, doi: 10.1016/0031-0182(91)90055-v, 1991.

Soloviev, S.G.: Iron oxide copper–gold and related mineralisation of the Siberian Craton, Russia: I – Iron oxide deposits in the Angara and Ilim river basins, southcentral Siberia. In: Porter TM (ed.) Hydrothermal Iron Oxide Copper–Gold and Related Deposits: A Global Perspective – Advances in the Understanding of IOCG Deposits, 4, 495–514. Adelaide: PGC Publishing, doi: 10.31223/x5c330, 2010a.

https://doi.org/10.5194/egusphere-2023-2091
Preprint. Discussion started: 29 January 2024


Soloviev, S.G.: Iron oxide copper–gold and related mineralisation of the Siberian Craton, Russia: 2 – Palaeoproterozoic and Mesozoic assemblages of iron oxide, Cu, Au and U deposits of the Aldan Shield, Southeastern Siberia. In: Porter TM (ed.) Hydrothermal Iron Oxide Copper–Gold and Related Deposits: A Global Perspective – Advances in the Understanding of IOCG Deposits, 4, 515–534. Adelaide: PGC Publishing, doi: 1013188/2330-0396.1000040, 2010b.

Spray, J.: Earth Impact Database (EID). http://passc.net/EarthImpactDatabase/New%20website_05-2018/Index.html., 2020.

Stalder, M., and Rozendaal, A.: Apatite nodules as an indicator of depositional environment and ore genesis for the Mesoproterozoic Broken Hill-type Gamsberg Zn- Pb deposit, Namaqua province, South Africa. Miner. Deposita, 39, 189–203, doi: 10.1007/s00126-003-0394-8, 2004.

Steinhorn, I.: The disappearance of the long term meromictic stratification of the Dead Sea. Limnol. Oceanogr., 30, 451–472, doi: 10.4319/lo.1985.30.3.0451, 1985.

Stoffell, B., Appold, M.S., Wilkinson, J.J., McClean, N.A., and Jeffries, T.E.: Geochemistry and evolution of Mississippi Valley-type mineralizing brines from the Tri-State and northern Arkansas districts determined by LA-ICP-MS microanalysis of fluid inclusions. Econ. Geol., 103, 1411-1435, doi: 10.2113/gsecongeo,103.7.1411, 2008.

Stueber, A.M., Walter, L.M.: Glacial recharge and paleohydrologic flow systems in the Illinois basin: Evidence from chemistry of Ordovician carbonate (Galena) formation waters. GSA Bulletin, 106, 1430-1439, doi: 10.1130/0016-7606(1994)106<1430:grapfs>2.3.co;2, 1994.

Sun, J., Zhang, L., Deng, C., Zhu, R.: Evidence for enhanced aridity in the Tarim Basin of China since 5.3 Ma. Quatern. Sci. Rev., 27, 1012–1023, doi: 10.1016/i.quascirev.2008.01.011, 2008.

Tang, L.J.: Multi-level Detachments and Petroleum Potential of the Tarim Basin. Acta Geologica Sinica, 5, 327-338, doi: 10.1111/j.1755-6724.1992.mp5004001.x, 1992.

Tang, M., Chen, K., Rudnick, R.L.: Archean upper crust transition from mafic to felsic marks the onset of plate tectonics. Science, 351 (6271), 372–375, doi: 10.1126/scienc.aad5513, 2016.

Tang, M., Chu, X., Hao, J.H., Shen, B.: Orogenic quiescence in Earth's middle age. Science, 371(6530), 728-731, doi: 10.1126/science.abf1876, 2021a.

https://doi.org/10.5194/egusphere-2023-2091
Preprint. Discussion started: 29 January 2024


Tang, M., Ji, W.Q., Chu, X., Wu, A.B., Chen, C.: Reconstructing crustal thickness evolution from europium anomalies in detrital zircons. Geology, 2021, 49, 76-80, doi: 10.1130/g47745.1, 2021b.

Tang, Q.Y., Zhang, M.J., Li, C.S., Yu, M., Li, L.W.: The chemical compositions and abundances of volatiles in the Siberian large igneous province: Constraints on magmatic CO2 and SO2 emissions into the atmosphere. Chem. Geol., 339, 84–91, doi: 10.1016/j.chemgeo.2012.08.031, 2013.

Taylor, A., Blum, J.D.: Relation between soil age and silicate weathering rates determined from the chemical evolution of a glacial chronosequence. Geology, 23(11), 979-982, doi: 10.1130/0091-7613(1995)023<0979:rbsaas>2.3.co;2, 1995.

Teng, X., Fang, X., Kaufman, A.J., Liu, C., Wang, J., Zan, J., Yang, Y., Wang, C., Xu, H., Schulte, R.F., Piatak, N.M.: Sedimentological and mineralogical records from drill core SKD1 in the Jianghan Basin, Central China, and their implications for late Cretaceous–early Eocene climate change. J. Asian Earth Sci., 182, 103936, doi: 10.1016/j.jseaes.2019.103936, 2019.

Thisse, Y.: Sédiments métallifères de la fosse Atlantis II (mer Rouge): Contribution à l'étude de leur contexte morpho-structural et de leurs caractéristiques minéralogiques et géochimiques. Thèse Université Orleans et BRGM, France, 155 pp, doi: 10.2113/gssgfbull.ii.3.511, 1982.

Thisse, Y., Guennoc, P., Pouit, G., Nawab, Z.: The Red Sea: A natural geodynamic and metallogenic laboratory. Episodes, 3, 3–9, doi: 10.18814/epiiugs/1983/v6i3/002, 1983.

Todd Ririe, G.: Evaporites and strata-bound tungsten mineralization. Geology, 17, 139-143, doi: 10.1130/0091-7613(1989)017<0139:easbtm>2.3.co;2, 1989.

Trewartha, G.T., Horn, L.H.: An Introduction to Climate. McGraw-Hill, New York, 416 pp, doi: 10.1126/science.120.3130.1067.b, 1980.

Utrilla, R., Pierre, C., Orti, F., Pueyo, J.J.: Oxygen and sulphur isotope compositions as indicators of the origin of Mesozoic and Cenozoic evaporites from Spain. Chem. Geol., 102, 229-244, doi: 10.1016/0009-2541(92)90158-2, 1992.

Valero Garces, B.L., Aguilar, J.G.: Shallow Carbonate Lacustrine Facies Models in The Permian of the Aragon-Bearn Basin (Western Spanish-French Pyrenees). Carbonate Evaporite, 7, 94-107, doi: 10.1007/bf03175624, 1992.

https://doi.org/10.5194/egusphere-2023-2091
Preprint. Discussion started: 29 January 2024


van der Meer, D.G., van den Berg van Saparoea, A.P.H., van Hinsbergen, D.J.J., van de Weg, R.M.B., Godderis, Y., Le Hir, G., Donnadieu, Y.: Reconstructing firstorder changes in sea level during the Phanerozoic and Neoproterozoic using strontium isotopes. Gondwana Res. 44, 22–34, doi: 10.1016/j.gr.2016.11.002, 2017.

Varol, B., Şen, Ş., Ayyıldız, T., Sözeri, K., Karakaş, Z., Métais, G.: Sedimentology and stratigraphy of Cenozoic deposits in the Kağızman-Tuzluca Basin, northeastern Turkey. Int. J. Earth Sci., 105, 107-137, doi: 10.1007/s00531-015-1201-3, 2016.

Veizer, J., Laznicka, P., Jansen, S.L.: Mineralization through geologic time: recycling perspective. Am. J. Sci., 289, 484–524, doi: 10.2475/ajs.289.4.484, 1989.

Viets, J.G., Hofstra, A.H., Emsbo, P., and Kozlowski, A.: The composition of fluid inclusions in ore and gangue minerals from Mississippi Valley type Zn-Pb deposits of the Cracow-Silesia region of southern Poland: Genetic and environmental implications. In Gorecka, E., and Leach, D.L., eds., Carbonate-hosted zinc-lead deposits in the Silesian-Cracow area, Poland. Warsaw, Poland, Prace Panstwowego Instytuti Geologicznego, v. 154, p. 85–104, doi: 10.5382/sp.04.09, 1996.

Visser, J.N.J., Kingsley, C.S.: Upper Carboniferous glacial valley sedimentation in the Karoo Basin, Orange Free State. Trans. Geol. Soc. S. Afr., 85, 71-79, doi: 10.1016/0031-0182(82)90065-7, 1982.

Volkova, N.I.: Geochemistry of rare elements in waters and sediments of alkaline lakes in the Sasykkul depression, East Pamirs. Chem. Geol., 147, 265–277, doi: 10.1016/s0009-2541(98)00020-5, 1998.

Volodin, R.N., Chechetkin, V.S., Bogdanov, Yu. V., Narkelyun, L.F., and Trubachev, A.I.: The Udokan cupriferous sandstones deposit (eastern Siberia). Geol. Ore Deposits, 36, 1-25, 1994.

Vysotsky, A. U., Galetsky, R.G., Krisrick, Y.U.: World potash deposit Basin. Yang, Q. (trans), Geological Press, Beijing (in Chinese), 2014.

Walker, R.N., Muir, M.D., Diver, W.L., Williams, N., Wilkins, N.: Evidence of major sulphate evaporite deposits in the Proterozoic McArthur Group, Northern Territory, Australia. Nature, 265, 526–529, doi: 10.1038/265526a0, 1977.

Walker, J.C.G., Hays, P.B., Kasting, J.F.: A negative feedback mechanism for the long–term stabilization of Earth's surface temperature. J. Geophys. Res. 86, 9776–9782, doi: 10.1029/JC086iC10p09776, 1981.

Wally, B.: CO2: Earth's Climate Driver. Geochem. Perspect., 7, 117–190, doi: 10.7185/geochempersp.7.2, 2018.

Walter, M.R.: Stromatolites: the main geological source of information on the evolution of the early benthos. In: Bengtson, S. (Ed.), Early Life on Earth, Nobel Symposium, vol. 84. Columbia University Press, New York, pp. 270– 286, 1994.

Walter, M.R., Heys, G.R.: Links between the rise of the metazoa and the decline of the stromatolites. Precambrian Res., 29, 149–174, doi: 10.1016/0301-9268(85)90066-X, 1985.

Wang, J.B., He, Z.L., Zhu, D.Y., Gao, Z.Q., Huang, X.W., Liu, Q.Y.: Organic-Inorganic Geochemical Characteristics of the Upper Permian Pusige Formation in a High-Saline Lake Basin, Tarim Basin: Implications for Provenance, Paleoenvironments, and Organic Matter Enrichment. Geofluids, 2021, 6651747, doi: 10.1155/2021/6651747, 2021.

Wang, R., Lang, X.G., Ding, W.M., Liu, Y.R., Huang, T.Z., Tang, W.B., Shen, B.: The coupling of Phanerozoic continental weathering and marine phosphorus cycle. Sci. Rep., 10, 5794, doi: 10.1038/s41598-020-62816-z, 2020.

Wang, Z.M., Xie, H.W., Chen, Y.Q., Qi, Y.M., Zhang, K.: Discovery and exploration of Cambrian subsalt dolomite original hydrocarbon reservoir at Zhongshen-1 well in Tarim Basin. China Petrol. Explor., 2014, 19, 1–13 (in Chinese with English abstract), doi: 10.3969/j.issn.1672-7703.2014.02.001, 2014.

Warren, J.K.: Evaporites: Sediments, Resources and Hydrocarbons. Springer, Berlin. 1036 p, doi: 10.1007/3-540-32344-9, 2006.

Warren, J.K.: Evaporites through time: Tectonic, climatic and eustatic controls in marine and nonmarine deposits. Earth-Sci. Rev., 98, 217-268, doi: 10.1016/j.earscirev.2009.11.004, 2010.

Warren, J.K.: Geochemistry of Evaporite Ores in an Earth-Scale Climatic and Tectonic Framework. In: Holland, H.D., Turekian, K.K. (Eds.) Treatise on Geochemistry 13, Elsevier, Oxford, pp. 569–591, doi: 10.1016/B978-0-08-095975-7.01125-6, 2014.

https://doi.org/10.5194/egusphere-2023-2091
Preprint. Discussion started: 29 January 2024


Warren, J.K., Havholm, K.G., Rosen, M.R., Parsley, M.J.: Evolution of gypsum karst in the Kirschberg Evaporite Member near Fredericksburg, Texas. J. Sediment. Petrol., 60, 721-734, doi: 10.1306/212F925A-2B24-11D7-8648000102C1865D, 1990.

Whelan, J.F., Rye, R.O., de Lorraine, W., Ohmoto, H.: Isotopic geochemistry of a mid-Proterozoic evaporite basin, Balmat, New York. Am. J. Sci., 290, 396–424, doi: 10.2475/ajs.290.4.396, 1990.

White, A.F., Buss, H.L.: Natural weathering rates of silicate Minerals, in Holland, H.D., and Turekian, K.K. (Eds.) Treatise on Geochemistry 7, 116–151. Oxford: Elsevier, doi: 10.1016/B0-08-043751-6/05076-3, 2014.

White, R.V., Saunders, A.D.: Volcanism, impact and mass extinctions: Incredible or credible coincidences. Lithos, 79, 299–316, doi: 10.1016/j.lithos.2004.09.016, 2005.

White, W.S.: A paleohydrological model for mineralization of the White Pine copper deposit, northern Michigan. Econ. Geol., 66, 1–13, doi: 10.2113/gsecongeo.66.1.1, 1971.

Wignall, P.B.: Large igneous provinces and mass extinctions. Earth. Planet. Sci. Lett., 53, 1–33, doi: 10.1016/S0012-8252(00)00037-4, 2001.

Williams, E.G.: Milankovitch-band cyclicity in bedded halite deposits contemporaneous with Late Ordovician-Early Silurian glaciation, Canning Basin, Western Australia. Earth Planet. Sci. Lett., 103, 143-155, doi: 10.1016/0012-821X(91)90156-C, 1991.

Williford, K.H., Van Kranendonk, M.J., Ushikubo, T., Kozdon, R., Valley, J.W.: Constraining atmospheric oxygen and seawater sulfate concentrations during Paleoproterozoic glaciation: In situ sulfur three-isotope microanalysis of pyrite from the Turee Creek Group, Western Australia. Geochim. Cosmochim. Ac., 75, 5686–5705, doi: 10.1016/j.gca.2011.07.010, 2011.

Willis, G.C.: Geologic map of the Salina quadrangle, Sevier Courtty, Utah. Utah Geol. Miner. Sur. Map, 83, 1986.

Wilson, J.T.: Did the Atlantic close and then re-open? Nature, 211, 676-681, doi: 10.1038/211676a0, 1966.

Wilson, T.P., Long, D.T.: Geochemistry and isotope chemistry of Ca-Na-CI brines in Silurian strata, Michigan Basin, U.S.A. Appl. Geochem., 8, 507-524, doi: 10.1016/0883-2927(93)90079-V, 1993.

https://doi.org/10.5194/egusphere-2023-2091
Preprint. Discussion started: 29 January 2024


Witkind, I.J.: The role of salt in the structural development of central Utah. USGS. Professional Paper, 1528, 145, doi: 10.3133/pp1528, 1994.

Wittrup, M.B., Kyser, T.K.: The petrogenesis of brines in Devonian potash deposits of western Canada. Chem. Geol., 82, 103-128, doi: 10.1016/0009-2541(90)90077-K, 1990.

Witzke, B.J., Bunker, B.J., Rogers, F.S.: Eifelian through lower Frasnian stratigraphy and deposition in the Iowa area, central Midcontinent, U.S.A., in McMillan, N.J., Embry, A.F., and Glass, D.J. (eds.), Devonian of the world. Can. Soc. Petrol. Geol., I, 221-250, 1988.

Wu, Y.P., Liu, C.L., Liu, Y.J., Gong, H.W., Awan, R.S., Li, G.X., Zang, Q.B.: Geochemical characteristics and the organic matter enrichment of the Upper Ordovician Tanjianshan Group, Qaidam Basin, China. J. Petrol. Sci. Eng., 208, 109383, doi: 10.1016/j.petrol.2021.109383, 2022.

Xiong, Y., Tan, X.C., Dong, G.D., Wang, L.C., Ji, H.K., Liu, Y., Wen, C.X.: Diagenetic differentiation in the Ordovician Majiagou Formation, Ordos Basin, China: Facies, geochemical and reservoir heterogeneity constraints. J. Petrol. Sci. Eng., 191, 107179, doi: 10.1016/j.petrol.2020.107179, 2020.

Yang, X.Y., Lai, X.D., Pirajno, F., Liu, Y.L., Ling, M.X., Sun, W.D.: Genesis of the Bayan Obo Fe-REE-Nb formation in Inner Mongolia, north China craton: a perspective review. Precambrian Res., 2017, 288, 39-71, doi: 10.1016/j.precamres.2016.11.008, 2017.

Yardley, B.W.D.: Metal concentrations in crustal fluids and their relationship to ore formation. Econ. Geol., 100, 613-632, doi: 10.2113/100.4.613, 2005.

Yu, K., Cao, Y., Qiu, L., Sun, P.: Depositional environments in an arid, closed basin and their implications for oil and gas exploration: The lower Permian Fengcheng Formation in the Junggar Basin, China. AAPG Bull., 103, 2073–2115, doi: 10.1306/01301917414, 2019.

Yu, K., Cao, Y., Qiu, L., Sun, P., Jia, X., Wan, M.: Geochemical characteristics and origin of sodium carbonates in a closed alkaline basin: The Lower Permian Fengcheng Formation in the Mahu Sag, northwestern Junggar Basin, China. Palaeogeogr. Palaeoclimatol. Palaeoecol., 511, 506–531, doi: 10.1016/j.palaeo.2018.09.015, 2018.

Zhang, C., Cai, Y.Q., Dong, Q., Xu, H.: Cretaceous–Neogene basin control on the formation of uranium deposits in South China: evidence from geology, mineralization ages, and H–O isotopes. Int. Geol. Rev., 62, 3, 263-310, doi: 10.1080/00206814.2019.1598898, 2019.

Zhang, C., Cai, Y.Q., Xu, H., Dong, Q., Liu, J.L., Hao, R.X.: Mechanism of mineralization in the Changjiang uranium ore field, South China: Evidence from fluid inclusions, hydrothermal alteration, and H-O isotopes. Ore Geol. Rev. 86, 225–253, doi: 10.1016/j.oregeorev.2017.01.013, 2017.

Zhang, C., Richard, A., Hao, W.L., Liu, C.H., Tang, Z.S.: Trace metals in saline waters and brines from China: Implications for tectonic and climatic controls on basin-related mineralization. J. Asian Earth Sci., 233, 105263, doi: 10.1016/j.jseaes.2022.105263, 2022.

Zhang, C., Richard, A., Hao, W.L.: Active metal deposition in a giant geothermal system. Terre Nova, 35, 313-328, doi: 10.1111/ter.12656, 2023a.

Zhang, C., Yang, H.T.: An Active Molybdenum (Polymetallic) – Enriching System in Foreland Basins. Journal of Geochemical Explorations, doi: 10.1016/j.gexplo.2023.107309, 2023b.

Zhang, C.J., Cao, J., Li, E.T., Wang, Y.C., Xiao, W.J., Qin, Y.: Revisiting Controls on Shale Oil Accumulation in Saline Lacustrine Basins: The Permian Lucaogou Formation Mixed Rocks, Junggar Basin. Geofluids, 2021, 5206381, doi: 10.1155/2021/5206381, 2021.

Zhang, S.H., Zhao, Y., Liu, Y.S.: A precise zircon Th-Pb age of carbonatite sills from the world's largest Bayan Obo deposit: Implications for timing and genesis of REE-Nb mineralization. Precambrian Res., 2017, 291, 202-219, doi: 10.1016/j.precamres.2017.01.024, 2017.

Zhao, G.C., Cawood, P.A., Wilde, S.A., Sun, M.: Review of global 2.1-1.8Ga orogens: implications for a pre-Rodinia supercontinent. Earth-Sci. Rev., 59, 125-162, doi: 10.1016/S0012-8252(02)00073-9, 2002.

Zharkov, M.A.: Evaporite sedimentation in the Precambrian as related to changes in biosphere and seawater chemistry. Article 1: Evaporites of the Archean and Lower Proterozoic. Stratigr. Geol. Correl., 13, 134–142, doi: 10.2113/108.1.135, 2005.

Zheng, M.P.: An Introduction to Saline Lakes on the Qinghai–Tibet Plateau. Boston, MA, Kluwer, 294, 1997.

Zheng, M.P., Xiang, J., Wei, X.J., Zheng, Y.: Saline lakes on the Qinghai–Xizang (Tibet) Plateau. Beijing, Beijing Scientific and Technical Publishing House, 1–404 (in Chinese with English abstract), 1989.

Zhong, R.C., Li, W.B., Chen, Y.J., Hou, H.L.: Ore-forming conditions and genesis of the Huogeqi Cu–Pb–Zn–Fe deposit in the northern margin of the North China Craton: evidence from ore petrologic characteristics. Ore Geol. Rev., 44, 107-120, doi: 10.1016/j.oregeorev.2011.09.008, 2012.

Zhu, G.Y., Yang, H.J., Zhang, B., Su, J., Chen. L., Lu. Y.H., Liu, X.G.: The geological feature and origin of Dina 2 large gas field in Kuqa Depression, Tarim Basin. Ac. Petrol. Sin., 28, 2479e92, doi: 10.1016/j.sedgeo.2012.06.004, 2012.

Ziegler, A.M., Eshel, G., Rees, P.M., Rothfus, T.A., Rowley, D.B., Sunderlin, D.: Tracing the tropics across land and sea: Permian to present. Lethaia, 36, 227–254, doi: 10.1080/00241160310004657, 2003.

Appendix A Major hydrothermal type uranium districts of the world, with showing their major enriched metal affinities and regional contemporaneous saline deposits and/or redbeds (detailed reference in Dahlkamp, 2009, 2010, 2016).

| No. | Continent | Country | Major U District (Belt) | Ore deposit type | Representative U Deposit | Resource | Mineralization Age | Contemporaneous Saline Giant (or Redbeds) in the Region? |
|---|---|---|---|---|---|---|---|---|
| 1 | Europe | Austria | Land Salzburg | Strata-bound and structure-controlled | Mitterberg | >700 t U, ~0.1% U | 290-260Ma, 90±5Ma | Permian and Jurassic evaporites in Europe |
| 2 | Europe | Bulgaria | Bukhovo district and other deposits | Structure-controlled, Vein type | Bortshe, Goten, Kamiko | >25000 t U, 0.02-3% U | 4Ma, 1-2Ma? | Messinian saline giant |
| 3 | Europe | Czech Republic | Northwest Bohemian U region | Structure-controlled, Vein type | Horni Rozmysl, Prisenice | >10000 t U, 0.1 to 1% U | 280-260Ma | Permian evaporites in Europe |
| 4 | Europe | Czech Republic | Horni Slavkov (Schlaggenwald) district | Structure-controlled, Lignite, Coal type | Barbora, Nadlesi, Zdar Buh | 1000 t U | 280-260Ma | Permian evaporites in Europe |
| 5 | Europe | Czech Republic | West Bohemian district | Structure-controlled, Vein type | Tachova, Vitkov I and II | >12000 t U, 0.05-0.2% U | 185±15Ma | Saline aquifers of Central Europe |
| 6 | Europe | Czech Republic | Central Bohemian U region | Structure-controlled, Vein type | Pribram district | >80000 t U, 0.15% U | 280-240 (265±15) Ma | Permian evaporites in Europe |

https://doi.org/10.5194/egusphere-2023-2091
Preprint. Discussion started: 29 January 2024


| | | | | | | | | |
|---|---|---|---|---|---|---|---|---|
| 7 | Europe | Czech Republic | Southwest Bohemian U region | Structure-controlled, Vein type | Dametice, Ustalec, Zelenov | > 3000 t U, 0.1-0.2% U | 280-240 (265±15) Ma | Permian evaporites in Europe |
| 8 | Europe | Czech Republic | West Moravian region | Structure-controlled, Vein type | Dancovice, Slavkovice | >25000 t U, 0.08-0.15% U | 270±15 Ma; 190±10Ma | Permian and Jurassic evaporites in Europe |
| 9 | Europe | Czech Republic | Other Major U deposits | Structure-controlled, Vein type | Rychlebskehory, Orlickehory | >5000 t U, 0.1-0.2% U | 280-250 (265) Ma | Permian evaporites in Europe |
| 10 | Europe | Finland | Proterozoic U deposits in Finland | Structure-controlled, Vein type, Polymetallic | Juomasuo, Hangaslampi | >1500 t U, >20 g/t Au, 0.03% Co, 0.18% Cu, 0.13% Mo, 0.20% U | 1900-1800Ma | Early Proterozoic evaporites in Baltica |
| 11 | Europe | France | La Crouzille district, Limousin | Structure-controlled, Vein type | Margnac-Peny ore field | 25000 t U, 0.1-0.3% U | 280-260 (270)Ma; 190-150Ma; 30Ma | Permian and Jurassic evaporites in Europe |
| 12 | Europe | France | La Marche | Structure-controlled, Vein type | Bernardan, Mas Grimaud, Piegut | 10000 t U, 0.03-1.5% U | 280-260 (270)Ma; 190-150Ma; 30Ma | Permian and Jurassic evaporites in Europe |
| 13 | Europe | France | Plateau de Millevaches | Structure-controlled, Vein type | Northern Millevaches | 2000 t U, 0.15-0.3% U | 270Ma; Oligocene-Early Miocene | Permian and Miocene evaporites in Europe |
| 14 | Europe | France | Forez District | Structure-controlled, Vein type | Bois Noirs-Limouzat | 7500 t U, 0.05-0.5% U | 270Ma; Oligocene-Early Miocene | Permian and Miocene evaporites in Europe |
| 15 | Europe | France | Morvan District | Structure-controlled, Vein type | Le Cartelet, Mazille, Niallin | 1500 t U, 0.1-0.4% U | 175±5Ma | Jurassic evaporites |
| 16 | Europe | France | Margeride district | Structure-controlled, Vein type | Le Vigan, Les Bondons | 4024 t U, 0.05-0.3% U | 188±12Ma | Jurassic evaporites |
| 17 | Europe | France | Rouergue-Levezou Massifs and adjacent regions | Structure-controlled, Vein type | Entraygues, Saint Leger de Peyre | 759.2 t U; 0.15% U | 180-170Ma | Jurassic evaporites |
| 18 | Europe | France | Mortagne Massif | Structure-controlled, Vein type | Le Chardon ore field | 15600 t U, 0.03-0.7% U | 420-390Ma; 345-310Ma; 280-260Ma (290-270Ma); 180Ma; 70Ma | Middle Devonian, Carboniferous, Permian, Jurassic, Late Cretaceous Saline deposits |
| 19 | Europe | Germany | Schneeberg-Schlema-Alberoda ore field | Structure-controlled, Vein type | Schneeberg, Bernsbach | 96603 t U; | 278-270Ma, 250-240Ma, 185-180Ma, 160-140Ma | Middle Devonian, Carboniferous, Permian, Jurassic Saline deposits |

https://doi.org/10.5194/egusphere-2023-2091
Preprint. Discussion started: 29 January 2024


| | | | | | | | | |
|---|---|---|---|---|---|---|---|---|
| 20 | Europe | Germany | Schwarzenberg ore field | Structure-controlled, Vein type | Bermsgrun, Weiber Hirsch | 1051.9 t U | 278-270Ma, 250-240Ma, 185-180Ma, 160-140Ma | Middle Devonian, Carboniferous, Permian, Jurassic Saline deposits |
| 21 | Europe | Germany | Johanngeorgenstadt ore field | Structure-controlled, Vein type | Rabenberg, Seifenbach | 4537 t U | 278-270Ma, 250-240Ma, 185-180Ma, 160-140Ma | Middle Devonian, Carboniferous, Permian, Jurassic Saline deposits |
| 22 | Europe | Germany | Pohla-Tellerhauser ore field | Structure-controlled, Vein type | Ehrenzipfel, Tellerhauser | 7918.6 t U | 278-270Ma, 250-240Ma, 185-180Ma, 160-140Ma | Middle Devonian, Carboniferous, Permian, Jurassic Saline deposits |
| 23 | Europe | Germany | Central Erzgebirge | Structure-controlled, Vein type | Barenstein-Niederschlag | 800 t U | 278-270Ma, 250-240Ma, 185-180Ma, 160-140Ma | Middle Devonian, Carboniferous, Permian, Jurassic Saline deposits |
| 24 | Europe | Germany | East Erzgebirge | Structure-controlled, Vein type | Barenhecke, Freiberg | 32000 t U | 278-270Ma, 250-240Ma, 185-180Ma, 160-140Ma | Middle Devonian, Carboniferous, Permian, Jurassic Saline deposits |
| 25 | Europe | Germany | Konigstein district, a northern extension of the North Bohemian Basin | Sandstone type | ? | 27812 t U | 74Ma, 49.5Ma, 24Ma | Late Cretaceous – Early Paleogene, Miocene evaporites |
| 26 | Europe | Germany | Dohlen Basin, Freital district | Lignite type U deposits | Heidenschanze, Gittersee | 3977 t U | 240Ma | Triassic evaporites |
| 27 | Europe | Germany | Kyhna-Schenkenberg | Structure-controlled, Vein type | Schenkenberg, Quering | 6660 t U | 250-280Ma, 76-40Ma | Permian, Late Cretaceous to Early Paleogene evaporites |
| 28 | Europe | Germany | Gera-Ronneburg Region, East Thuringia | Black Shale | Ronneburg, Stolzenberg | 200 000 t U | 280-260Ma, 240Ma, 120-90Ma | Permian, Triassic, Late Cretaceous to Early Paleogene evaporites |
| 29 | Europe | Germany | East Thuringian Anticline | Black Shale | ? | 15 300 t U | 280-260Ma, 240Ma, 120-90Ma | Permian, Triassic, Late Cretaceous to Early Paleogene evaporites |
| 30 | Europe | Germany | Grobschloppen-Hebanz/Weibenstadt Granitic Massif | Structure-controlled, Vein type | Grobschloppen, Rudolfstein | >2000 t U | ~268Ma, ~233Ma | Permian and Triassic evaporites |
| 31 | Europe | Germany | Poppenreuth-Mahring area | Structure-controlled, Vein type | Hohensteinweg, Waldel | ? | ~336±17Ma, 295±5Ma | Carboniferous and Permian evaporites |
| 32 | Europe | Germany | Schwarzach Valley/Neunburg Massif | Structure-controlled, Vein type | Altfalter | ? | ~360Ma? ~210Ma? | Carboniferous and Triassic evaporites |

https://doi.org/10.5194/egusphere-2023-2091
Preprint. Discussion started: 29 January 2024


| | | | | | | | | |
|---|---|---|---|---|---|---|---|---|
| 33 | Europe | Germany | Other deposits in Northeast Bavaria | Structure-controlled, Vein type | Schonthan, Wolsendorf-Nabburg | ? | ~295±14Ma? | Permian evaporite |
| 34 | Europe | Germany | Menzenschwand district | Structure-controlled, Vein type | Krunkelbach Mine | ? | 310±3Ma, 65Ma, 295±7Ma, 50±8Ma | Triassic, Permian, Late Cretaceous to Early Paleogene evaporites |
| 35 | Europe | Germany | Upper Kinzigtal district | Structure-controlled, Vein type | Stammelbach Valley, Wittichen | ? | 230-245Ma; 240Ma | Triassic evaporites |
| 36 | Europe | Germany | Other deposits in Schwarzwald region | Structure-controlled, Vein type | Sulzburg, St. Ulrich, Fischerhof | ? | ~240Ma, 160±20Ma | Triassic and Jurassic evaporites |
| 37 | Europe | Polland | Kowary Ore Field, Kletno Ore Field | Structure-controlled, Vein type | ? | 760 t U | 265Ma, 70Ma | Triassic, Late Cretaceous to Early Paleogene evaporites |
| 38 | Europe | Romania | Major deposits in Romania | Structure-controlled, Vein type | Arieseni, Avram lancu | 16500-17000 t U | 280Ma, 230Ma, 110Ma | Permian, Triassic, and Cretaceous evaporites |
| 39 | Europe | Russian Federation | Lake Ladoga district | Unconformity-related, Hydrothermal metasomatic type | Salmi, Shotkusa | 35 000 t U | 1.8-1.75Ga; 1.5Ga; 412±11Ma | Paleo-Proterozoic, Meso-proterozoic, and Late Silurian to Early Devonian evaporite |
| 40 | Europe | Russian Federation | Lake Onega district | Metasomatism type | Srednaya Padma, Tsarevskoye, | 9 000 t U | 1740±30Ma | Paleo-Proterozoic evaporite |
| 41 | Europe | Russian Federation | Northern Caucasus region | Structure-controlled, Volcanic type | Naratinskoye, Dakhovskoye | ? | 190Ma, 140Ma, 115Ma, 40Ma? | Jurassic, Cretaceous, and Early Paleogene evaporites |
| 42 | Europe | Slovak Republic | Gemer zone | Structure-controlled, Volcanic type | Cierna hora, Haniskova | 25000 t U; >3000 t Mo | 240±30Ma, 130±20Ma | Triassic and Cretaceous evaporites |
| 43 | Europe | Slovak Republic | Kozie Chrbty Mountains and Northern Lower Tatra | Stratiform type | Vikartov-Cierny Vah zone | >3000 t U, >0.10% U | 160Ma, 105-70Ma | Jurassic and Cretaceous evaporite |
| 44 | Europe | Slovak Republic | Major deposits in Slovak Republic | Structure-controlled, Volcanic type | Kalnica, Krajna dolina, Selec | >2000 t U, 0.1% U | 160Ma | Jurassic evaporite |
| 45 | Europe | Portugal | Beiras (Guarda-Viseu) U region | Structure-controlled, Vein type | | >10 000 t U, 0.1-0.25% U | 100-60Ma, 57-37Ma | Late Cretaceous to Early Paleogene evaporite |
| 46 | Europe | Spain | South Spain region | Structure-controlled, Vein type | Aguila, Alameda, Villar, Retortillo ore field | 36700 t U, 0.05% U | 57-37Ma | Early Paleogene evaporites |

https://doi.org/10.5194/egusphere-2023-2091
Preprint. Discussion started: 29 January 2024


| | | | | | | | | |
|---|---|---|---|---|---|---|---|---|
| 47 | Europe | Sweden | Petrozoic U deposits in Sweden | Structure-controlled, Vein type, Metasomatism | Arvidsjaur, Arjeplog, and Sorsele region | 10000 t U, 0.03-0.1% U | 1738±10Ma, 1736-1767Ma | Paleo-Proterozoic evaporites |
| 48 | Europe | Sweden | Other U deposits in Sweden | Structure-controlled, Vein type | Flistjarn, Klappibacken | >2000 t U | 420±1Ma | Late Silurian evaporites |
| 49 | Europe | Switzerland | Les Marecottes-La Creusa area | Structure-controlled, Vein type | Gisiger, Juillard | > 1000 t U | 270Ma, 240Ma | Permian and Triassic evaporites |
| 50 | Europe | Ukraine | Kirovograd-Smolino region | Structure-controlled, Metasomatism | Michurinsk ore field | 250 000 t U, 0.08-0.14% U | 1812±42 to 1753±42Ma; 1.84-1.80Ga; 1.8-1.7Ga | Paleo-Proterozoic evaporites |
| 51 | Europe | Ukraine | Krivoy Rog region | Structure-controlled, Metasomatism | Annovskoye, Krasnogvardeiskoye | >25000 t U, 0.1% U | 1770±50Ma | Paleo-Proterozoic evaporites |
| 52 | Europe | Ukraine | Pobuzhsky region | Structure-controlled, Metasomatism | Kalinovskoye, Lozovatskoye | >15000 t U, 0.5-0.22% U | 1770±50Ma | Paleo-Proterozoic evaporites |
| 53 | Europe | Ukraine | Ingul Megablock | Structure-controlled, Vein type | Geikovskoye, Lagodovskoye | >3000 t U, >0.10% U | 1770±50Ma | Paleo-Proterozoic evaporites |
| 54 | Europe | Ukraine | Dnieper Block | Structure-controlled, Vein type | Sergeevskoye | >3000 t U, >0.10% U | 1770±50Ma | Paleo-Proterozoic evaporites |
| 55 | Europe | Ukraine | Priazov Block | Structure-controlled, Vein type | Barbasovskoye, Dibrovskoye | >3000 t U, >0.10% U | 1770±50Ma | Paleo-Proterozoic evaporites |
| 56 | Europe | United Kingdom | Southwest U region in U.K. | Structure-controlled, Vein type | Restormel Royal, South Terras | >2000 t U | 280-270Ma, 244-212Ma, 175-160Ma, 75-55Ma | Permian, Triassic, Jurassic and Late Cretaceous to Early Paleogene evaporites |
| 57 | Asia | China | Wuyishan Belt | Structure-controlled, Vein type | Maoyangtou | >50000 t U | 127-137Ma, ~81Ma, 71-75Ma | Cretaceous evaporites |
| 58 | Asia | China | Taoshan-Zhuguang Belt | Structure-controlled, Vein type | Juntian, Dabu | >50000 t U | ~147-152Ma, ~101-110Ma, ~82-89Ma; ~65-67Ma, ~52-57Ma, ~42-45Ma | Late Jurassic to Early Paleogene evaporites |
| 59 | Asia | China | Chenzhou-Qinzhou U Belt | Structure-controlled, Vein type | Jiuyishan | >50000 t U | ~70Ma, ~55-64Ma | Late Cretaceous to Early Paleogene evaporites |
| 60 | Asia | China | Gan-Hang Belt | Structure-controlled, Vein type | Xiangshan district | >50000 t U | ~141-148Ma, ~120-130Ma, ~84-94Ma | Late Jurassic to Early Paleogene evaporites |
| 61 | Asia | China | Xixia-Luzong Belt | Structure-controlled, Vein type | Xixia | >20000 t U | 110-120MaMa, 60Ma | Late Cretaceous to Early Paleogene evaporites |
| 62 | Asia | China | Mufushan-Hengshan Belt | Structure-controlled, Vein type | Jinguanchong, Baofengyuan | >20000 t U | ~5-14Ma, ~24-26Ma | Miocene evaporite |

https://doi.org/10.5194/egusphere-2023-2091
Preprint. Discussion started: 29 January 2024


| | | | | | | | | |
|---|---|---|---|---|---|---|---|---|
| 63 | Asia | China | Xuefengshan-Jiuwandashan Belt | Structure-controlled, Vein type | Silihe | >20000 t U | ~316-360Ma, ~60-71Ma, ~73-88Ma, ~44Ma | Carboniferous, Late Cretaceous to Early Paleogene evaporites |
| 64 | Asia | China | Jungar-Tien Shan | Structure-controlled, Vein type | Baiyanghe | >1000 t U | ~230Ma | Triassic evaporites and redbeds |
| 65 | Asia | China | Liaoning Region/Yinshan-Liaohe Belt | Structure-controlled, Vein type | Lianshanguan | >3000 t U | 1894Ma; 1829Ma; 1810Ma; 1823Ma | Paleo-Proterozoic evaporites and redbeds |
| 66 | Asia | China | Yanshan Belt | Structure-controlled, Vein type | Dashiqiao | 4 000 t U | 1763-1794Ma; 226Ma | Paleo-Proterozoic, Triassic evaporites and redbeds |
| 67 | Asia | China | Taihangshan Belt | Structure-controlled, Vein type | Wutaishan | 1500 t U | 1765-1746Ma; 103Ma; 122Ma | Paleo-Proterozoic, Cretaceous evaporites and redbeds |
| 68 | Asia | China | Qinglong Region/Yinshan-Liaohe Belt | Structure-controlled, Vein type | Qinglong | 8000 t U; 0.03 to 0.1% U | 124Ma | Cretaceous evaporites |
| 69 | Asia | China | Guyuan Region/Yinshan-Liaohe Belt | Structure-controlled, Vein type | Zhangmajing | > 3000 t U | ~90Ma; ~24Ma | Late Cretaceous evaporites |
| 70 | Asia | China | Hongshanzi Region/Yinshan-Liaohe Belt | Structure-controlled, Vein type | Hongshanzi | ~3000 t U | ~90Ma | Late Cretaceous evaporites |
| 71 | Asia | China | Longshoushan region/Qilian-Qinling | Structure-controlled, Vein type | Hongshiquan | 1500-3000 t U, 0.03-0.1% U | ~1760Ma; 700-600Ma | Paleo-Proterozoic redbeds, |
| 72 | Asia | China | Longshoushan region/Qilian-Qinling | Structure-controlled, Vein type | Jiling | 1500-3000 t U, 0.03-0.1% U | 430-400Ma; 383-357Ma | Devonian evaporites |
| 73 | Asia | China | North Qinling region/Qilian-Qinling | Structure-controlled, Vein type | Lantian | ~8000 t U, 0.171 % U | 96Ma | Late Cretaceous |
| 74 | Asia | China | North Qilian region/Qilian-Qinling | Structure-controlled, Vein type | | <3000 t U | 280-260Ma | Permian evaporites |
| 75 | Asia | China | Ruoergai region/Qilian-Qinling | Structure-controlled, Vein type | Luojungou | >3000 t U | 130-45Ma | Late Cretaceous to Early Paleogene evaporites |
| 76 | Asia | India | Singhbhum Cu-U Belt | Structure-controlled, Vein type | Khadandungri-Purandungri ore field | 56000 t U | 1766+82Ma; 1.5-1.6Ga | Paleo-Proterozoic redbeds |

https://doi.org/10.5194/egusphere-2023-2091
Preprint. Discussion started: 29 January 2024


| | | | | | | | | |
|---|---|---|---|---|---|---|---|---|
| 77 | Asia | India | Cuddapah Basin | Unconformity-proximal, and fracture-controlled types | Nalgonda and Guntur Districts/ Srisailam Subbasin | 22 000 t U | 1756 ± 29 Ma | Paleo-Proterozoic redbeds |
| 78 | Asia | India | Bhima Basin | Unconformity-proximal, and fracture-controlled types | | 1300 t U; 0.16% U | 1756 ± 29 Ma; | Paleo-Proterozoic redbeds |
| 79 | Asia | Iran | Saghand Ore Field | Metasomatic and hydrothermal vein type | | 1400 t U | ? | ? |
| 80 | Asia | Kazakhstan | Kokshetau region | Vein-stockwork type | Ishimsky Ore Field, Forty uranium deposits | 230000 t U; 0.1-0.2% U | ~380-360Ma | Devonian evaporites |
| 81 | Asia | Kazakhstan | Kendyktas-Chuily-Betpak Dala region | Vein-stockwork type | Dzhideli Ore Field | 65000 t U; 0.1-0.3% U | 370-350Ma; 285-265Ma | Devonian and Permian evaporites |
| 82 | Asia | Kyrgyzstan | Eastern Karamazar-Northeastern Fergana Region | Vein-stockwork type | Charkasar, Mayluu-Suu, Shakaptar, and Malisay | 12000 t U; 0.1-0.3% U | 370-350Ma; 285-265Ma | Devonian and Permian evaporites |
| 83 | Asia | Mongolia | Mardai, Ugtam, Turgen, Engershand | Vein type, volcanic type | Dornod, Gurvan bulag | 57 000 t U; 0.16% U | 138-136Ma | Cretaceous evaporites |
| 84 | Asia | Russian Federation, Asian Territory | Yenisey Region | Vein type, volcanic type | Labyshkoye, Solonechnoye | >2000 t U, 0.1% U | 350-370Ma | Devonian evaporites |
| 85 | Asia | Russian Federation, Asian Territory | Streltsovsk district | Vein type, volcanic type | 19 deposits, Streltsovskoye , Tulukuyevskoye, and Octyabrskoye | 28 0000 t U; 0.1-0.3% U | 136-134Ma; 18-17Ma | Cretaceous, Miocene evaporites |
| 86 | Asia | Russian Federation, Asian Territory | Central Transbaykal region | Vein type, volcanic type | Olovskoye and Imskoye | 40000 t U; 0.01-0.1% U | 110-100Ma | Cretaceous evaporites |
| 87 | Asia | Russian Federation, Asian Territory | Elkon district | vein-stockwork-type | Agdinskaya, Severnoye, Sokhsolookhsk | 342 000 t U; 0.1-0.15% U | 135-130Ma | Cretaceous evaporites |

| | | | | | | | | |
|---|---|---|---|---|---|---|---|---|
| 88 | Asia | Russian Federation, Asian Territory | Bureinsky District | vein-stockwork type | Lastochka, Kamenushinskoye, Skalnoye, Svetloye | 29000 t U; 0.03-0.2% U | 136-134Ma | Cretaceous evaporites |
| 89 | Asia | Russian Federation, Asian Territory | Tas-Kastabyt | Volcanic type, vein type | | >3000 t U; 0.1-0.3% U | 119-89Ma; 127Ma; 72Ma; 60-50Ma | Cretaceous to Early Paleogene evaporites |
| 90 | Asia | Turkmenistan | Karamazar Uranium Region | vein stockwork type | Chauli, Alatanga | 20 000 t U; 0.1-0.3% U | 275-267Ma; 280-270±10Ma | Permian evaporites |
| 91 | America | USA | Arizona Strip Area | Collapse Breccia Pipes | Orphan Lode | 12000-15000 t U; 0.3-0.7% U | 260Ma; 200±20Ma; 141Ma | Permian and Jurassic evaporites |
| 92 | America | USA | Spokane Mountain Area | Vein type | Midnite and Sherwood | 15000 t U; | 51Ma | Late Cretaceous to Early Paleogene evaporites |
| 93 | America | USA | Ralston Buttes | Vein type | Schwartzwalder | >7500 t U; 0.408% U | 70-52Ma; 69.3 ± 1.1 Ma | Late Cretaceous to Early Paleogene evaporites |
| 94 | America | USA | Marshall Pass District | Vein type | Pitch deposit | >11 000 t U; >0.1% U | Laramide to Mid-Teritary age | ? |
| 95 | America | USA | McDermitt Caldera District, Nevada-Oregon; | Vein type | Aurora | >10000 t U; 0.04% U | 13.3 ± 2 Ma; 12.3 ± 7 Ma | Miocene redbeds and evaporites |
| 96 | America | USA | Lakeview District, Oregon | Vein type | White King | >200 t U | | ? |
| 97 | America | USA | Spor Mountain/Thomas Caldera, Utah | Vein type | ? | ? | 21Ma | Miocene redbeds and evaporites |
| 98 | America | USA | Marysvale Volcanic Complex, Utah | Vein type | ? | 540 t U | ~20Ma; 19-18Ma | Miocene redbeds and evaporites |
| 99 | America | USA | Date Creek Basin, Arizona | Vein type | ? | 12000 t U; 0.06% U | ~20Ma; 19-18Ma | Miocene redbeds and evaporites |
| 100 | America | USA | Sierra Ancha/Apache Proterozoic Basin, Arizona | Vein type | ? | 38 00 t U; 0.15-0.32% U | 1.8-1.7Ga? | Paleo-Proterozoic redbeds and evaporites |
| 101 | America | USA | Coles Hill | Vein type, Disseminated impregnation-type | ? | 45770 t U; 0.05% U | 562 ± 5 Ma; 417Ma | Neo-Proterozoic redbeds and evaporites; Late Silurian |
| 102 | America | Mexico | Sierra de Peña Blanca | Vein type | Nopal-1 | 4000 t U; 0.1% U | 43.8-37.3Ma | Early Paleogene |
| 103 | America | Brazil | Caetité Massif | Metasomatite type | Ten deposits | 85 000 t U; 0.15% U | 1400Ma? | ? |
| 104 | America | Brazil | Central Ceará Region, Itataia | Vein type | Santa Quitéria Deposit | 12 0000 t U; 0.08% U | 1.8-1.7Ga | Paleo-Proterozoic redbeds and evaporites |

https://doi.org/10.5194/egusphere-2023-2091
Preprint. Discussion started: 29 January 2024


| | | | | | | | | |
|---|---|---|---|---|---|---|---|---|
| 105 | America | Brazil | Poços de Caldas Region | Vein type | Cercado and Agostinho | 27000 t U; 0.07% U | 80-60Ma; | Late Cretaceous to Early Paleogene |
| 106 | America | Brazil | Seridó Region | Metasomatite type | Espinharas Deposit | 4240 t U; 0.04% U | 450Ma? | ? |
| 107 | America | Brazil | Parana Basin | | | 11000 t U; | Triassic | ? |
| 108 | America | Canada | Great Bear Batholith | Vein type, Metasomatite type | | 20000 t U | 1860±20Ma, 1424±29Ma, 1076±96Ma, 457±26Ma, 511±86Ma, 415±29Ma, 536±66Ma, 339±22Ma, 125±48Ma | Episodic evaporites and redbeds of Paleo-Proterozoic to Neo-Proterozoic |
| 109 | America | Canada | Athabasca Basin | Unconformity type | | 150000 t U | 1770-1730Ma (1740Ma), 1590Ma, 1500-1520Ma, 1440Ma, 1350-1330Ma, 1290Ma, 1250Ma, 1190Ma, 1150Ma, 1120Ma, 1075Ma, 1030Ma, 1000Ma, 920Ma, 825Ma, 750Ma, 671Ma, 643Ma, 530Ma, 250Ma, 116Ma | Episodic evaporites and redbeds of Paleo-Proterozoic to Neo-Proterozoic |
| 110 | America | Canada | Thelon | Unconformity type, vein type | | 5 0000 t U | 1860Ma, 1667-1640Ma, 1520-1500Ma, 1284Ma, 1200Ma, 1131-1100Ma, 982Ma, 577Ma, 532Ma, 513Ma, 489Ma, 284Ma | Episodic evaporites and redbeds of Paleo-Proterozoic to Neo-Proterozoic |
| 111 | America | Canada | Beaverlodge | Vein type | | 100000 t U | 2058±34Ma, 1875-1855Ma, 1740Ma, | Episodic evaporites and redbeds of Paleo- |

https://doi.org/10.5194/egusphere-2023-2091
Preprint. Discussion started: 29 January 2024


| | | | | | | | |
|---|---|---|---|---|---|---|---|
| | | | | | | 1450Ma, 1200Ma, 422±38Ma, 340±4Ma | Proterozoic to Neo-Proterozoic |
| 112 | Australia | Australia | Kombolgie Basin | Unconformity type, vein type | 3 0000 t U | 1690-1680Ma, 1650-1600Ma, 1521±8Ma, 1445±20Ma, 1348±16Ma, 1040Ma, 474±6Ma | Episodic evaporites and redbeds of Paleo-Proterozoic to Neo-Proterozoic |
| 113 | Australia | Australia | North Olary Province | Vein type | 3 0000 t U | 1705Ma, 1580Ma, 580Ma, 513Ma | Episodic evaporites and redbeds of Paleo-Proterozoic to Neo-Proterozoic |
| 114 | Australia | Australia | Pink Creek Inlier | Unconformity type | 5 0000 t U | 1740Ma, 1723Ma, 1680Ma, 1650-1600Ma, 1560Ma | Episodic evaporites and redbeds of Paleo-Proterozoic to Neo-Proterozoic |
| 115 | Australia | Australia | Mounte Isa | Na-Metasomatite type | 3 0000 t U | 1750-1730Ma, 1640Ma, 1534Ma, 1523-1505Ma | Episodic evaporites and redbeds of Paleo-Proterozoic to Neo-Proterozoic |
| 116 | Australia | Australia | South Australia | Olympic Dam | 30 0000 t U | 1590Ma | Episodic evaporites and redbeds of Paleo-Proterozoic to Neo-Proterozoic |
| 117 | Africa | Gabon, Africa | Franceville | Unconformity type | 5 0000 t U | 1950±40Ma, 890-860Ma, 500Ma | Episodic evaporites and redbeds of Paleo-Proterozoic to Neo-Proterozoic |

Appendix B Inferred and direct evidence of evaporites from Proterozoic to Cenozoic, based on the compilation by Pope and Grotzinger (2003), Bekker et al. (2006), Schroder et al. (2008).

| No. | Location | Age (Ga) | Units | Evaporite evidence | Thickness | Notes | Reference |
|---|---|---|---|---|---|---|---|
| 1 | Canada | Ca. 2.22-2.3 | Gordon Lake Formation, Huronian Supergroup | Ba (as beds), silicified and pristine anhydrite and gypsum nodules and layers, Si-tr-An, beds of anhydrite | Multiple horizons in >300m | SG, marine, passive margin, supratidal and sabkha zone, correlated with | Cameron, 1983; Bekker et al., 2006 |

https://doi.org/10.5194/egusphere-2023-2091
Preprint. Discussion started: 29 January 2024


| | | | | | | | |
|---|---|---|---|---|---|---|---|
| | | | | nodules | | Chocolay Group | |
| 2 | USA | Ca. 2.22-2.3 | Kona Dolomite, Chocolay Group | Si-ps-Gy, Si-ps-An, ps-Ha (moulds), sc-breccias | 30-1000m | SG, marine, associated with volcanics, intracratonic basin, open to passive margin, correlated with Gordon lake Formation | Bekker et al., 2006 |
| 3 | Australia | Ca. 2.2 | Bartle Member, Killara Formation, Yerrida Group | Si-ps-An, Si-ps-Gy, Kao-ps-Gy or An, An (relics), ps-Sh, ps-Tro | ? | Playa lake (Alkaline) | Pirajno and Gray, 2002 |
| 4 | Africa | 2.2 | Pretoria Group, South Africa | Ps-Mir | < 2m | Sodic lake deposits in a playa setting | Pope and Grotzinger, 2003 |
| 5 | Australia | Ca. 2.15 (2.2) | Bubble Well Member, Juderina Formation, Yerrida Group | Si-Evp, Q-ps-Gy, Q-ps-An | Ca. 100m | SG, Marine or marginal marine, associated with volcanics | El-Tabakh et al., 1999 |
| 6 | Africa | Ca. 2.15 (2.10-2.20) | Lucknow Formation, Olifanshoek Group and Transvaal Supergroup, South Africa | Q-ps-Gy, Q-ps-An, molds after gypsum and anhydrite | ? | Marine, passive margin | Bekker et al., 2006; Schro¨der et al., 2008 |
| 7 | Canada | Ca. 2.15 | Laparre Formation, Peribonca Group, Otish Supergroup | Dol-ps-Gy, Dol-ps-An (after crystals and nodules) | ? | Passive margin | Bekker et al., 2006 |
| 8 | USA | Ca. 2.15 | Lower part of the Nash Fork Formation, Snowy Pass Supergroup | Molds after anhydrite nodules and gypsum crystals | ? | Passive margin | Bekker et al., 2006 |
| 9 | Africa | Ca. 2.2-2.0 | Francevillian C Formation, Francevillian | Ca-ps-An, Ca-ps-Gy | ? | Marine, supratidal-sabkha | Preat et al., 2011 |

| | | | | | | | |
|---|---|---|---|---|---|---|---|
| | | | Group, Gabon | | | environment | |
| 10 | Africa | Ca. 2.15 | Norah Formation, Deweras Group, Zimbabwe | An, as layers | ? | Intracratonic rift basin | Bekker et al., 2006 |
| 11 | Russia | Ca. 2.1 | Fedorovka (Fedorov) Formation (Aldan Shield) | An, as layers and veins | ? | Passive margin | Zharkov, 2005; Bekker et al., 2006 |
| 12 | Russia | Ca. 2.09 | Tulomozero Formation, Upper Jatulian Group | Ca-ps-Gy, Dol-ps-Gy, Si-ps-Gy, An, pseudomorphs after anhydrite and gypsum crystals and nodules, ps-Ha, sc-breccias, enterolithic and chicken wire structures | Multiple units >20m, within ca. 500m of total thickness | SG, passive margin, playa lake, marine sabkha, intertidal flats | Melezhik et al., 2005; Brasier et al., 2011; Reuschel et al., 2012 |
| 13 | Africa | 2.06 | Dewaras Group, South Africa | Gy | | Lacustrine environment in rift | Pope and Grotzinger, 2003 |
| 14 | Canada | Ca. 1.95 | Rocknest Formation, Coronation Supergroup, Slave craton | Dol-ps-Gy, ps-An, ps-Ha | Traces of evaporites dispersed within carbonates | SG, marine, lagoon on inner shelf, passive margin | Evans, 2006 |
| 15 | Canada | 1.8-2.0 | Kasegalik and Mc-Leary formations, Belcher Group | Ps-Gy, ps-Ha | Ca. 150m | Marine | Pope and Grotzinger, 2003 |
| 16 | Canada | Ca. 1.87 | Stark and Hearne formations, Great Slave Lake Supergroup | Ps-Ha, silicified hopper casts, and pagoda halite, ps-Gy, sc-megabreccia | 200-600m, reconstructed thickness of evaporites are ca. 100m | SG, Marine to non-marine, halite>>gypsum | Pope and Grotzinger, 2003; Evans, 2006 |
| 17 | Canada | 1.81-1.91 | Tavani Formation, Hurwitz Group | Q-ps-Gy, Dol-ps-Gy, halite moulds | ? | Coastal pans, marine to non-marine | Aspler and Chiarenzelli, 2002 |
| 18 | Russia | 1.8-1.9 | | Ps-Gy, ps-An | ? | Associated with barite, sabkha | Pope and Grotzinger, 2003 |
| 19 | Canada | 1.8 | Brown Sound | Ps-Ha, ps-Gy, sc- | Ca. 300m | Marine to non- | Pope and |

| | | | | | | | |
|---|---|---|---|---|---|---|---|
| | | | Formation | breccias | | marine halite>>gypsum | Grotzinger, 2003 |
| 20 | Canada | 1.8 | Cowles Lake Formation | Ps-Ha, ps-Gy, sc-breccias | >200m | Marine to non-marine halite>>gypsum | Pope and Grotzinger, 2003 |
| 21 | India | >1.7 | Vempalle Formation, Papaghni Group | Ps-Ha, ps-Gy | ? | Marine, associated with lava flows | Pope and Grotzinger, 2003 |
| 22 | Australia | 1.74 (1.54-1.74) | Corella Formation, McArthur-Mt Isa basins | Ps-Sh, ps-Gy, quartz replacing anhydrite nodules | Ca. 500m | SG, alkaline lake suggested by shortite | Walker et al., 1977; Muir, 1987; Evans, 2006 |
| 23 | Australia | 1.66 | Mallapunyah, Paradise Greek, Esperanza, Staveley formations, McArthur-Mt Isa basins | Ps-Gy, ps-Ha, botryoidal quartz nodules after anhydrite, massive replacement by gypsum | >10m | SG, marine sabkha | Walker et al., 1977; Evans, 2006 |
| 24 | Australia | 1.645 | Myrtle, Emmerugga, and other formations, McArthur-Mt Isa basins | Ps-Gy, ps-Ha | Ca. 200m | SG | Walker et al., 1977; Evans, 2006 |
| 25 | Australia | 1.635 | Lynott Formation, McArthur-Mt Isa basins | Ps-Gy, ps-Ha, cauliflower cherts | Ca. 300m | SG, marine sabkha | Walker et al., 1977; Evans, 2006 |
| 26 | Australia | 1.61 | Balbirini Formation, McArthur-Mt Isa basins | Ps-Ha, pseudomorphs after sulfates, ps-Sh, Cauliflower cherts | ? | SG, alkaline lake suggested by shortite | Walker et al., 1977; Evans, 2006 |
| 27 | Australia | 1.5 | Discovery Formation, Edmund Group, Bangemall Supergroup, Bangemall basin | Ps-Gy, or ps-An | 70 | SG, marine, several evaporite horizons | Evans, 2006 |
| 28 | USA, Canada | 1.46 | Waterton, Altyn, Prichard, and Wallace formations, Belt Supergroup | Ps-Evp, ps-Gy, ps-An, ps-Ha, length-slow chalcedony, chicken-wire textures, scapolite | 100 m | SG, marine, two evaporite horizons | Evans, 2006 |

https://doi.org/10.5194/egusphere-2023-2091
Preprint. Discussion started: 29 January 2024


| | | | | | | | |
|---|---|---|---|---|---|---|---|
| 29 | USA | 1.15-1.3 | Upper Marble, Grenville Series | An, as lenses and beds | Beds (or lenses) > 40m thick | Metamorphosed evaporites | Whelan et al., 1990 |
| 30 | Canada | 1.2 | Society Cliffs Formation, Victor Bay Group, Borden Basin | Gy, ps-Ha, sc-breccias | Multiple beds a few cm's to meter's thick, >100 m | SG, restricted marine | Kah et al., 2001; Evans, 2006 |
| 31 | Africa | Ca. 1.2 | Char Group, Mauritania, Douik Group, Algeria, Mauritania | ps-Ha | Ca. 50m | SG, marine, possibly correlate with evaporites in Atar and EI Mreiti Groups | Evans, 2006 |
| 32 | Africa | Ca. 1.1 | Qued Tarioufet Formation, Atar Group, Gouamir and Tenoumer formations, EI Mreiti Group, Taoudeni Basin, Mauritania | Ca-Evp, Ca-ps-Gy or Ar, ps-Ha, sc-breccias, chicken-wire texture | Ca. 50 m | SG, marine | Kah et al., 2012 |
| 33 | Canada | 0.7-1.2 | Minto inlet and Kilian formations, Shaler Group | Gy | Multiple gypsum beds up to 30m thick | Marine | Pope and Grotzinger, 2003 |
| 34 | Australia | 0.80-0.83 | Centralian superbasin | Gy, Ha | SG, ~140 000km3 | intracratonic basin | Babel and Schreiber, 2014 |
| 35 | Africa | 0.30-0.27 | Dwyka Formation, Karoo Basin, South Africa | Ha, Gy | ? | Intracratonic basin | Visser and Kingsley, 1982 |
| 36 | Africa | 0.16-0.13 | Late Jurassic to Early Cretaceous, Morocco, Casamance River, Old Bahama Channel | Gy, Ha | SG | marine | Burke, 1975 |
| 37 | Africa | 0.23-0.20 | Upper Triassic, basins in North Africa | An, Gy, Ha, Syl | Multiple horizons in >20m | SG, marine | Vysotsky et al., 2014 |

https://doi.org/10.5194/egusphere-2023-2091
Preprint. Discussion started: 29 January 2024


| | | | | | | | |
|---|---|---|---|---|---|---|---|
| 38 | Asia | 0.54-0.52 | Salt Mountain Formation, Lower Cambrian, Salt Range, Pakistan | Ha, Gy, An, as layers; Dol-ps-Gy | Multiple horizons in > 100m | SG, marine | Vysotsky et al., 2014 |
| 39 | Asia | 0.02-0.01 | Badenian, Middle Miocene, Carpathian Region | Ha, Gy | SG, Multiple horizons in > 10m | Intracratonic basin | Galamay et al., 2021 |
| 40 | Asia | 0.30-0.25 | Kungurian Salt, Permian, Caspian Sea | Gy, Ha, An | SG | Intracratonic basin | Vysotsky et al., 2014 |
| 41 | Australia | 0.51-0.49 | Saline River Formation, Northwest Territories | Ha, An; Dol-ps-An | Multiple horizons in > 200m | SG, marine to lagoonal, sub-tidel to peritidal environment, similar to Sabkahs | Vysotsky et al., 2014 |
| 42 | Australia | 0.54-0.52 | Ouldburra Formation, Lower Cambrian, Officer basin, South Australia | Ha, An | Multiple horizons in > 20m | SG, marginal to restricted marine environments, mudflat | Kovalevych, 1988, 1990; Kovalevych et al., 2006 |
| 43 | Australia | 0.46-0.44 | Carribuddy Group, Late Ordovician to Early Silurian, Canning basin, Western Australia | Ha, An, Dol-ps-An | Multiple horizons in > 100m | SG, marginal marine to ephemeral saltpan and saline mudflat | Williams, 1991 |
| 44 | Australia | 0.45-0.41 | Dirk Hartog Group, Silurian, Southern Carnarvon Basin | An, Gy, Evaporite karst | ? | Subtidal, peritidal, mudlfat | El-Tabakh et al., 2004 |
| 45 | Australia | 0.63-0.54 | Gillen Member, Undoolya Sequence, Late Proterozoic, Amadeus Basin | An, Gy, Ha | ? | Intracratonic basin, marginal marine | Kennedy, 1993 |
| 46 | Australia | 0.9 | Bitter Spring Formation | Gy, Ha | SG | Marine | Preiss, 1972; Marjoribanks |

https://doi.org/10.5194/egusphere-2023-2091
Preprint. Discussion started: 29 January 2024


| | | | | | | | |
|---|---|---|---|---|---|---|---|
| | | | | | | | and Black, 1974 |
| 47 | Canada | 0.42-0.41 | Salina Formation, Upper Silurian, Great Lake | An, Gy, Dol-ps-An | ? | intracratonic basin | Vysotsky et al., 2014 |
| 48 | Canada | 0.36-0.30 | Carboniferous, Sverdrup Basin, Arctic Canada | Gy, An | SG, evaporite diapirs | Intracratonic basin | Balkwill, 1978 |
| 49 | Canada | 0.40-0.38 | Fort Vermilion Formation, Western Canada basins | An, Gy, Ha, Syl, Car | SG, Multiple horizons in > 100m | Sabkham marginal marine | Klingspor, 1969; Wittrup and Kyser, 1990 |
| 50 | Canada | 0.40-0.38 | Elk Point Group, Middle Devonian, Saskatchewan, Western Canada | Ha, Gy, An, | SG, Multiple horizons in > 10m | Intracratonic basin | Horita et al., 1996 |
| 51 | Canada | 0.39-0.36 | Wabamun Group, Alberta Basin, West Canada | An, Dol-ps-An | ? | Intracratonic basin | Anfort et al., 2001 |
| 52 | Canada | 0.35-0.33 | Windsor Group, Early Middle Visean, Nova Scotia, New Brunswick, Atlantic Canada | Ha, Gy, An | SG, Multiple horizons in > 100m | Intracratonic basin | Schenk et al., 1994a, b; Ravenhurst et al., 1989 |
| 53 | China | 0.53-0.50 | Wusonggeer Formation, Sayilike Formation, Awatage Formation, Lower-Middle Cambrian, Tarim basin, NW China | An, Dol-ps-An | Multiple horizons in > 100m | SG, lagoonal to tidal flat, | Wang et al., 2014 |
| 54 | China | 0.53-0.50 | Meishucun Formation, Canglangpu Formation, Qingxu Formation, | Gy, Ha, An; Dol-ps-An | Multiple horizons in > 100m | SG, marine to lagoonal, to intracontinental, tidal flat | Huang, 1993; Goldberg et al., 2005 |

| | | | | | | | |
|---|---|---|---|---|---|---|---|
| | | | Qiongzhusi Formation, Shilengshui Formation, Lower-Middle Cambrian, Yangtz Block | | | | |
| 55 | China | 0.46-0.44 | Tanjianshan Group, Qaidam basin | Gy | ? | Marginal marine, restricted basin | Wu et al., 2022 |
| 56 | China | 0.36-0.30 | Carboniferous, Tarim | Gy, | ? | Marginal marine to restricted basin | Chen et al., 2016 |
| 57 | China | 0.47-0.46 | Majiagou Formation, Middle Ordovician carbonate-evaporite sequence, Ordos basin | Gy, Ha, Ca-ps-An | SG, Multiple horizons in > 20m | Inter-tidal | Meng et al., 2019; Xiong et al., 2020 |
| 58 | China | 0.06-0.03 | Paleogene, Tarim | Gy | ? | Marginal marine to restricted basin | Chen et al., 2016 |
| 59 | China | 0.02-0.005 | Suwiyi Formation, Miocene, Tarim Basin | Gy, An, Ha | SG, Multiple horizons in > 10m | Intracratonic basin | Tang, 1992 |
| 60 | China | 0.36-0.32 | Lower Carboniferous, Tarim Basin | Gy, An, Ha | SG, Multiple horizons in > 10m | Intracratonic basin | Tang, 1992 |
| 61 | China | 0.01-present | Quaternary, Qaidam Basin | Gy, Ha, An | SG, Multiple horizons in > 10m | Foreland basin | Schubel and Lowenstein, 1997 |
| 62 | China | 0.28-0.26 | Lucaogou Formation, Fengcheng Formation, Permian, Junggar Basin | Ha, Gy | ? | Intracratonic basin | Zhang et al., 2021; Yu et al., 2018, 2019 |
| 63 | China | 0.28-0.26 | Pusige Formation, | Ha, Gy | ? | Intracratonic basin | Wang et al., 2021 |

https://doi.org/10.5194/egusphere-2023-2091
Preprint. Discussion started: 29 January 2024


| | | | | | | | |
|---|---|---|---|---|---|---|---|
| | | | Permian, Tarim Basin | | | | |
| 64 | China | 0.23-0.20 | Jialingjiang Formation, Leikoupo Formation, Triassic, Sichuan Basin | Gy, An | ? | Intracratonic basin, Tidal flats, lagoon | Liu et al., 2018 |
| 65 | China | 0.10-0.06 | Mengyejing Formation, Yunlong Formation, Late Cretaceous, Simao Basin, | Gy, An, Ha, Syl | ? | Marginal marine | Liu et al., 2018 |
| 66 | China | 0.10-0.03 | Tuyiluoke Formation, Altash Formation, Kumugelimu Formation, Late Cretaceous to Oligocene, Tarim Basin | Gy, An | ? | Marginal marine | Liu et al., 2018 |
| 67 | China | 0.18-0.16 | Qiangtang basin | Gy, An | ? | Intracratonic basin, lagoonal, subkha | Li et al., 2008a, b |
| 68 | China | 0.01-present | Late Miocene to Pliocene, Qaidam Basin, China | Gy, Ha | ? | Intracratonic basin | Guo et al., 2018 |
| 69 | China | 0.06-0.02, 0.01-present | Eocene, Qaidam, Tarim, Junggar, Bohai Bay, Subei, Nanxiang, Jianghan Basin, South China Grabens | Gy, Ha | ? | Intracratonic basin | Guo et al., 2020; Jiang et al., 2013 |
| 70 | China | 0.15-0.03 | South China graben, Middle-Lower reaches of Yangtze River | GY, Ha, An | SG | Intracratonic basin | Teng et al., 2019 |
| 71 | China | 0.06-0.02 | Paleogene, Tarim basin | Gy, An | Multiple horizons | SG, marine | Zhu et al., 2012 |

https://doi.org/10.5194/egusphere-2023-2091
Preprint. Discussion started: 29 January 2024


| | | | | | | | |
|---|---|---|---|---|---|---|---|
| | | | | | in >200m | | |
| 72 | Europe | 0.48-0.43 | Middle Ordovician to Late Silurian red beds, Baltic basin | Red beds | ? | Intracratonic sedimentary basin | Kiipli et al., 2009 |
| 73 | Europe | 0.26-0.25 | St. Bees evaporites, Upper Permian, England | An, Gy | ? | Intracratonic basin | Arthurton and Hemingway, 1972; Kiersnowski et al., 1995 |
| 74 | Europe | 0.32-0.25 | Late Carboniferous to Permian, Lodeve Basin, Autun Basin, Bourbon l' Archambault basin, Saar-Nahe Basin, Thuringian Forest Basin, Saale Basin, North German-Polish Basin, Central and Western Bohemian Basins, Intra-Sudetic Basin, Boskovice Graben, Moroccan Basins | Ha, Gy, An | SG, Multiple horizons in > 100m | Intracratonic basin | Roscher and Schneider, 2006 |
| 75 | Europe | 0.27-0.25 | Permian, Zechstein Basin | Ha, Gy, An | SG, Multiple horizons in > 10m | Isolated deep basin | Regenspurg et al., 2016; Lüders et al., 2010 |
| 76 | Europe | 0.28-0.25 | Rotliegend Supergroup, South Permian Basin, Europe | Ha, Gy | SG, Multiple horizons in > 100m | Intracratonic basin | Kiersnowski et al., 1995; Gaupp et al., 2000 |
| 77 | Europe | 0.28- | Unidad Roja | Ha, Gy | ? | Intracratonic | Valero Garces |

https://doi.org/10.5194/egusphere-2023-2091
Preprint. Discussion started: 29 January 2024


| | | | | | | | |
|---|---|---|---|---|---|---|---|
| | | 0.25 | Superior Group, Permian, Aragon-Bearn Basin, Pyrenees basins | | | basin | and Aguilar, 1992 |
| 78 | Europe | 0.23-0.20 | Late Triassic, Foreland basins of pyrenees | Gy, An | ? | Intracratonic rift basin | Puigdefabregas and Souquet, 1986 |
| 79 | Europe | 0.23-0.20 | Keuper Formation, Late Triassic, Central Europe | Gy, An, Ha | ? | Intracratonic basin | Barth, 2000 |
| 80 | Europe | 0.02-0.01 | Miocene, Ebro Basin | Gy, An, Ha | ? | Intracratonic basin | Sanchez et al., 1999 |
| 81 | Europe | 0.23-0.20 | Mercia Group, Upper Triassic, Bristol Channel Basin, U.K. | Gy, An, Ha | ? | Intracratonic basin | Nemcok and Gayer, 1996 |
| 82 | Europe | 0.30-0.20 | Permian, Triassic, Upper Triassic, Bay of Biscay, Europe basins | Gy, An, Ha | SG | Intracratonic basin | Bourquin et al., 2011 |
| 83 | Europe | 0.06-0.02 | Paleocene to Miocene, Ebro, Tajo, Calatayud and Teruel basin, Spain | Gy, Ha | ? | Intracratonic basin | Utrilla et al., 1992 |
| 84 | Europe | 0.40-0.38 | Middle Devonian, Morsov Basin | Gy, An, Ha, Syl | Multiple horizons in >20m | SG, marine | Vysotsky et al., 2014 |
| 85 | Europe | 0.39-0.36 | Upper Devonian, Dnieper Donets basin | Gy, An, Ha, Syl | Multiple horizons in >20m | SG, marine | Vysotsky et al., 2014 |
| 86 | Europe | 0.39-0.36; 0.30-0.25 | Upper Devonian, Pripyat depression | Gy, An, Ha, Syl | Multiple horizons in >20m | SG, marine | Vysotsky et al., 2014 |
| 87 | Europe | 0.30-0.25 | Permian, Dnieper Donets basin | Gy, An, Ha, Syl | Multiple horizons in >20m | SG, marine | Vysotsky et al., 2014 |
| 88 | Latin America | 0.16-0.14 | Minas Viejas Formation, Late | Gy, An, Ha | SG | Marine to lagoonal | Guzman, 1962 |

https://doi.org/10.5194/egusphere-2023-2091
Preprint. Discussion started: 29 January 2024


| | | | | | | | |
|---|---|---|---|---|---|---|---|
| | | | Jurassic, Sierra Madre Oriental, Mexico | | | | |
| 89 | Latin America | 0.16-0.14 | Upper Jurassic, Mexican Gulf Coastal Plain, Mexico | Gy, An, Ha | SG | Marginal basin | Guzman, 1962 |
| 90 | Latin America | 0.16-0.13 | Late Jurassic to Early Cretaceous, Caribbean | Gy, Ha | SG | marine | Iturralde-Vinent, 2006 |
| 91 | Mediterranean and Black Sea | 0.07-0.05 | Messinian Saline Gaint, Late Miocene, Mediterranean | Gy, Ha, An, Dol-ps-An | $10^6$km$^3$ | SG, Desiccating deep basin | Mu¨ller and Hsu¨, 1987 |
| 92 | Middle-East | 0.63-0.50 | Birba Formation, U/Athel Formation, Al Noor Formation, South Oman Salt Basin | Ha, An, Ca-ps-Ha | Multiple horizons in > 200m | SG, marginal to restricted marine environments | Ramseyer et al., 2013 |
| 93 | Middle-East | 0.02-present | Miocene, Pleistocene, Danakil depression, Ethiopian rift, Red Sea Basin | Ha, Gy, Eva | Multiple horizons in > 200m | SG, Marine | Hutchinson and Engels, 1970 |
| 94 | Middle-East | 0.04-0.01 | Tuzluca Formation, Kagizman and Tuzluca basin, Anatolian basins | Gy, Ha | SG | Marginal marine | Palmer et al., 2004; Varol et al., 2015 |
| 95 | North Atlantic-Canada | 0.23-0.18 | Argo Formation, Late Triassic to Early Jurassic, Scotian Basin | Ba, Gy, An | SG | Intracratonic basin | Pe-Piper et al., 2015 |
| 96 | Russia | 0.68-0.57 | Motaya Formation, Eastern Siberia | An, as layers; Ca-ps-Gy; Ps-Ha | Multiple horizons in > 20m | SG, non-marine to marine | Vysotsky et al., 2014 |
| 97 | Russia | 0.54-0.51 | Jonov Formation, Huchtuisk Formation, | Ha, Gy, as layers; Ca-ps-Gy | Multiple (16) horizons in > 400m | SG, non-marine to marine, >600000 km$^3$ | Vysotsky et al., 2014 |

https://doi.org/10.5194/egusphere-2023-2091
Preprint. Discussion started: 29 January 2024


| | | | | | | | |
|---|---|---|---|---|---|---|---|
| | | | Eastern Siberia, Ussoli Formation, Lower Cambrian | | | | |
| 98 | Russia | 0.30-0.25 | Permian, Ural depression | Gy, An, Ha, Syl | Multiple horizons in >20m | SG, marine | Vysotsky et al., 2014 |
| 99 | South America | 0.15-0.08 | Caqueza Group, Villeta Group, Cretaceous, Cordillera Oriental, Columbia | An, Gy | SG, Multiple horizons in > 5m | foreland basin | McLaughlin, 1972 |
| 100 | South America | 0.28-0.25 | Rio Bonito Formation, Permian, Parana Basin, Brazil | Ha, Gy | ? | Intracratonic basin | Ketzer et al., 2009 |
| 101 | South America | 0.28-0.25 | Motuca Formation, Parnaiba Basin, Brazil | Ha, Gy | SG, ? | Intracratonic basin | Abrantes Jr et al., 2019 |
| 102 | South America | 0.13-0.06 | Codocedo Formation, Quebrada Monardes Formation, Atacama region | Gy, An | ? | Marginal marine | Bell and Suarez, 1993 |
| 103 | South America | 0.04-present | Purilactis Group, Oligocene-Pliocene, Salar de Atacama basin | Gy, An | SG | Intracratonic basin | Mpodozis et al., 2005 |
| 104 | South America | 0.06-present | Cenozoic, Central Andes | Gy, Ha, An | SG | Intracratonic basin | Diaz, 1988 |
| 105 | South America | 0.30-0.25 | Permian, Amazon Basin, Brazil | Gy | ? | ? | Vysotsky et al., 2014 |
| 106 | Southeast Asia | 0.10-0.06 | Late Cretaceous, Laos-Khorat basin | Gy, An | ? | Marginal marine | Liang and Xu, 2022 |
| 107 | Southeastern Asia | 0.10-0.06 | Upper Cretaceous, | Gy, An, Syl | Multiple horizons | SG | Vysotsky et al., 2014 |

| | | | | | | | |
|---|---|---|---|---|---|---|---|
| | | | Nam Kam Basin | | in >20m | | |
| 108 | USA | 0.46-0.44 | Ordovician Galena Group, Illinois basin | Gy, An | ? | Marginal basin | Stueber and Walter, 1994 |
| 109 | USA | 0.43-0.42 | Niagara and Salina Group, Silurian, Michigan basin | Ha, Gy, Car, Ca-ps-Gy | SG, >500m thick | Intracratonic sedimentary basin | Wilson and Long, 1993; Elliott and Aronson, 1993 |
| 110 | USA | 0.42-0.40 | Detroit River Group, Lower Devonian, Michigan basin | Gy, Ha, An | SG, Multiple horizons in > 30m | Intracratonic basin | Wilson and Long, 1993 |
| 111 | USA | 0.43-0.41 | Salina Group, Appalachian basin | Ha, Gy, Car, Ca-ps-Gy | SG, >500m thick | Intracratonic sedimentary basin | Johnson, 1997 |
| 112 | USA | 0.36-0.32 | Mississippian Michigan Formation, Michigan basin | Gy | SG, Multiple horizons in > 1-10m | Intracratonic sedimentary basin | Johnson, 1997 |
| 113 | USA | 0.33-0.32 | St. Louis Formation, Illinois basin | Evaporite karst | ? | Intracratonic basin | McGrain and Helton, 1964 |
| 114 | USA | 0.41-0.36 | Wapsipinicon Group, Cedar Valley Group, Devonian, Forest City basin | Gy, An, Evaporite karst | Multiple horizons in > 1-10m | Intracratonic basin | Witzke et al., 1988; Cody et al., 1997 |
| 115 | USA | 0.20-0.15 | Fort Dodge Formation, Jurassic, Forest City basin | Evaporite karst | Multiple horizons in > 1-10m | Intracratonic basin | Witzke et al., 1988; Cody et al., 1997 |
| 116 | USA | 0.17-0.15 | Louann Salt and Salt Domes, Gulf Coast basin | Ha, Gy, Evaporite karst | Multiple horizons in > 500m | SG, marine | Babel and Schreiber, 2014 |
| 117 | USA | 0.27-0.25 | Schnebly Hill Formation, Holbrook basin | Ha, Gy, Evaporite karst | ? | SG | Neal and Johnson, 2002 |
| 118 | USA | 0.32-0.30 | Hermosa Formation, Paradox basin | Ha, Evaporite karst | ? | Salt anticline | Hite and Lohman, 1973; Doelling, 1988 |
| 119 | USA | 0.17-0.15 | Jurassic Arapien Formation, | Ha, Evaporite karst | ? | Salt anticline | Willis, 1986; Witkind, 1994 |

https://doi.org/10.5194/egusphere-2023-2091
Preprint. Discussion started: 29 January 2024


| | | | | | | | |
|---|---|---|---|---|---|---|---|
| | | | Paradox basin | | | | |
| 120 | USA | 0.26-0.25 | Castile Formation, Salado Formation, Rustler Formation, Delaware basin | Gy, Ha, An, Evaporite karst | SG, Multiple horizons in > 500m | Intracratonic basin | Dean and Johnson, 1989; Kirkland and Evans, 1980 |
| 121 | USA | 0.26-0.25 | Castile Formation, Salado Formation, Rustler Formation, Midland basin | Gy, Ha, An, Evaporite karst | SG, Multiple horizons in > 500m | Intracratonic basin | Dean and Johnson, 1989; Kirkland and Evans, 1980 |
| 122 | USA | 0.27-0.25 | Artesia Group, San Andres Formation, New Mexico | Gy, Ha, An, Evaporite karst | SG, Multiple horizons in > 100m | Intracratonic basin | Forbes and Nance, 1997 |
| 123 | USA | 0.27-0.25 | Blaine Formation, Cloud Chief Formation, Texas and Oklahoma | Gy, Ha, An, Evaporite karst | SG, Multiple horizons in > 5m | Intracratonic basin | Johnson, 1990, 1992 |
| 124 | USA | 0.14-0.10 | Terrett Formation, Cretaceous, Central Texas | Gy, Evaporite karst | >10m | Intracratonic basin | Warren et al., 1990 |
| 125 | USA | 0.30-0.25 | Permian, Palo Duro Basin, Texas | Gy, An | SG | Intracratonic basin | Gu and Eastoe, 2021 |
| 126 | USA | 0.25-0.20 | Spearfish Formation, South Dakota, | Gy, Evaporite karst | ~5m | Intracratonic basin | Rahn and Davis, 1996; Davis and Rahn, 1997 |
| 127 | USA | 0.36-0.32 | Madison Formation, Wyoming | Gy, Evaporite karst | ? | Intracratonic basin | Sando, 1988 |
| 128 | USA | 0.28-0.25 | Permian, Appalachian basin | An, Gy | ? | Intracratonic basin | Rowen et al., 2015 |

https://doi.org/10.5194/egusphere-2023-2091
Preprint. Discussion started: 29 January 2024


| | | | | | | | |
|---|---|---|---|---|---|---|---|
| 129 | USA | 0.28-0.26 | Opeche Shales, Nippewalla Group, Ochoan Series, Summer Group, Chase Group, Wolfcampian Formation, Salado Formation, Permian, Palo Duro Basin, Denver Basin, Paradox Basin, Central Basin, Delaware Basin, Midland Basin, North Amercia | Ha, Gy, An, Syl, Ca | SG, Multiple horizons in > 100m | Intracratonic basin | Benison et al., 1998; Engle et al., 2016 |
| 130 | USA | 0.23-0.19 | Newark Supergroup, North Amercia grabens | Gy | ? | Intracratonic basin | Smoot et al., 1991 |
| 131 | USA | 0.14-0.10 | Edwards Group, Lower Cretaceous, Gulf Basin, Texas | Gy, An | SG | Marginal marine | Land and Prezbindowski, 1981; Hanor and Mcintosh, 2007 |
| 132 | USA | 0.02-present | Late Great Salt Lake, Picacho basin, Safford basin, Tucson basin, SE North Amercia | Gy, Ha | ? | Intracratonic basin | Kowalewska and Cohen, 1998 |

Saline Giants (SG), with volume > 1000km3;
An, anhydrite;
Ank-ps-Gy, ankerite pseudomorphs after gypsum;
Ba, barite; Ba-ps-Gy, barite pseudomorphs after gypsum;
Ca-Evp, calcitized evaporites; Ca-ps-Ar, carbonate pseudomorphs after aragonite;
Ca-ps-An, carbonate pseudomorphs after anhydrite;
Ca-ps-Gy, carbonate pseudomorphs after gypsum;
Ca-ps-Gy or -Ar, carbonate pseudomorphs after gypsum or aragonite;
Dol-ps-An, dolomite pseudomorphs after anhydrite;
Dol-ps-Gy, dolomite pseudomorphs after gypsum; Gy, gypsum;
Kao-ps-Gy or An, kaolinite pseudomorphs after gypsum or anhydrite;

https://doi.org/10.5194/egusphere-2023-2091
Preprint. Discussion started: 29 January 2024


ps-An, pseudomorphs after anhydrite;
ps-Evp, pseudomorphs after evaporites;
ps-Gy, pseudomorphs after gypsum;
ps-Mir, pseudomorphs after mirabilite;
ps-Nah, pseudomorphs after nahcolite;
ps-Nat, pseudomorphs after natron;
ps-Ha, pseudomorphs after halite;
ps-Sh, pseudomorphs after shortite;
ps-Tro, pseudomorphs after trona;
Q-ps-An, quartz pseudomorphs after anhydrite;
Q-ps-Gy, quartz pseudomorphs after gypsum;
sc-breccias, solution collapse breccias;
Si–Evp, silicified evaporites;
Si-ps-An, silicified pseudomorphs after anhydrite;
Si-ps-Ar, silicified pseudomorphs after aragonite;
Si-ps-Gy, silicified pseudomorphs after gypsum;
Si-ps-Nah, silicified pseudomorphs after nahcolite;
Si-tr-An, quartz filled traces after anhydrite;
Si-tr-Gy, quartz filled traces after gypsum.